ISBN 90-6256-600-6
NUGI 742

Free University Press
De Boelelaan 1105
1081 HV Amsterdam

telefoon 020-444355
telex 18191 vuboe nl

MR Imaging of Laryngeal Cancer J.A.Castelijns

MR Imaging of Laryngeal Cancer

J.A.Castelijns

VRIJE UNIVERSITEIT TE AMSTERDAM

MR Imaging of Laryngeal Cancer

ACADEMISCH PROEFSCHRIFT

ter verkrijging van de graad van doctor aan
de Vrije Universiteit te Amsterdam,
op gezag van de rector magnificus
dr. C. Datema,
hoogleraar aan de faculteit der letteren,
in het openbaar te verdedigen
ten overstaan van de promotiecommissie
van de faculteit der geneeskunde
op vrijdag 11 december 1987 te 15.30 uur
in het hoofdgebouw van de universiteit,
De Boelelaan 1105

door

JOHANNES ADRIANUS CASTELIJNS

geboren te Bladel en Netersel

VU Uitgeverij
Amsterdam 1987

Promotoren: prof.dr. J. Valk
prof.dr. G.B. Snow
Referent: prof.dr. A.E. van Voorthuisen

Voor Mladenka
Aan mijn ouders

The publication of this thesis was made possible through a grant from Kodak and General Electric Medical Systems.

ISBN 90-6256-600-6 CIP
NUGI 742

Free University Press
De Boelelaan 1105
1081 HV Amsterdam
The Netherlands

Telephone 020-44 43 55
Telex 18191 vuboe nl

MAGNETIC RESONANCE IMAGING OF LARYNGEAL CANCER

CONTENTS

INTRODUCTION

This study concerns the role of magnetic resonance imaging (MRI) in the diagnostic work-up of laryngeal cancer. Radiation therapy and/ or surgery are the modalities of choice for the treatment of laryngeal cancer in non-previously treated patients. The choice depends mainly on the risk of tumor recurrence and that of complications, as well as on the functional results after treatment, such as the quality of the voice. The response of laryngeal cancer to radiotherapy is related to general conditions, such as the general physical state of the patient, as well as to local conditions, such as origin, extent of the tumor and histological characteristics and the nature of involved tissues. Tumor infiltration into muscular and in particular cartilagineous structures increases the risk of therapeutic failures and complications, particularly if high doses of irradiation treatment are applied. Surgery, and in particular conservation surgery, requires detailed knowledge of the superior, inferior and lateral extent of the lesion.

If a choice has been made between radiation therapy and surgery, local properties of the lesion may still influence the plan of treatment. The radiation dose may be adjusted to the TNM staging, anatomic site and volume of the tumor. Reduction of the size of treatment portal is an essential part of the treatment planning. Similarly both the procedures of partial and total laryngectomy may be modified according to the extent of the primary tumor within or outside the larynx.

It is evident that accurate assessment of the extent of local disease is of great importance with regard to correct choice of treatment modality and technique. Laryngoscopic examination reveals a great deal of information of site, volume and extent of the intralaryngeal lesion. However, it does not provide information of the submucosal extension of the lesion and some hidden regions, such as the subglottic area or areas, concealed by a large tumor mass.

Radiological examination can provide additional information on the extent of the disease. The conventional radiological modalities , such as contrast laryngography and conventional tomography, have been largely supplanted by computer tomography (CT). The contribution of CT to diagnostic imaging is based on its capability to visualize much smaller differences in X-ray absorption than conventional radiological techniques and to demonstrate submucosal changes by axial imaging. CT scanning provides useful information of areas that are hidden from visual inspection by bulky tumors, such as the subglottic area. More importantly it reveals submucosal extension not visible by other means. It is particularly capable of detecting gross cartilage invasion and of demonstrating extralaryngeal extension.

However, CT also has its limitations. Its potential to discriminate soft tissues, although superior to that of conventional radiological modalities, still is relatively poor. Furthermore CT is insufficiently capable to image accurately in the frontal and the sagittal planes. CT does not reveal minor cartilage invasion and is unable to differentiate between post-irradiation fibrosis and recurrent carcinoma.

Of late it has become clear that MRI has the potential to provide additional value in the diagnostic work-up. In condensed phases, liquids and solids, nuclear magnetic resonance (NMR) was first observed by both Bloch and Purcell in 1946 (1,2). In 1973 MR Imaging started to develop, due mainly to the work of Lauterbur, who introduced linear gradients for spatial localisation of NMR signals (3). MRI is a non-ionizing diagnostic method, providing images with high soft-tissue contrast at any plane of the human body. The density relationships of various tissues are quite different on MRI when compared to CT. CT is based on photon absorption in tissues of different density. MR imaging depends on the presence of hydrogen atoms, certain tissue characteristics and the

presence or absence of blood flow.

At the start of the investigations in december 1984, reports on MR imaging of the larynx were limited to a few examples of normal anatomy of the neck area (4,5). The techniques of MR imaging of the larynx were certainly not explored. Investigations as to comparisons between MR images, CT scans and corresponding histopathological sections had not been carried out.

The aim of this study is firstly to optimize MRI technique of the larynx and to describe MR images of the laryngeal anatomy in detail. Subsequently, the potential of MRI to demonstrate site and extent of laryngeal cancer, and particularly its ability to detect cartilage invasion, is analyzed by comparing MR images with corresponding CT scans and histopathological sections of surgical specimens.

Chapter 1 deals with general aspects of laryngeal cancer. In particular, the therapeutical implications will be discussed.

In chapter 2 the clinical relevance of various radiological examinations of the larynx, such as conventional tomography, contrast laryngography and computer tomography, in regard to the assessment of the extent of laryngeal cancer, will be discussed.

Chapter 3 covers the basic principles of magnetic resonance imaging and reviews its technical potentials and limitations.

In chapter 4 the experiences are described in optimizing laryngeal images by introducing the use of surface coils and by applying various MR techniques and pulse parameters, with a view to maximize signal-to-noise ratio and soft tissue contrast. A detailed description of axial, frontal and sagittal MR images of normal anatomical laryngeal structures is given.

Chapter 5 deals with MR imaging of laryngeal cancer in previously untreated patients and in patients with recurrent disease after radiotherapy, by comparing pre-operative MRI findings with post-operative histopathological findings in surgical specimens.

Chapter 6 covers a detailed description of MRI of non-ossified and ossified laryngeal cartilages, both normal and invaded by cancer, in untreated patients.
In chapter 7 MRI and CT results are evaluated in detecting laryngeal cartilage invasion by cancer in previously untreated patients, by comparing both CT- and MR images with histopathological findings in corresponding sections of surgical specimens and assessing the accuracy of observations, done by CT- and MRI-observers.
In chapter 8 the clinical relevance of MRI and other radiological investigational procedures will be discussed in relation to the therapeutical management of laryngeal cancer.

REFERENCES

1. Bloch F, Hansen WW, Packard M. Nuclear induction. Phys rev 1946;69:127-131.

2. Purcell EM, Torrey HC, Pound RV. Resonance absorption by nuclear magnetic moments in a solid. Phys rev 1946;69:37-42.

3. Lauterbur PC. Image formation by induced local interactions: examples employing NMR. Nature;242:191-192.

4. Lufkin RB, Larson SG, Hanafee WN. Work in progress: NMR anatomy of the larynx and the tongue base. Radiology 1983;148:173-175.

5. Stark DD, Moss AA, Gamsu G, Clark OH, Gooding GAW, Webb WR. Magnetic resonance imaging of the neck. Normal anatomy. Radiology 1984;150:447-454.

Chapter 1. GENERAL ASPECTS OF LARYNGEAL CANCER

1.1 INTRODUCTION

1.1.1 Incidence

Cancer of the larynx is the most commonly occuring malignant tumor in the head and neck area in the western hemisphere. Eighty per cent of laryngeal cancers occur in the fifth, sixth, and seventh decades of life; approximately 40 percent occur in the sixth decade (1,2).
The general range of incidence rates in the U.S.A. is as follows: glottic, 60 to 70 per cent; supraglottic, 25 to 35 per cent and in about 5 percent, subglottic (1,3). It is interesting, but not yet explained, that the incidence of supraglottic malignant tumors is relatively much higher in some other parts of the world; particularly in Finland, Yugoslavia, Italy and the Southeast Asian countries, the 70/30 ratio of glottic to supraglottic involvement is reversed (1,2).
The incidence of cervical node metastasis with lesions, confined to the glottic region, is very low (about 1%). In contrast, supraglottic and subglottic lesions show a much higher frequency of lymphatic spread: 21-32% (4). The first nodal stations of lymphatic spread of laryngeal tumors include the jugulodigastric, jugulo-omohyoid and paratracheal nodes (5). Hematogeneous spread is rare on admission and uncommon. If it occurs, the lungs are the most frequent site of metastatic deposits, followed by the skeletal system (5).
Almost all laryngeal cancers are squamous cell carcinomas (more than 90%) (6).

1.1.2 Predisposing factors

Epidemiological examinations have shown a relationship between excessive tobacco usage and laryngeal cancer. The risk of developing cancer of the larynx has been related to the amount and type of tobacco consumed. Excessive alcohol consumption in the presence of tobacco use is an additional etiologic factor, particularly in supraglottic cancer (4,6,7). Furthermore, it has been demonstrated that irradiation has a carcinogenic effect (6).

1.2 TNM STAGING

1.2.1 Introduction

The two staging systems most frequently used are that proposed by the American Joint Commission (AJC), and that proposed by the International Union Against Cancer (UICC) (5,8). Although they differ in several details, these systems are almost identical concerning laryngeal tumors. The most current and widely accepted classification of carcinoma of the larynx is the TNM-staging as proposed by the UICC (8).

1.2.2 Clinical classification

In the classification, as proposed by the UICC, the larynx is divided into three anatomical sites (supraglottis, glottis and subglottis) and these sites are subdivided in subsites:

A. Supraglottis
   Epilarynx (including the marginal zone)
   1) Suprahyoid epiglottis
   2) Aryepiglottic fold
   3) Arytenoid
   Supraglottis (excluding the epilarynx)
   4) Infrahyoid epiglottis
   5) False cords
   6) Laryngeal ventricles
B. Glottis
   1) Vocal cords
   2) Anterior commissure

   3) Posterior commissure
C. Subglottis

Clinical classification, as proposed by the UICC (8):

T-staging

Supraglottis:

T1 Tumor limited to one subsite of supraglottis with normal vocal cord mobility
T2 Tumor invades more than one subsite of supraglottis or glottis, with normal vocal cord mobility
T3 Tumor limited to the larynx with vocal cord fixation and/ or invades postcricoid area, medial wall of piriform sinus or pre-epiglottic tissues
T4 Tumor invades through thyroid cartilage and/ or extends to other tissues beyond the larynx, e.g. to oropharynx, soft tissues of the neck

Glottis:

T1 Tumor limited to vocal cord(s) (may involve anterior and posterior commissures) with normal mobility
T1a Tumor limited to one vocal cord
T1b Tumor involves both vocal cords
T2 Tumor extends to supraglottis and/or subglottis, and/or with impaired vocal cord mobility
T3 Tumor limited to the larynx with vocal cord fixation
T4 Tumor invades through thyroid cartilage and/or extends to other tissues beyond the larynx, e.g. to oropharynx, soft tissues of the neck

Subglottis

T1 Tumor limited to the subglottis
T2 Tumor extends to vocal cord(s) with normal or impaired mobility

T3 Tumor limited to the larynx with vocal cord fixation
T4 Tumor invades through cricoid or thyroid cartilage and/or extends to other tissues beyond the larynx, e.g. to oropharynx, soft tissues of the neck

N-staging

The definitions of the N categories for all head and neck sites except thyroid gland are:
N0 No regional lymph node metastasis
N1 Metastasis in a single ipsilateral lymph node, 3 cm or less in greatest dimension
N2 Metastasis in a single ipsilateral lymph node, more than 3 cm but not more than 6 cm in greatest dimension, or in multiple ipsilateral lymph nodes, none more than 6 cm in greatest dimension, or in bilateral or contralateral lymph nodes, none more than 6 cm in greatest dimension
N3 Metastasis in a lymph node more than 6 cm in greatest dimension

M-staging

The definitions of all M categories for all head and neck sites are:

M0 No distant metastasis
M1 Distant metastasis

The term transglottic carcinoma is used for extensive deep tumor invasion passing the ventricle in vertical direction with subglottic extension. All transglottic carcinomas are characterized by invasion into the paraglottic space (9).

1.3 DIAGNOSTIC ASPECTS

1.3.1 History

Patient's complaints correlate with the intralaryngeal origin of the tumor. Glottic cancers cause hoarseness in an early stage. In contrast, patients with a supraglottic tumor have relatively vague complaints of throat soreness, particularly during swallowing. Sometimes they complain of otalgia ("referred pain") or have noticed a mass in the neck due to lymphatic spread. Patients with a subglottic lesion are suffering from vague complaints of coughing in an early stage. In a more advanced stage they may complain of hoarseness, due to infiltration of the vocal muscles or dyspnea due to obstruction of the airway (10).

1.3.2 External examination

Signs of advanced, extralaryngeal tumor spread may be detected by external examination. The assessment of the status of neck nodes is still based on clinical palpation. The fallibility of palpating the neck is well known and large interobserver variations have been reported (11,12). The palpability of a lymph node depends on its location, consistency, size, and type of neck. In a neck of average size and in the hands of an experienced examiner, the lower limit of palpability is approximately 0.5 cm in a superficial area such as the submental and submandibular area. Therefore, nodes containing small deposits of carcinoma may not be clinically palpable. Moreover, not all the enlarged lymph nodes contain metastatic deposits (11). Spread to some regional lymph nodes, such as the paratracheal nodes, almost invariably goes undetected clinically (13).

1.3.3 Laryngoscopy

Indirect and direct laryngoscopic examination reveal a great deal of information about site, volume and extent of the intralaryngeal lesion. Indirect laryngoscopy provides an overall survey of superficial intralaryngeal structures. It does not interfere with the normal mobility, and during phonation the mobility of the cords may be examined. Direct laryngoscopy allows a more precise study of superficial structures. The anterior commissure, the apex of the piriform sinuses and the greater part of the laryngeal ventricles can be examined as well. This diagnostic procedure also provides an adequate opportunity of removing tissue for histopathological examination.

However, laryngoscopy fails to demonstrate the submucosal extent of the tumor. Moreover, some intralaryngeal areas still remain less accessible, such as the inferior surfaces of the false and true vocal cords and the lateral extent of the laryngeal ventricles (14). The failure to appreciate the extent of minor subglottic spread is also an accepted limitation of direct laryngoscopy.

1.4 THERAPEUTICAL OPTIONS

1.4.1 Radiotherapeutical options

1.4.1.1 Technique

Treatment of patients with laryngeal cancer is performed with megavoltage radiation by left-to-right fields, wedged or unwedged, to pursue a homogeneous radiation dose in the target area. The size of the treatment field depends on the T-stage, extent of the primary tumor, and the presence or probability of lymphatic spread. The extent of the tumor volume, the degree of differentiation, and the rate of regression of the tumor during irradiation treatment each influence the total radiation dose. The extent of the target volume influences the fractionation schedule.

If lymphatic spread is present, both the primary and the enlarged lymph nodes are treated with a curative radiation dose. Because the supraglottic tumors have a high tendency to metastasize, the first echelon of lymphatic drainage is irradiated electively if invasion is not clinically demonstrated.

1.4.1.2 Prognostic factors of irradiation treatment

The treatment results regarding the locoregional tumor-free survival depends on several factors:

1. The response is related to several general factors, including the physical condition, age, and sex of the patient (15). Furthermore, the presence of general disease such as diabetes, hypertension, chronic cardiovascular and pulmonary failures and infections in the target volume are risk bearing factors in radiotherapy (16).
2. Other more local factors, such as location and stage of the tumor and loss of cord mobility influence the response to radiotherapy (17). Radiotherapy is almost invariably incapable of the sterilization of malignant cells invading the cartilages other, than at the cost of osteomyelitis, chondronecrosis and sequestration of the diseased cartilage (10,18,19,20,21). Loss of cord mobility seriously impairs the response to irradiation treatment (19,22,23,24,25).

1.4.1.3 Complications due to radiation therapy

Irradiation treatment of laryngeal cancer may be complicated, sooner or later, by several reactions:

1. In regard to early reactions, it is known that the response of the larynx to radical radiation doses consists of patchy or confluent mucositis, temporary hoarseness and swallowing complaints.
2. Following a larger period of time after the start of irradiation treatment, the cure may be complicated by severe edema and radiation necrosis of bone or cartilages. Complications mainly occur in cases of high fractions of radiation dose, high total dose or due to invasion of bone or cartilage (25,26).

Furthermore, radiotherapy increases the surgical complication rate of salvage surgery when this has to be carried out to counter recurrent disease.

1.4.2 Surgical options

1.4.2.1 Laser therapy and microsurgical stripping.

The carbon dioxide laser provides a precise tool to excise endoscopically selected T1 glottic and carcinoma in situ lesions. Whether or not the laser excision is curative depends, amongst other factors, upon the accuracy with which the extent of the disease is estimated. Inadequate exposure, or extension of the carcinoma into the anterior commissure, arytenoid or subglottic area are contra-indications to this approach (27).

1.4.2.2 Laryngofissure and cordectomy

This surgical procedure implies removal of a vocal cord, at times including adjacent subglottic and supraglottic tissue. A malignant T1a-lesion involving the true vocal cord, not extending anteriorly into the anterior commissure and posteriorly beyond the vocal process of the arytenoid cartilage, and having good mobility, can be resected by this method (28).

1.4.2.3 Vertical partial laryngectomy

This implies the removal of nearly all of the ipsilateral thyroid ala with the exception of a vertical posterior strip, together with the vocal cord, ventricle and false cord on one side, but with preservation of the external perichondrium of the resected ala (29). Usually the anterior commissure is included in the resection. In selected cases this procedure may be extended to include the arytenoid on the involved side or the anterior one third of the contralateral vocal cord.

This procedure is commonly applied in Northern America as primary treatment for T1 and T2 glottic carcinomas. In most Western-European countries the application of the procedure is almost exclusively limited to small recurrences of T1 and selected T2 glottic carcinomas after previous radiotherapy (30).

Whatever the indication, the extent of the tumor should fulfill a number of precise criteria. The posterior extension may involve the vocal process or anterior surface of the arytenoid, but it may not involve either the crico-arytenoid joint or the posterior surface of the arytenoid (31). The tumor may have 8 to 9 mm of subglottic extension in the anterior or midportion of the true cord, but no more than 3 to 4 mm of subglottic extension posteriorly. Extension to the ventricular surface of the false cord indicates a transglottic tumor, which is a contra-indication for partial laryngectomy. Hemilaryngectomy should not be attempted in such cases (32). All three criteria are recommended, because these findings are often associated with invasion of the thyroid and/or cricoid cartilage: a feature that disqualifies the lesion for hemilaryngectomy because the tumor margins are unpredictable (33,34).

Some authors report that in selected cases glottic lesions with a fixed cord, fulfilling strict criteria, can be adequately resected by partial vertical laryngectomy (32,35,36).

1.4.2.4 Antero-frontal laryngectomy for excision of the anterior commissure

On occasion, the anterior commissure of the larynx will be involved to the extent that radiation therapy is not practical. Such a lesion may be amenable to resection of the anterior commissure. The anterior portions of both vocal cords and thyroid cartilage, comprising the central segment between two thyrotomies placed about 1 cm on either side of the midline, are excised (23,37).

1.4.2.5 Supraglottic laryngectomy

Supraglottic lesions, even if they involve the vallecula, base of the tongue, ary-epiglottic folds, and the walls of the piriform sinus, to a level of 1 cm above its apex, should be considered for supraglottic laryngectomy. The lesion should not extend to the lateral pharyngeal wall or into the interarytenoid space. There must be a 5 mm margin between the lower margin of the tumor and the anterior commissure. The true vocal cords and arytenoids should function normally. Invasion of cartilage, other than that of the epiglottis, is a contra-indication for supraglottic partial laryngectomy. It is possible to remove one arytenoid cartilage and fix the vocal cord on this side to the midline, and at the same time preserve laryngeal function (38,39).

1.4.2.6 (Wide-field) total laryngectomy

In the classical technique of total laryngectomy the plane of resection is directly on the laryngeal skeleton. Small tumor masses may be left behind on the deep surface of the infrahyoid strap muscles. It is stated that the wide-field technique of total laryngectomy should be the procedure of choice in all cases. When tumor infiltration is anteriorly extensive, so that the skin appears tethered, even the wide-field technique is on its own insufficient. In that case the involved wide skin should be also resected (40).

1.4.3 Chemotherapeutical options

Chemotherapy can be administered to a patient as single agent therapy (methotrexaat, bleomycine or cisplatin), combination therapy or combined modality therapy, as an adjuvant to surgery and/ or radiotherapy. Chemotherapy as yet has no significant impact on long term survival and only occasionally offers brief palliation (41,42). Integration of chemotherapy into primary treatment of head and neck cancer is still in an investigational stage.

1.5 THERAPEUTICAL MANAGEMENT

In various countries, traditional choices of treatment still influence the preferential therapeutical procedures. Whereas in the United States surgery is generally the preferred choice of treatment, in England and Canada irradiation treatment is usually favoured. The reported cure rates vary considerably. The difficulty in staging the primary tumor by laryngoscopy or radiographic methods is likely to be one of the main reasons for this disparity.

T1- and T2-glottic carcinomas

The management of T1 glottic carcinomas is basically decided by the need for optimal conservation of the voice (43). Vermund has reviewed the results of both surgery and radiotherapy from more than 20 published reports. High cure rates have been reported with either modality. He concluded that glottic T1N0 lesions can be cured very well by adequate radiotherapy with preservation of the voice (44). Succesful surgical techniques include laryngofissure and cordectomy, partial laryngectomy and CO2 laser surgery (28,36).

For T2-glottic lesions, different cure rates are recorded from different institutions (45). Kirchner reported that cure rates with vertical partial laryngectomy are better than with radiotherapy (71% vs. 35%) (46). Cocke reviewed reports of 15 major centres, and reported less discrepancy between these modalities (73% vs. 61%) (47).

T1- and T2-subglottic carcinomas

Radiotherapy is preferable in small subglottic tumors (9).

T1- and T2-supraglottic carcinoma

T1-supraglottic and selected supraglottic T2-lesions, which meet the above-mentioned criteria, (see 1.4.2.5) are succesfully treated by supraglottic laryngectomy. In general, radiotherapy is the choice of method in the treatment of the other T2 supraglottic lesions (33).

T3- and T4-laryngeal cancer.

The recurrence rate after irradiation therapy is much higher with T3 and T4 lesions than with T1 and T2 lesions (20,44). Therefore in most centres these advanced tumors are treated with surgery. In most instances this will entail a wide-field laryngectomy, often combined with post-operative radiotherapy (20,40,48).

As stated above, partial vertical laryngectomy may be suitable for the occasional fixed-cord lesion that fulfills strict criteria (31,32,33,34). Also, an extended supraglottic laryngectomy has been recommended for selected T3 and T4 supraglottic carcinomas (34).

In contrast, others, like Harwood et al and Snow et al, hold the view that radiation therapy with surgery in reserve is the preferred treatment for T3 glottic cancer, in view of its potential for laryngeal preservation and better quality of life (10,18).

Nodal metastasis

Generally, surgery is favoured over radiation therapy for the treatment of regional lymph node metastasis. Because it is preferred to apply the same procedure of treatment for both the primary tumor and metastatic lymph nodes, the presence of lymphatic spread will favour the option of surgical treatment (10).

REFERENCES

1. Bryce DP. Cancer of the larynx. In: Chretien PB, Johns ME, Shedd DP, Strong EW, Ward PH, eds. Head and neck cancer. Saint Louis: The CV Mosby Company 1985: 194-195.

2. Ali S, Tiwari R, Snow GB, van der Waal I. Incidence of squamous cell carcinoma of the head and neck. J Laryngol Otol 1986;100:315-327.

3. Ogura JH, Spector GJ. The larynx. In: Nealon TF, ed. Management of the patient with cancer. Philadelphia: WB Saunders Company, 1976:206-238.

4. Ogura JH, Thawley Se. Cysts and tumors of the larynx. In: Paperella MM, Shumrick DA, eds. Otolaryngology. Vol III, Head and Neck. 2nd edition. Saunders Co 1980: 2504-2527.

5. Beahrs OH, Myers MH. Manual for staging of cancer. Second edition. Philadelphia: JB Lippincott Company 1983:37-43.

6. Batsakis JG. Neoplasms of the larynx. In: Batsakis JG, ed. Tumours of the head and neck- clinical and pathological considerations. 2nd edition, Williams &Wilkins Co., 1979:135-154.

7. Wynder EL, Bross IDJ, Day E. A study of environmental factors in cancer of the larynx. Cancer 1956;9;86-110.

8. International union against cancer. TNM classification of malignant tumors. Geneva, 3rd edition, 1978, enlarged and revised 1987.

9. Gerritsen GJ. Computed tomography and laryngeal cancer. Academic thesis. Amsterdam: Free University of Amsterdam, 1984.

10. Snow GB, Karim ABMF. Behandeling van larynxcarcinoom. NTvG 1982;126:1096-1100.

11. Ali S, Tiwari RM, Snow GB. False-positive and false-negative neck nodes. Head&neck surgery 1985;8:78-82.

12. Sako K, Pradier RN, Marchetta FC, Pickren JW. Fallibility of palpation in the diagnosis of metastases to cervical lymph nodes. Surg gynaecol obstet 1964;118:989-990.

13. Bocca E. Conservative neck dissection. Laryngoscope 1975;85:1511-1515.

14. Jafek BW. Fiberoptic endoscopy. In: English GM, ed. Otolaryngology. Revised Edition, Harper & Bow, 1982:572-584.

15. Lederman M. Cancer of the larynx. Part 1: natural history in relation of treatment. Br J Radiother 1971;44:521-525.

16. Bryce DP. Management of laryngeal cancer. J Otolaryngol 1979;8:105-108.

17. Karim ABMF, Kralendonk JH, Yap LY, Njo KH, Tierie AH, Tiwari RM, Snow GB, Gerritsen GJ, Hasman A. Int J Radiat Oncol Biol Phys 1987;13:313-317.

18. Harwood AR. Cancer of the larynx. The Toronto experience. J Otolaryngol 1982;11(suppl.11).

19. Lederman M. Radiotherapy of cancer of the larynx. J Laryngol Otol 1970;84:867-896.

20. Gerritsen GJ, Valk J, van Velzen DJ, Snow GB. Computed tomography: a mandatory investigational procedure for T-staging of advanced laryngeal cancer. Clin Otolaryngol 1986;11:307-316.

21. Kirchner JA. Invasion of the framework by laryngeal cancer- Surgical and radiological implications. Acta Otolaryngol 1984;97:392-397.

22. Biller HF, Ogura JH, Pratt LL. Hemilaryngectomy for T2 glottic cancers. Arch Otolaryngol 1971;93:238-243.

23. Kirchner JA, Som ML. The anterior commissure technique of partial laryngectomy: clinical and laboratory observations. Laryngoscope 1975;85:1308-1317.

24. Fletcher GH, Jing BS. The head and neck- an atlas of tumor radiology. Chicago: Year book medical 1968:258-265.

25. Harwood AR, DeBoer G. Prognostic factors in T2 glottic cancer. Cancer 1980;45:991-995.

26. Harwood AR, Tierie AH. Radiotherapy of early glottic cancer. Part II. Int J Radiat Oncol Biol Phys 1979;5:477-482.

27. Strong MS, Laser excision of carcinoma of the larynx. Laryngoscope 1975;85:1286-1289.

28. Neel HB iii, Devine KD, DeSanto LW. Laryngofissure and cordectomy for early glottic carcinoma: outcome in 181 patients. Otolaryngol Head and Neck Surg 1980;88:79-84.

29. Silver CE. Conservation Surgery for glottic carcinoma. In: Silver CE. Surgery for cancer of the larynx 1982:83-121.

30. Croll GA, van den Broek P, Tiwari RM, Manni JJ, Snow GB. Vertical partial laryngectomy for recurrent glottic carcinoma after irradiation. Head&Neck Surgery

1985;7:390-393.

31. Som ML. Cordal cancer with extension to vocal process. Laryngoscope 1975;85:1298-1305.

32. Kirchner J. Som Ml. Clinical significance of fixed vocal cord. Laryngoscope 1971;81:1029-1034.

33. Kirchner JA. Two hundred laryngeal cancers: patterns of growth and spread as seen in serial section. Laryngoscope 1977;87:474-482.

34. Hordijk GJ. De behandeling van larynxcarcinoom. Academic thesis, University of Leiden, 1977.

35. Kirchner JA. Treatment of laryngeal cancer. In: Chretien PB, Johns ME, Shedd DP, Strong EW, Ward PH, eds. Head and Neck cancer. Saint Louis: the CV Mosby company, 1985:199-201.

36. Bailey BJ, Stiernberg CM. Surgical management of advanced laryngeal cancer. In: Chretien PB, Johns ME, Shedd DP, Strong EW, Ward PH, eds. Head and Neck cancer. Saint Louis: The CV Mosby company, 1985:207-212.

37. Som ML, Siver CE. The anterior commissure technique. Arch Otolaryng 1968;87:139-145.

38. Bocca E, Pignataro O, Mosciaro O. Supraglottic surgery of the larynx. Ann Otol 1968;77:1005-1026.

39. Dedo HH. Supraglottic laryngectomy, indications and techniques. Laryngoscope 1968;78:1183-1194.

40. Lam KH. Extralaryngeal spread of cancer of the larynx: a study with whole-organ sections. Head & Neck surgery 1983;5:410-424.

41. Ross WE. General principles for treatment of cancers in the head and neck: chemotherapy. In: Million RR, Cassini NJ. Management of head and neck cancer- a multidisciplinary approach. Philadelphia: JB Lippincott company 1984:97-105.

42. Snow GB, Vermorken JB, Pinedo HM. Adjuvant chemotherapy: the EORTC trials. In: Bloom HJG, Hanham IWF, Shaw HJ, eds. Head and neck oncology. New York: Raven press 1986:83-92.

43. Karim ABMF, Snow GB, Sick HTH, Njo KH. The quality of voice in patients irradiated for laryngeal carcinoma. Cancer 1983;51:47-49.

44. Vermund H. Role of radiotherapy in cancer of the larynx as related to the TNM system of staging. A review. Cancer 1970;25:485-504.

45. Karim ABMF, Snow GB, Ruys PN, Bosch H. The heterogenity

of the T2 glottic carcinoma and its local control probability after radiation therapy. Int J Radiat Oncol Biol Phys 1980;6:1653-1657.

46. Kirchner JA, Owen JR. Five hundred cancers of the larynx and pyriform sinus. Laryngoscope 1977; 87:1288-1303.

47. Cocke EW Jr. Management of malignant neoplasms of the larynx. In: English GM, ed. Otolaryngology. Rev ed. vol. 5. Philadelphia: Harper & Row, 1981, Chapter 34.

48. Bardwil JM. Cancer of the vocal cord. Cancer 1972;29:31-36.

Chapter 2. THE RADIOLOGICAL EXAMINATION OF THE LARYNX

2.1 INTRODUCTION

Radiologists have devised many radiologic procedures of varying complexity over a period of many years to study the normal and abnormal states of the larynx. These include plain films, tomography, fluoroscopy, cinefluorography, xeroradiography and laryngography (1-5). In recent years computed tomography (CT) has been added. The following techniques are most commonly used: conventional tomography (planigraphy), contrast laryngography and computer tomography.

2.2 PHONATION MANOEUVERS

In many radiological techniques, examining the larynx, physiologic manoeuvers, which will test laryngeal functions, have successfully been used. In total, five basic manoeuvers are utilized (1,6):

1. Quiet inspiration results in a maximum amount of abduction of the true and false cords;

2. Phonation E. The patient is told to attempt to say E softly for a prolonged period of time. The true cords are adducted to the midline indicating their mobility and configuration. The false cords become paramedian in position. The laryngeal vestibule will open slightly. The piriform sinuses will be in a slightly distended position.

3. Valsalva manoeuver. In this manoeuver the patients are instructed to inhalate deeply and to squeeze with closed lips. The false and true cords come forcefully together in the midline. The subglottic space changes in configuration from an arched roof to a flattened roof. Any disparity between the two sides becomes significant.

4. In the modified Valsalva manoeuver, the patients are instructed to hold their breath and puff out their cheeks. By expiring against pursed lips with a little bit of air

being exhaled, the true and false cords are paramedian and the piriform sinuses become distended.

5. Phonation during inspiration or "reverse E". The patient is instructed to make noise (any noise) while breathing in slowly. The true cords descend and there is lateral distension of the laryngeal ventricles.

2.3 FRONTAL TOMOGRAPHY

In conventional tomography (or planigraphy) the X-ray tube and the X-ray film are moved in opposite directions so that all points within one specific plane are located in the same position on the film. The structures in this specific plane are sharply defined. The images of the other planes are highly blurred, because the shadows of the structures in these planes are continuously in motion (7).

A frontal tomography often demonstrates the presence of a lateral subglottic lesion of a vocal cord. Occasionally, minimal subglottic extension may be overlooked or be indistinguishable from the deformity caused by a bulky tumor of the cord (6,8). When the ventricle is well demonstrated, cranial extension of a glottic lesion towards the false cord can be excluded; but when the ventricular air shadow is obliterated, the superior extent of the lesion is often underestimated (8).

In the diagnosis of tumors of the false cords, a frontal tomogram often demonstrates thickening of the false cord, obliteration or depression of the ventricle, and enlargement of the adjacent structures when they are involved. However, it can not differentiate a tumor mass from edema, as laryngography may do. Frontal tomography has little to offer in the evaluation of the supraglottic lesion originating from the epiglottis.

2.4 CONTRAST LARYNGOGRAPHY

Laryngography is a radiologic investigation in which the inner side of the larynx and hypopharynx is coated with a

thin layer of contrast medium. With radiographs in antero-posterior frontal and lateral projections during inspiration and phonation, the true and modified Valsalva manoeuvers give good information of endolaryngeal pathology and laryngeal function.

A contrast laryngogram can reveal almost all early tumors of true vocal cords, particularly if the tissues are freely mobile (6,8,9). Thickening and mucosal irregularity of the vocal cord indicate the presence of a tumor. The contrast laryngogram can accurately reveal the presence or absence of subglottic involvement. Any change in the contour of the normal acute subglottic angle indicates the presence of subglottic extension (8).

The ventricle is very well outlined by contrast medium even when it is reduced to a narrow slit (6,8). Normal appearance of the false cords between inspiration and phonation manoeuvers and normal distensibility of the ventricle on reverse phonation manoeuver rule out the possibility of false cord involvement. Fixation of a true cord is well demonstrated by the inspiration and phonation manoeuvers. Contrast laryngography can accurately delineate superficial spread of tumors of the epiglottis or ary-epiglottic folds by showing deformity and distortion of soft tissues and/or mucosal irregularity (8).

However, except for some of the above mentioned blind areas, laryngograms tend to duplicate the information obtained from direct laryngoscopy, particularly with regard to mucosal changes and laryngeal function (6,10). Furthermore, this diagnostic procedure may cause morbidity due to anesthesia and contrast reactions (8).

2.5 COMPUTED TOMOGRAPHY

The contribution of CT to diagnostic imaging is based on two unique properties:

1. The capability of CT to differentiate much smaller differences in radiologic densities than conventional techniques may do;

2. The capability to provide axial images.

CT complements direct laryngoscopy and biopsy better than any other radiologic examination. It provides helpful information about areas that may be hidden from visual inspection by bulky tumors, such as the subglottis, the apex of the piriform sinus and the laryngeal ventricle. It reveals deep extension not visible by other means. CT helps to clarify suspected pathology in submucosal laryngeal structures, where overlapping structures prevent a full two-dimensional evaluation. Furthermore, it demonstrates nodal metastasis not clinically evident (10,11). Caution must be used in diagnosing cartilage invasion by CT because of the random distribution of calcification and ossification within the normal cartilage (12-19). CT only identifies changes in density, and does not permit a histological diagnosis. Consequently, fibrosis or edema in adjacent tissues can simulate malignant extension on CT (20,21). Minor mucosal abnormalities will not be imaged with CT, but this is generally of no clinical importance since such irregularities can be depicted by laryngoscopy. Another shortcoming of CT is its inability to consistently define a transition zone from the true to the false cords. An opened ventricle is not demonstrated by CT in all patients. Spread of the tumor from the false to the true cords, or vice versa, can be difficult to determine on CT (20).

CT fails to demonstrate axial and frontal images in an sufficiently accurate manner. Furthermore injection of contrast material is needed to detect lymphatic spread. There is also some hazard associated with CT scanning in the form of X-ray exposure and the use of intravenous contrast agents.

2.6 CT VERSUS CONVENTIONAL RADIOLOGICAL TECHNIQUES

2.6.1 CT versus conventional tomography

Conventional tomography only gives inferential data concerning the submucosal margins of the tumor. CT is superior in showing cartilage invasion and distortions as well as in showing extralaryngeal extension of the tumor. The diagnostic procedure has largely been supplanted by CT and is regarded as obsolete by some investigators (6,22,23).

2.6.2 CT versus contrast laryngography

In different reports it is stated that CT is more accurate than laryngography in identifying areas of tumor involvement. Deep extension of neoplasms, invading the pre-epiglottic space (PES), paraglottic space (PGS) and the subglottic region can more directly be visualized by CT and need not to be inferred as with laryngography (9,10,14,15). CT provides an additional advantage of direct visualization of laryngeal cartilages (12).

Technologic improvements (narrow collimation, rapid scanning time, thinner slices) in CT equipment have provided the means to carry out detailed studies of the larynx during physiologic manoeuvers. Functional impairment of the glottis and the arytenoid cartilages can readily be detected by obtaining CT scans during rest, E-phonation, forced inspiration and Valsalva-manoeuvers (9,14,15,21,25). It has been stated that the laryngeal ventricle is seen in essentially all patients, employing 2 mm thick sections with and without E-phonation (21). Moreover, CT is cost-competitive with laryngography (20). The patient can be positioned comfortably and no anesthetic is needed.

Laryngography will be more reliable in detecting small mucosal exophitic growths. However, information obtained by laryngography mostly duplicates findings which are obtained by laryngoscopy. It is concluded by different authors that contrast laryngography is now obsolete (22,24), or to be regarded as an unusual diagnostic procedure (9,10,20,21,23,24).

Conventional radiological techniques are available as "fall back" options if necessary. Conventional modalities might still be performed in patients in whom clinical circumstances make it possible to perform direct laryngoscopy under general anesthesia. If a CT scan cannot be performed because of excessive patient motion or unfavourable habitus, one can revert to other diagnostic modalities (23).

REFERENCES

1. Landman GHM. Laryngografie en cinelaryngografie. De toepassing van contrastmiddelen in de rontgendiagnostiek van de larynx. Academic thesis. Nijmegen: University of Nijmegen, 1966.

2. Doust BD, Tig VM. Xeroradiography of the larynx. Radiology 1974;110:727-730.

3. Fabrikant JI, Dickson RJ. The use of cinefluorography for the radiologic examination of the larynx and hypopharynx in cases of suspected carcinoma. BJR 1965;38:28-38.

4. Pastore RN, May M, Gildersleeve GA. The laryngopharyngogram as a diagnostic aid. Laryngoscope 1964;74:723-737.

5. Woener ME, Braun EJ, Sander I. Xeroradiographic zonography of larynx and hypopharynx. Ann Otol Rhinol Laryngol 1974;83:42-48.

6. Hanafee WN. Radiography of the pharynx and the larynx. In: Valvassori GE, Potter GD, Hanafee WN, Carter BL, Buckingham RA, eds. Radiology of the ear, nose and throat. Stuttgart- New York: Georg Thieme Verlag Stuttgart- New York 1982:242-301.

7. Ziedses des plantes BG, Westra D, Penn WM. Methods of examination. In: van Voorthuisen AE, ed. Textbook of radiodiagnosis. Oxford: Oxford university press. 1979: 28-43.

8. Jing BS. Malignant tumors of the larynx. In: Radiol Clin North Amer 1978;16:247-260.

9. Archer CR, Sagel SS, Yeager VL, Martin S, Friedmann WH. Staging of carcinoma of the larynx: comparative accuracy of CT and laryngography. AJR 1981;136:571-575.

10. Mancuso AA, Hanafee WN. A comparative evaluation of computed tomography and laryngography. Radiology 1979;133:131-138.

11. Mancuso AA, Maceri D, Rice D, Hanafee WN. CT of cervical lymph node cancer. AJR 1981;136:381-385.

12. Archer CR, Yeager VL. Evaluation of laryngeal cartilages by computed tomography. J Comput Assist Tomogr 1979;3:604-611.

13. Yeager VL, Lawson C, Archer CR. Ossification of laryngeal cartilages as it relates to computed tomography. Invest Radiol 1982;17:11-19.

14. Gerritsen GJ. Computed tomography and laryngeal cancer. Academic thesis. Amsterdam: Free University of Amsterdam, 1984.

15. Von Zaunbauer W, Haertel M. Zur computertomographischer diagnostik maligner larynxtumoren. Fortschr Geb Rontgenstr Nuklearmed Erganzungsband 1982;136:694-699.

16. Archer CR, Yeager VL, Herbold DR. CT versus histology of laryngeal cancer. Their value in predicting laryngeal cartilage invasion. The laryngoscope 1983;93:140-147.

17. Hoover LA, Calcaterra ThC, Walter GA, Larsson SG. Preoperative CT scan evaluation of laryngeal carcinoma: correlation with pathologic findings. The laryngoscope 1984;94:310-315.

18. Silverman PM, Bossen EH, Fisher SR. Carcinoma of the larynx and hypopharynx: computed tomographic-histopathologic correlations. Radiology 1984;151:697-702.

19. Mafee MF, Schild JA, Valvassori GE, Capek V. Computed tomography of the larynx: correlation with anatomic and pathologic studies in cases of laryngeal carcinoma. Radiology 1983;147:123-128.

20. Sagel SS, AufDerHeide JF, Aronberg DJ, Stanley RJ, Archer CR. The laryngoscope 1981;91:292-300.

21. Scott M, Forsted DH, Rominger CJ, Brennan M. Computed tomograpic evaluation of laryngeal neoplasms. Radiology 1981;140:141-144.

22. Ward PH, Hanafee WN, Mancuso AA, Shallit J, Berci G. Evaluation of computerized tomography, and laryngography in determining the extent of laryngeal disease. Ann Otol 1979;88:454-462.

23. Mancuso AA, Hanafee WN. Larynx, hypopharynx, and cervical nodes- malignant tumors. In: Mancuso AA, Hanafee WN. Computed tomography of the head and neck. Baltimore/London: Williams & Wilkins, 1982:26-38.

24. Friedman WH, Archer CR, Yeager VL, Katsantonis GP. CT versus laryngography: a comparison of relative diagnostic

value. Otolaryngol Head Neck Surg 1981;89:579-586.

Chapter 3. GENERAL ASPECTS OF MAGNETIC RESONANCE IMAGING

3.1 INTRODUCTION

The new diagnostic image modality, magnetic resonance imaging (MRI), receives a great deal of attention in the medical community. The reason for this is the capability of MRI to generate high resolution images with excellent soft tissue contrast in all planes of the human body without ionizing radiation. The high contrast levels make the use of contrast agents unnecessary in most instances.

In 1946, Felix M. Bloch and Edward M. Purcell published independently their observations on Nuclear Magnetic Resonance (NMR). The idea of magnetic resonance resulted from the observation that energy is absorbed and subsequently released by nuclei at specific frequencies following excitation by radiofrequency (RF) electromagnetic energy (1,2). In 1973 magnetic resonance imaging was developed, thanks to the work of Paul C. Lauterbur, who introduced linear gradients for spatial localization of the NMR signal (3).

3.2 TECHNICAL CONSIDERATIONS

3.2.1 Magnetic properties of atomic nuclei

Magnetism is the result of the motion of electric charges. Electric charges, like electrons, can produce a magnetic field by their intrinsic spin movement, which can be visualized as a rotation of the electrons around a central axis. The particles that compose the atomic nucleus, both the protons and neutrons, also have a "spin" and an electric charge. Nuclei with odd numbers of protons, neutrons, or both have a magnetic moment. If these nuclei are placed in an external magnetic field, they will have a tendency to align with the field. Magnetic moments of atomic nuclei can only adopt a few discreet orientations in the external magnetic field.

Protons, the nuclei of hydrogen atoms, have two possible energy states in the external static magnetic field. The lower energy state is associated with a nuclear magnetic moment pointing along the field (parallel) and the higher one with the antiparallel direction. Given the fixed values of the magnetic moments of each type of nucleus, and a fixed magnetic field strength, the transition between states involves an exact amount of energy; the stronger the field the higher the energy.

3.2.2 Resonance

Transitions between parallel and antiparallel states can occur if the right amount of energy is absorbed or released. Because the interaction is with a magnetic element, the necessary energy can be provided by a magnetic field. One way to obtain such a field is by utilizing electromagnetic radiations. These consist of photons of energy, proportional to frequency.

The equation f=1/(2.pi).gamma.(Ho) should be considered as a "resonance condition": the protons can change their orientation if the frequency f of the radiation and the magnitude Ho of the magnetic field fit each other. If this is not the case, the radiation has little or no effect (4). When the nuclei, originally in the parallel state, are irradiated at the resonant frequency they can adopt the antiparallel stand. When they return to the equilibrium (if the field is unchanged) they will emit energy at the same frequency.

3.2.3 Behavior of a sample of nuclei

It is practical to consider the magnetic moments of a sample of nuclear spins in stead of that of a single one. At room temperature and in the absence of a magnetic field, the nett magnetization vector is zero. If the external magnetic field of the main magnet is applied to the sample

of nuclei, the nett magnetization vector points along the field; its length is proportional to the number of nuclei in the sample and the field strength. The length and direction of this vector characterize the equilibrium magnetization M of the sample, that is, the state that it will revert to after being disturbed if enough time is allowed to pass. The vector can be disturbed from the equilibrium and will align with the nett field, by application of a second external magnetic field which is superimposed on the first one. When the second field is removed, the nett magnetization returns to the equilibrium and the nuclei release the stored energy to the environment as radiofrequency (RF) energy. The field along the main magnet is called the longitudinal field and the component of the nett magnetization along the main magnet is called the longitudinal magnetization Ml. The superimposed field is called the axial field and the component of the nett magnetization, orthogonal to the longitudinal field, is called the axial magnetization Ma.

If the axial field is switched rapidly by radiofrequent irradiation emitted by a transmitter coil, Ml is reduced from its equilibrium value. The intensity and duration of the RF pulse determines the magnitude of the flip angle, e.g. 90 or 180 grades (a 90-pulse or 180-pulse). After a 90-pulse the longitudinal magnetization has changed into axial magnetization. The magnetization will return slowly to its equilibrium value in a relaxation process, which can be characterised by tissue parameters: T1- and T2-tissue characteristics. Longitudinal magnetization Ml begins to grow again towards its equilibrium value M. The growth is exponential with a time constant T1, so that Ml=M.(1-exp(-t/T1)), where t is the time since irradiation. During this process Mt decays exponentionally with a time constant T2, so that Mt=M0.exp(-t/T2), where M0 is the value of Mt immediately after irradiation. T2-value can never be longer than T1-value.

The signal, obtained from hydrogen nuclei at the same field strength, is much higher than that from an equal number of other nuclei. The nucleus which is used for MRI is the hydrogen atom, and because the nucleus of the hydrogen atom contains only a single proton the technique of MRI may be referred to as proton MRI.

3.2.4 Proton density, Tissue-characteristics.

As stated above, RF stimulation by a RF transmitter coil causes the nuclei to absorb energy, lifting them to an excited state. The nuclei in their excited state can return to the ground state only by dissipating their excess energy to the lattice. This process is termed T1- or spin-lattice relaxation. In the T2 relaxation process, no energy is transferred from the nuclei to the lattice. Rather, the nuclei in the excited and equilibrium state exchange energy with each other. It is the rate of loss of axial magnetization that determines the relaxation time.

When a RF pulse interacts with protons, its absorption is basically proportional to the proton density. However rather than differences in proton density, the T1- and T2-tissue characteristics are the primary determinants of relative contrast in MR images. The protons giving rise to an MRI signal are mainly those in water and lipid. Protons in large biological macromolecules such as proteins and DNA, and those in solid structures, e.g. bone, have such tissue characteristics, so that these protons usually do not contribute to the signal (5,6). Fat consists of approximately 50%-80% lipid and 10%-30% water, whereas the other soft tissues consist of approximately 70%-80% water and 5%-10% lipid (7).

Medium sized molecules, such as lipids, relax faster than small molecules, such water, and macromolecules. Efficient relaxation is consistent with short T1-relaxation times. For instance, in fat, T1 is of the order of a few hundreds of milliseconds, whereas in pure water, it is about 3 seconds. The relaxation time is indirectly related to the field strength of the main magnet field. For this reason, when T1 relaxation times are reported, the field strength

must be indicated. In contrast, T2-relaxation is less susceptible to the magnitude of the external field. T2-relaxation is more efficient in large molecules. Typically, T2 values in biologic tissue have a range from about 50 to 150 ms (8).

Although free water relaxes slowly due to long relaxation time, the water in biologic tissue is found to relax much faster, typically with relaxation times of several hundred milliseconds. A fraction of this water in tissue is bound to the surface of proteins. Fast equilibrium exists between free and bound water (9). This equilibrium is probably disturbed in certain pathologic conditions. The elevated T1 and T2-tissue characteristics, found in tumors, may be caused by a release of bound water with a concomitant increase of the free water fraction (8,10).

3.2.5 Spin Echo

The MR imaging techniques now in use are saturation recovery, inversion recovery and spin echo. The latter technique is probably the most useful type of MR Imaging mode from the point of clinical utility (4).

In the Spin Echo (SE) technique both T1 and T2 relaxation times contribute to the signal intensity and thus to the contrast. A short time (T') after a 90 grades pulse, a 180 grades pulse is applied to the tissue. In abbreviated form the SE sequence can be expressed as (90-T'-180-T''-90 etc.), at which repitition time (TR) can be defined as T'+T'' and echo time (TE) as 2xT' (4).

Manipulation of equations permits an insight into the dependence of the MRI signal intensity on intrinsic (proton density,T1,T2) and operator-selectable (TE,TR) parameters. The dependence of the MRI signal intensity I on these parameters can be shown to be:
$I=N(H)f(v)\exp(-TE/T2)(1-\exp(-TR/T1))$. This equation shows that image intensity is dependent on the proton density N(H), relaxation times (T1 and T2), repetition (TR), and echotime (TE). From the above equation it can be inferred

that the SE signal intensity increases when:
1. T1 decreases
2. T2 increases.

The effects on signal intensity, when the pulse timing parameters are changed, can now be evaluated. If repitition time (TR) is long compared to the longest T1 tissue-relaxation times, then the exp(-TR/T1) approaches zero. The signal intensity becomes independent of T1 since the magnetization for all protons has completely recovered at the time of the new 90 grades excitation pulse. In this case, the signal is only modulated by T2-relaxation processes and possibly by proton density. So called T2-weighted images should have a repetition time of at least 2000ms and an echo time of at least 100ms. If, on the other hand, the echo time (TE) is shortened relative to T2, then exp (-TE/T2) approaches unity. Under these conditions the signal intensity is only related to T1. So called T1-weighted images should have a repitition time, equal to the T1-relaxation time (about 500ms) and an echo time as small as possible (11).

3.2.6 Signal-to-noise ratio

The method of improving the signal-to-noise ratio consists of data averaging. When an MRI experiment is repeated and the MR signals obtained are recorded each time, the MR signals will add up. The random noise signals will also add up, but at a slower rate because of the statistical nature of the noise. For "NxN" data averaging runs, the nett increases of signal-to-noise ratio will be "N".

On images acquired with longer echo times (T2-weighted images vs. T1-weighted images) the MR signal intensity gradually decreases. This decrease in intensity is a manifestation of the signal diminution caused by T2 decay. An adjustment of the relative brightness ("level" adjustment) is usually made to equalize the overall brightness of the images. Although the intensity of all

tissues decreases in each successive echo, the signals from those tissues with long T2 values decay more slowly than those from tissues with short T2 values. After brightness adjustment, the region consistent with a long T2 will have higher absolute intensity in the later echoes, as compared to the intensity in earlier echoes. With lengthening of the echotime, the overall signal-to-noise ratio also decreases. For this reason, images of higher echo order become progressively noisier.

3.2.7 RF antennas.

Imagers may use two antennas, one as transmitter and one as receiver, or a single antenna switching between the transmitter and the receiver mode. Since the RF magnetic field has to be 90 grades to the main field, the antenna shape varies according to the direction of the main magnetic field with respect to the body axis. If the direction of the main field is perpendicular to the axis, a solenoidal antenna can be used. If it is along the axis, as in superconductors, saddle-shaped antennas are used. There are also variations of these shapes. It has been stated that solenoidal antennas are two or three times more sensitive than saddle-shaped ones (12). Were this to be the case, magnets that provide fields that cross the body axis would become favoured. However, from other investigations it is reported that using equal antenna aperture and length, both antennas provide equal signal-to-noise ratio (13).

Coils which are placed on the body nearest to the organ of interest, so-called surface coils, are a recent welcome addition. They are typically circular or elliptical. The proximity of the antenna to the region of interest and its small sensitive volume, realizes a larger signal-to-noise level, at the expense of the uniformity and the magnitude of the imaged volume.

As the strength of the field increases, it becomes more difficult to obtain efficient antennas unless their size is decreased. Consequently, uniformity and magnitude of the imaged volume will be less (13).

3.3 DISADVANTAGES OF MRI

3.3.1 Claustrophobia

The long barrel of the magnet induces claustrophobia in about 1%-5% of the patients, who consequently refuse to complete the study. Dyspnoeic patients may find the enclosed space inside the imager claustrophobic. Sedation may be a help, but most often gentle persuasion is the best policy.

3.3.2 Artifacts

Although with MR imaging no streaking artifacts are found, as with CT scanning, several other factors may degrade image quality:

1. Due to the long scanning times (approximately 2-8 minutes), patient movement and blood flowing in vascular structures causes both blurring of the image and ghost images in the phase-encoded axis of the image (14). However, MRI may be less sensitive than CT to small intermittent motion artifacts.
2. Ferromagnetic or paramagnetic materials such as dental stainless steel, "crowns" and hearing aids may produce artifacts in MR images. The MR image distortion caused by a magnetic material arises from the disruption of the magnetic field and, therefore, a disruption in the relationship between position and frequency which is necessary for accurate image reconstruction. Consequently, a magnetic object in MRI may cause an artifact, even when it is located outside the slice since the field lines passing through the region being imaged are distorted (15).

3.3.3 Contra-indications

MRI examination is contra-indicated for patients, bearing:

1. A pacemaker, which may be affected by the electrical fields generated during imaging, in particular from the gradient fields. The electric fields may cause problems in the pacing unit and thus give rise to false pacing signals. This is an obvious and easily avoidable hazard and nobody with a pacemaker should be allowed near the magnet (16). Another hazard is the force which is exerted on the pacemaker by the static magnetic field. This may cause the patient much discomfort and even harm (12).
2. Aneurysm clips. Any patient with a history of intracranial aneurysm must be carefully examined. Many of the clips used in clipping these aneurysms are ferromagnetic and move in a magnetic field. The risk of detachment of these clips increases with the magnitude of the static field employed.

From experiments with seven different types of widely used metallic stapedectomy protheses, Applebaum and Valvassori concluded that there is no apparent danger that these protheses become displaced in stapedectomy patients subjected to the electromagnetic fields of MRI units (17).

It is considered safe to image patients with a history of epilepsy or cardiac arrhythmias.

REFERENCES

1. Bloch F, Hansen WW, Packard M. Nuclear induction. Phys rev 1946;69:127-131.

2. Purcell EM, Torrey HC, Pound RV. Resonance absorption by nuclear magnetic moments in a solid. Phys rev 1946;69:37-42.

3. Lauterbur PC. Image formation by induced local interactions: examples employing NMR. Nature;242:191-192.

4. Valk J, MacLean C, Algra PR. Basic principles of nuclear magnetic resonance imaging. Amsterdam: Elsevier, 1985.

5. Wehrli FW, MacFall JR, Shutts D, Breger R, Herfkens RJ. Mechanisms of contrast in NMR Imaging. J Comput Assist Tomogr 1984;8(3):369-380.

6. Young IR, Burl M, Clark GJ, et al. Magnetic resonance properities of hydrogen: imaging the posterior fossa. AJR 1981;137:895-901.

7. Davis PL, Kaufman L, Crooks LE. Tissue characterization. In: Margulis AR, Higgins CB, Kaufman L, Crooks LE, eds. Clinical magnetic resonance imaging. San Francisco, 1983.

8. Wehrli FW, MacFall JR, Glover GH, Grisby N. The dependence of nuclear magnetic resonance (NMR) image contrast on intrinsic and pulse sequence timing parameters. Magnetic Resonance Imaging 1984;2:3-16.

9. Hazelwood CF. A view of the significance and understanding of physical properities of cell-associated water. In: Drost-Hansen W, Clegg J. Cell-associated water. New-York: Academic press,1979.

10. Mansfield P, Morris PG. NMR Imaging in biomedicine. New York:Academic press, 1982:29-30.

11. M. Sprenger. Personal communication.

12. Hoult DI, Richards RE. Signal-to-noise ratio of nuclear magnetic resonance experiment. J Magnet Reson 1976;24:71.

13. Kaufman L, Crooks LE. Instrumentation. In: Margulis AR, Higgins CB, Kaufman L, Crooks LE. Clinical magnetic resonance imaging. Radiology research and education foundation. San Francisco. 1983:31-39.

14. Kean D. Practical aspects of clinical imaging. In: Kean D, Smith M. Magnetic resonance imaging-principles and applications. William heinemann medical books. London. 1986:70-75.

15. Pavlicek W, Geisinger M, Castle L, Borkowski GP, Meany TF, Bream BL, Gallagher JH. The effects of NMR on patients with cardiac pacemakers. Radiology 1983;147:149-153.

16. Anonymous. Safety of nuclear magnetic resonance imaging. Lancet 1980;2:103.

17. Applebaum EL, Valvassori GE. Effects of magnetic resonance imaging fields on stapedectomy protheses. Arch Otolaryngol 1985;820-825.

Chapter 4. MAGNETIC RESONANCE IMAGING OF THE NORMAL LARYNX

Authors: J.A. Castelijns (B.Sc., M.B.) (1)
J. Doornbos (Ph.D) (1)
B. Verbeeten, Jr (M.D.) (2)
G.J. Vielvoye (M.D.) (1)
J.L. Bloem (M.D.) (1)

(1) Dept. of Diagnostic Radiology
University Hospital
Leiden

(2) Dept. of Diagnostic Radiology
Academic Medical Centre
Amsterdam

Institution: Dept. of Diagnostic Radiology 30a
University Hospital
Rijnsburgerweg 10
2333 AA Leiden
The Netherlands

Abstract

Magnetic resonance imaging of the larynx was performed on 15 volunteers. Searching for optimal images in the sagittal, frontal and axial planes, we compared images made with a special surface coil and the standard head coil, images with different slice thicknesses, images with different repetition times (TR) and images with different matrices. The field of view and the scan times were kept as small as possible. Using a surface coil, we obtained high resolution images in all three planes. These images provide clinically relevant information, not shown by current radiological techniques: hyoepiglottic ligament, thyrohyoid ligament, thyroepiglottic ligament and cricothyroid ligament, the borders between the preepiglottic space and both paraglottic spaces (PGS), the borders between both PGS and thyroid cartilage, and the vocalis and thyroarytenoid muscles. Short TR is preferred because, with shorter scan time, more measurements could be made. Images with a 128 x 128 matrix size had a much better signal-to-noise ratio than images with a 256 x 256 matrix size. Magnetic resonance has great potential in imaging normal and pathological anatomy of the larynx.

Index Terms : Ligaments-Larynx, anatomy-Nuclear magnetic resonance.

In the diagnostic work-up of patients with laryngeal neoplasms the conventional techniques (i.e., soft tissue radiography, frontal tomography, and contrast laryngography) are of great value. However, they do not give a detailed delineation of tumor invasion or destruction of the laryngeal framework and of invasion in specific areas important for planning therapy (1).

The fundamental value of Computer Tomography (CT) in the diagnosis of laryngeal cancer is its ability to visualize tumor extension in the axial plane. CT is therefore important for visualization of tumor infiltration into the preepiglottic space (PES), the thyroid cartilage, and the extralaryngeal soft tissues. The use of CT in the visualization of the paraglottic space (PGS), the anterior commissure region, and the subglottic larynx appears less important(1). Frontal and sagittal reconstructions obtained from standard 5 mm thick sections have not added significant information. Thin-section multiplanar reconstructions of CT images yields improvement in spatial resolution of the epiglottis and PES (2). To our knowledge CT has not succeeded in imaging ligaments, the partition membrane between PES and PGS, or the vocalis and thyroarytenoid muscles: all clinically relevant structures. Furthermore, the contrast between the PGS and the thyroid cartilage obtained by CT is not optimal (3).

Since magnetic resonance (MR) is able to produce high contrast images in any desired plane, this modality has great potential in displaying normal and pathological laryngeal anatomy. In the present paper we optimize laryngeal MR images, using standard MR techniques and a specially designed radiofrequency coil. We also describe in detail the normal anatomy of the larynx in sagittal, frontal, and axial planes. The potential of MR to improve the diagnosis of different modes of invasion of laryngeal cancer will be discussed.

MATERIALS AND METHODS

Magnetic resonance imaging of the larynx was performed on 15 volunteers whose age varied between 22 and 60 years, with an average of 30 years. All persons were healthy and had no known trauma of the larynx. Images were obtained with a 0.5 T MR system (Philips Gyroscan S5). Sagittal, frontal, and axial slices were made using the standard 30 cm aperture head coil as well as a single turn, saddle-shaped, surface coil placed adjacent to the larynx as a receiver antenna. Recent literature reports on the use of surface coils (4-7).

Single slice scanning, multiple slice scanning two-dimensional Fourier transform (2DFT), and volume acquisition three-dimensional Fourier transform (3DFT) were utilized. The slice thickness was 3 mm (3DFT), 4 mm (2DFT, single slice), or 5 mm (2DFT, multiple slice). Images with 128x128 matrix were compared with images with 256x256 matrix for different planes. Gradient zooming was used to keep the field of view as small as possible (125x125-180x180 mm). Spin echo (SE) images were acquired with repetition time (TR) varying from 250 to 2,000 ms using echo time (TE) =50, 100, and 150 ms (multiecho technique). To compare the practical applicability of the various TR values, the total acquisition time was kept constant, e.g., TR = 250 ms applied with eight measurements requires the same amount of time as TR = 2,000 ms with one measurement. The phase-encoding gradient direction, which is standard left-to-right, was changed in the axial scanning in some images to the anteroposterior direction. Few images were obtained with the inversion recovery (IR) technique (IR, inversion time = 400 ms, TR = 1,400 ms, TE = 50 ms).

RESULTS AND DISCUSSION

Sagittal MR Anatomy

The cricoid cartilage, thyroid cartilage, and the greater

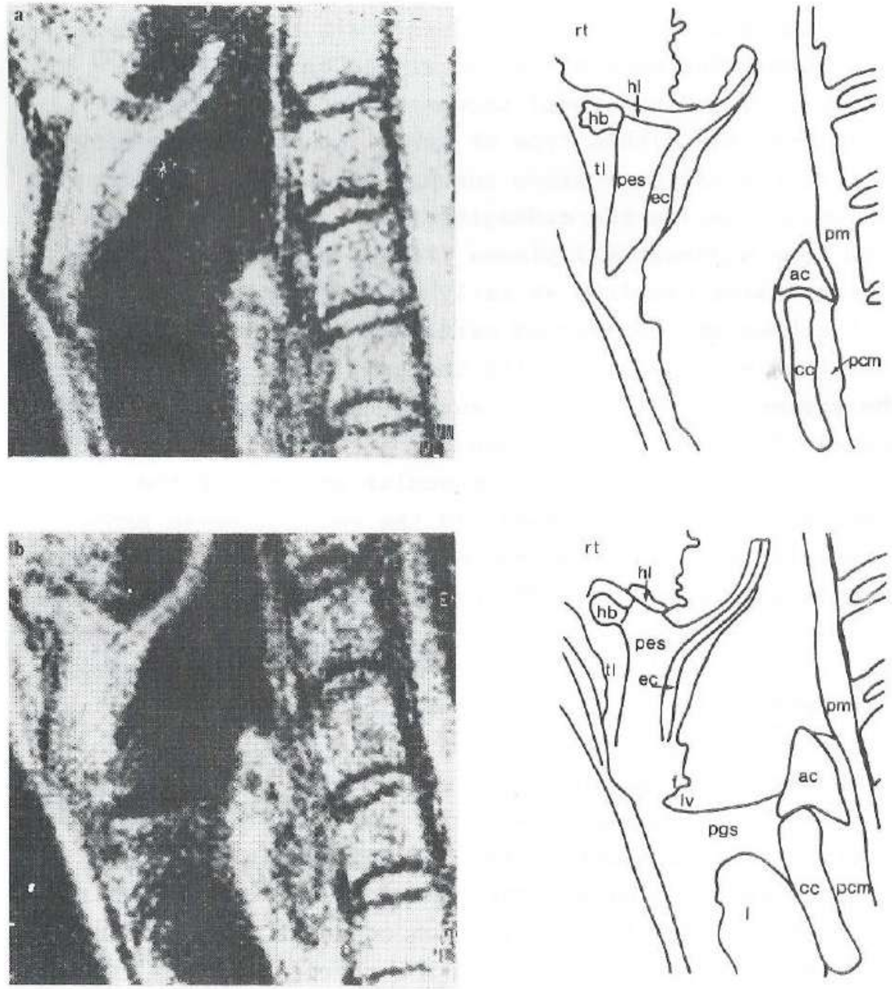

FIG.1.
A: Parasagittal images of a 31-year-old man; distance off center: 3mm; field of view: 180x180mm; slice thickness: 5mm; measurements: 2; SE: 1,000/50; matrix: 256x256. Standard head coil. Single slice.
B: Similar to (a); distance off center: 6mm.
For key to abbreviations in schemes see appendix.

part of the arytenoid cartilage consist of hyaline cartilage and are subject to ossification like all hyaline structures. The epiglottic cartilage, corniculate cartilages, and the vocal processes consist of yellow fibrocartilage ; this type of cartilage does not ossify (8). In the sagittal plane surveys of laryngeal structures are only shown in the midsagittal and parasagittal (within 8 mm from midsagittal) planes (Figs.1 and 2). The hyoid bone, already ossified at early age, the cricoid cartilage, the isthmus of the thyroid cartilage (Fig.2), the freestanding epiglottis with the epiglottic cartilage, and the arytenoid cartilage can easily be recognized (Figs.1 and 2). Nonossified cartilage has a fairly low intensity (SE 500/50, SE 250/50). The muscular process of the arytenoid projects backward and the vocal process projects ventrally (Fig. 1b). The posterior surface of the cricoid cartilage is covered by the posterior cricoarytenoid muscle. The latter muscle is separated from the inferior constrictor pharyngis muscle by the collapsed hypopharynx.

The PES is triangular in the sagittal plane (Figs.1 and 2). Its anterior wall is formed by the hyoid bone, the hyoid membrane, and the upper wall of the thyroid cartilage; the posterior wall is the epiglottic cartilage. Anterior to this membrane the thyrohyoid ligament is situated in the midline. The superior wall of the PES is the hyoepiglottic ligament, which connects the hyoid bone with the epiglottic cartilage. The thyroepiglottic ligament connects this cartilage with the back of the thyroid cartilage. The cricothyroid ligament is visualized in Fig.2. The MR images of ligaments have a low intensity (SE 1,000/50). The two lateral PGSs are filled with loose areolar tissue and the PES is filled with more dense connective tissue, including collagen bundles between mucous glands (9). The PGS has a high intensity (SE 250/50), the PES has a fairly high intensity (SE 1,000/50, 500/50, 250/50). Parasagittal (Fig. 1b) sections of the PGS contain the true vocal cord, which connects the vocal process of the arytenoid with the back of the thyroid

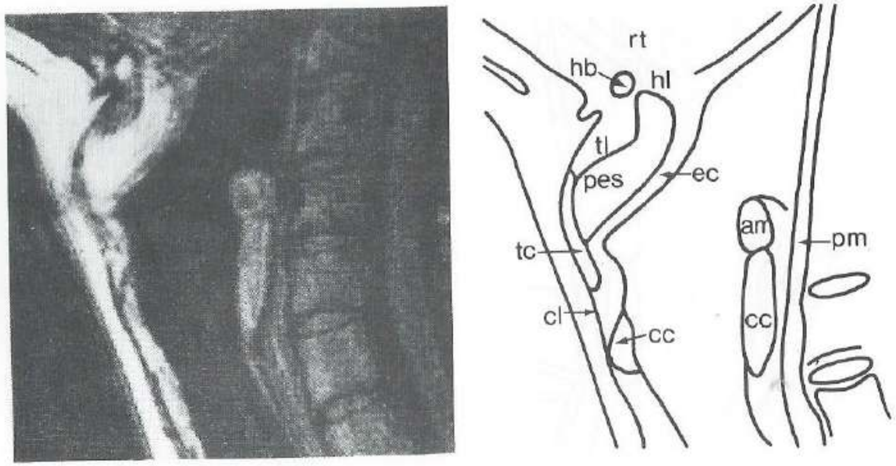

FIG.2.
Midsagittal image of a 25-year-old man; field of view: 170x170mm; slice thickness: 5mm; measurements: 4; SE: 500/50; matrix: 128x128. Surface coil. Single slice. For key to abbreviations in scheme see appendix.

APPENDIX

Index to abbreviations in figures:
ac, arytenoid cartilage; af, aryepiglottic fold; am, arytenoid muscles: ca, common carotid artery; cc, cricoid cartilage; cl, cricothyroid ligament; coc, corniculate cartilage; e, epiglottis, ec, epiglottic cartilage; f, false vocal cord; hb, hyoid bone; hl, hyoepiglottic ligament; shc, superior horn of cartilage; ihc, inferior horn of cartilage; im, infrahyoid muscles; jv, internal jugular vein; lm, lateral cricoarytenoid muscle; lv, laryngeal ventricle; pcm, posterior cricoarytenoid muscle; pes, preepiglottic space; pf, piriform fossa; pgs, paraglottic space; pm, constrictor pharyngis muscle; rt, root of the tongue; sm, sternocleidomastoid muscle; sv, superior laryngeal vein; tc, thyroid cartilage; tel, thyroepiglottic ligament; tg, thyroid gland; tl, thyrohyoid ligament; tme, thyrohyoid membrane; vb, vertebral body; vn, vagus nerve; vtm, vocalis/thyroarytenoid muscle.

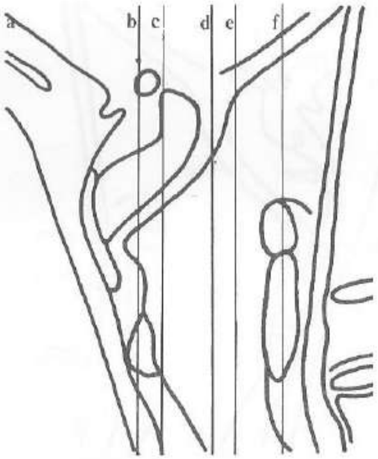

FIG.3.
A: Levels at which frontal images were taken.
B-F: Frontal images of man; level shown on (A); field of view: 125x125mm; slice thickness: 4mm; measurements: 2; SE 250/50; matrix 128x128. Surface coil. Single slices.
For key to abbreviations in schemes see appendix.

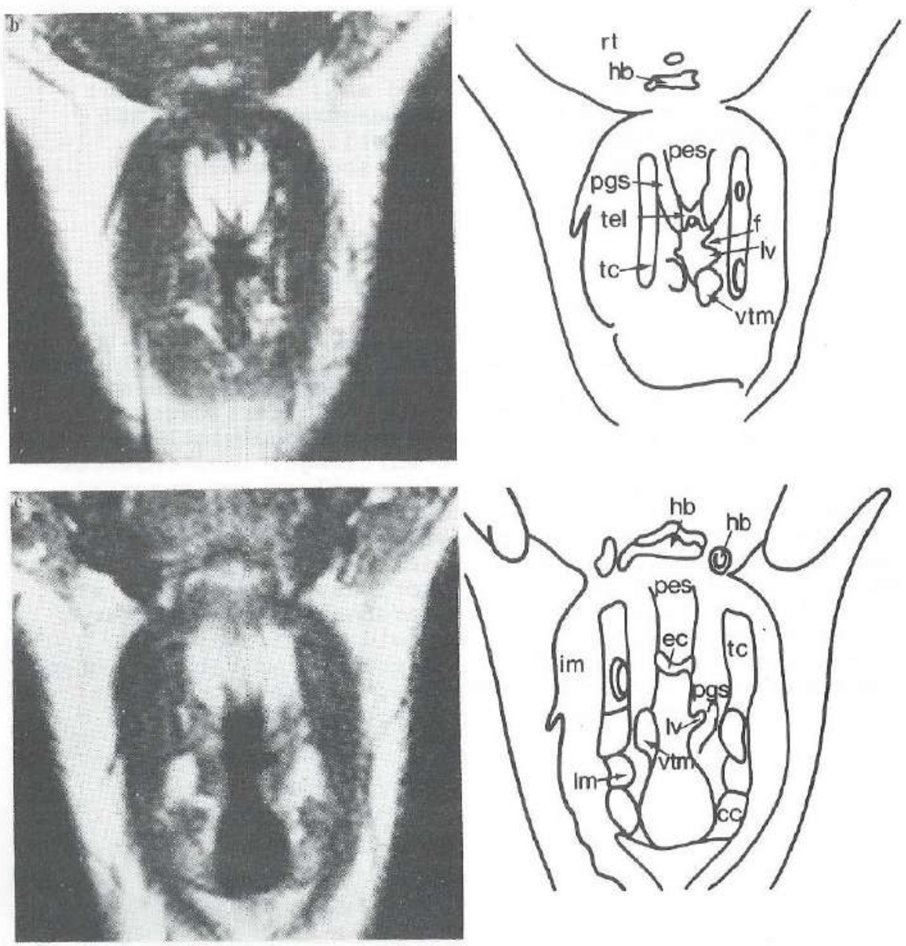

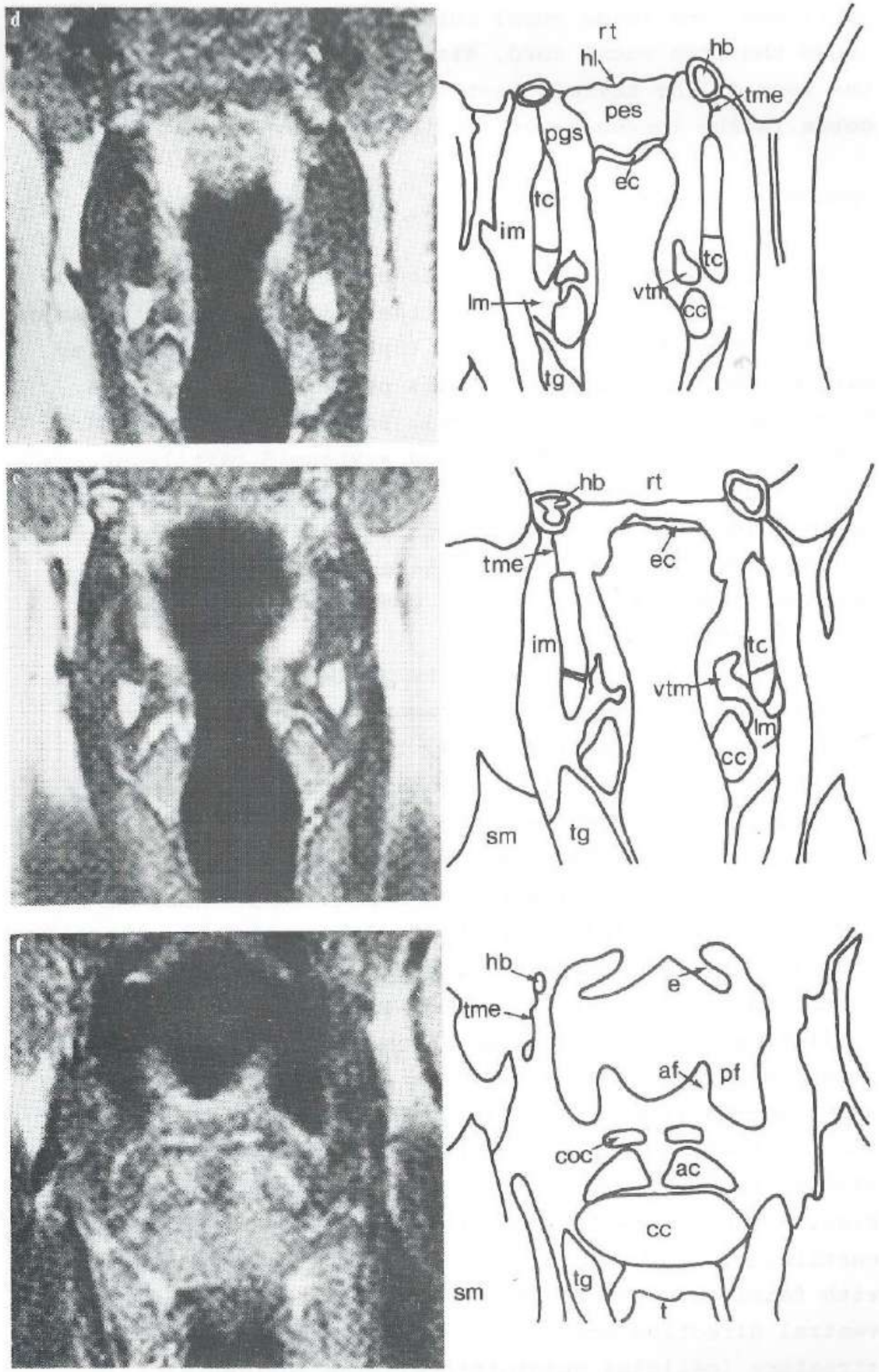

cartilage. The false vocal cord (Fig. 1b), which is found above the true vocal cord, also connects the arytenoid with the back of the thyroid cartilage. Between the two vocal cords is the laryngeal ventricle.

Frontal MR anatomy

Frontal images were taken perpendicular to the plane of the vocal cords. In Figs. 3c-e the cricoid arch is shown as a fairly bright oval structure (SE 250/50). The superior part of the cricoid cartilage is ossified in this case (Figs. 3d and e; age, 25 years). In Fig.3f the cricoid lamina is visualized. The paired arytenoid cartilages are located at the lateral part of the superior border of the lamina. The apex of each arytenoid is surmounted by a small conical cartilage: the corniculate cartilage. The arytenoids are situated in the posterior parts of the aryepiglottic folds.

The thyroid cartilage consists of two laminae, 3 cm in height, and the connection between these, the isthmus, which lies in the medial plane. In Fig.3b the thyroid cartilage is recognizable on both sides as two linear, vertical, partly ossified structures. Figures 3c-e show the caudal part of the thyroid cartilage as an ossified structure; the cranial part has the low signal intensity of cartilage. Ossification of the caudal part of the thyroid cartilage is in accordance with the ossification pattern described by Chievitz (8). The signal intensity of the hyaline cartilage is similar to that of the laterally situated infrahyoid muscle. This similarity is consistent with reports in other areas (10). The body of the hyoid bone is visible in Figs. 3b and 3c; bone marrow has high signal intensity and cortex has a low signal intensity. In Figs. 3c-f the greater horn is shown. The epiglottic cartilage is shown in Figs. 3c-f as a wing-shaped structure with fairly low signal intensity. This cartilage narrows in ventral direction and Fig. 3b shows it as a dotlike structure (petiolus epiglottidis). The thyroepiglottic ligament fills up the greater part of the low intensity structure.

The PES and both PGS are visible in Figs. 3b-d. At the supraglottic region the space enclosed by the thyroid laminae is divided into three compartments: the two lateral PGS and the medial PES. The PGS extends inferiorly along the thyroid cartilage and becomes part of the glottic region. The cricoarytenoid and vocalis muscles occupy the inferior portions of the PGS (Figs. 3b-e). The PES has a lower signal intensity than the PGS. The hyoepiglottic ligament is situated in the midline of the clearly imaged border between the above-mentioned spaces and the root of the tongue.

The false vocal cord (superior to the laryngeal ventricle) and the true vocal cord can be identified as two separate structures (Figs.3b and c). The vocal cords are normally seen in an abducted position during quiet breathing. In Fig.3b the true vocal cords (low signal intensity, SE 250/50) meet each other in the anterior commissure. The false vocal cords contain mainly adipose tissue and therefore show up bright (11) (Figs.3b-e, SE 250/50). In Figs. 3c-e the thyroarytenoid muscle (lateral part), the vocal muscle (medial part), and the lateral cricoarytenoid muscle are visible.

The laryngeal ventricle is imaged in Figs.3b and c. Between the posterior portions of the vocal cords, the ventricle is not recognizable. The piriform fossa, another air-filled space, is situated laterally to the aryepiglottic fold but medially to the thyroid cartilage (Fig.3f).

Axial MR Anatomy

The cricoid is displayed as an interrupted circular structure, which is mainly ossified (Fig. 4a). On the luminal side the cricoid is covered by the very bright mucosal tunica. The thyroid cartilage is not easily distinguished from the infrahyoid muscle group

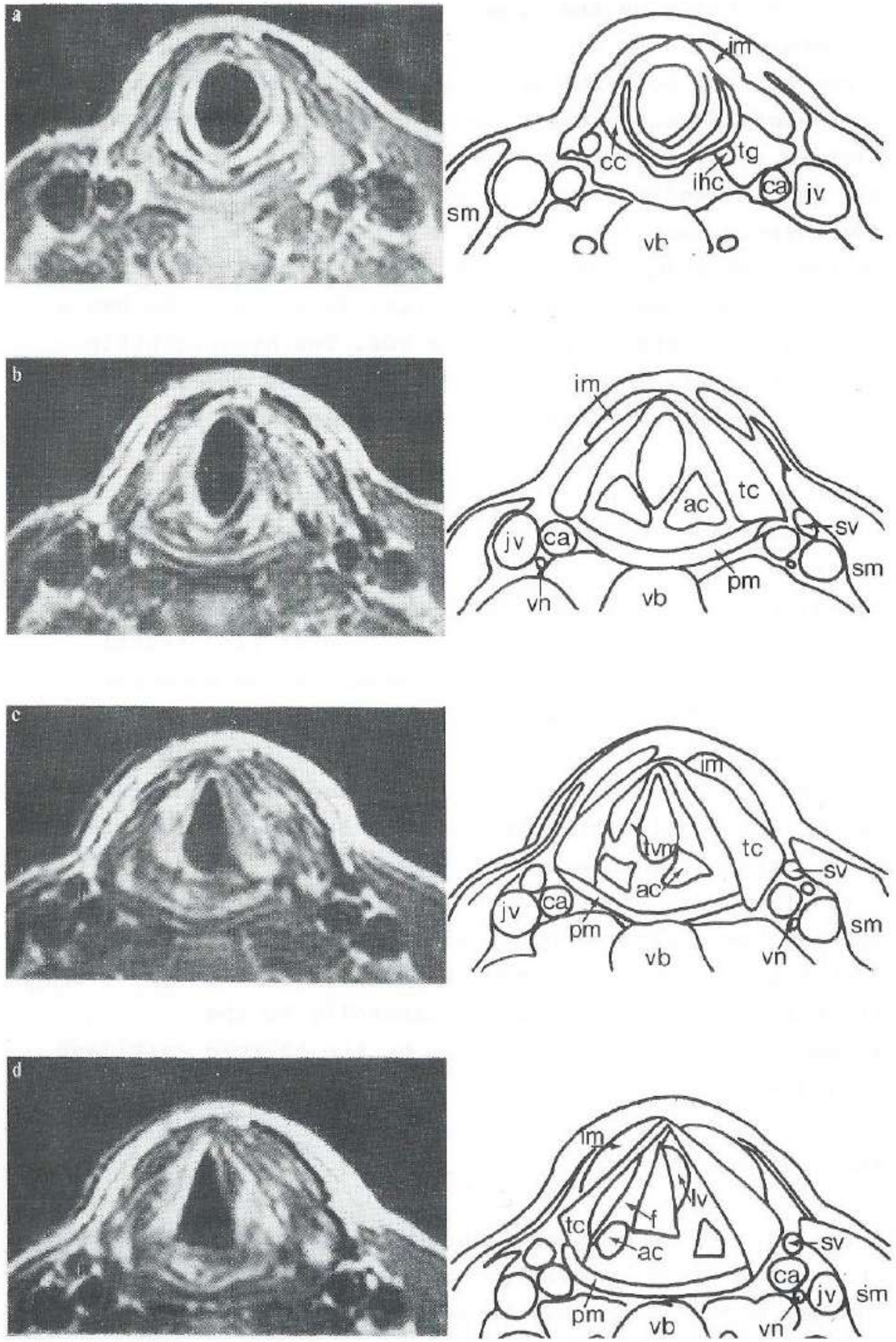

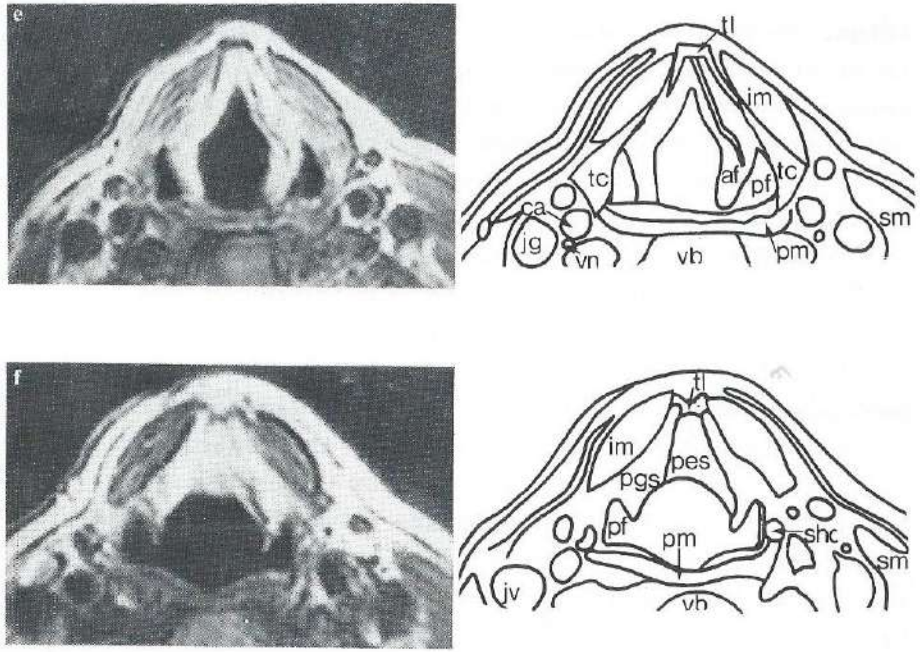

FIG.4.
Axial images of a 32-year-old man; field of view: 180x180 mm; slice thickness: 5 mm; SE: 250/50; matrix: 128x128. Surface coil. Multiple slice.
Levels: A: cricoid cartilage; B: caudal part of arytenoid cartilages; C: true vocal cords; D: false vocal cords; E: Thyroid notch; F: superior horn of the thyroid cartilage. For key to abbreviations in schemes see appendix.

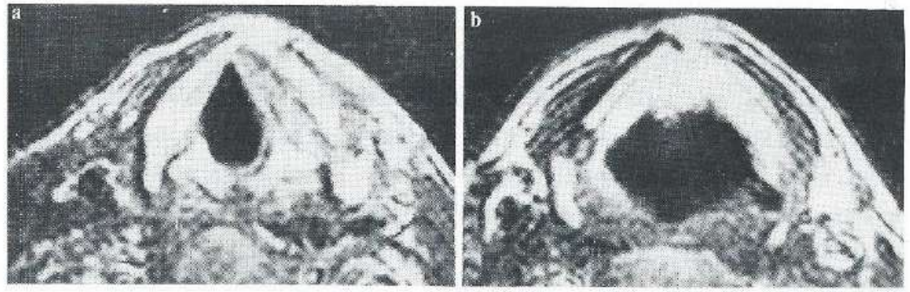

FIG. 5.
A and B: Axial images of 60-year-old man; field of view: 140x140mm; slice thickness: 4mm; measurements: 4; SE: 300/50; matrix: 128x128. Surface coil.

(Figs. 4b-d). The dorsal portion of the thyroid cartilage is ossified. The arytenoids are imaged as triangular structures in Figs.4b-d. The vocal muscles attach to the vocal process (Fig.4c). Above the true cords the false cords are attached to the arytenoid cartilage (Fig.4d, left). The laryngeal ventricle separates the false and true vocal cord. In accordance with CT experience (12) this space is imaged as a lateral dilatation of the laryngeal lumen (Fig.4d, right).

The walls of the PES can be recognized: the thyrohyoid membrane (and anteriorly the thyrohyoid ligament) (Fig. 4f) and the thyroid cartilage (Fig.4e) as the ventral wall; the epiglottic cartilage as the posterior wall (Fig. 4f). Laterally to the PES, both PGS are situated. The conus elasticus (caudal) and the fibroelastic membranes (cranial) constitute the medial walls of the PGS. The lateral walls are the thyroid cartilage and the thyrohyoid membrane. The cricoarytenoid and vocal muscles, lying within the conus elasticus, occupy the inferior portions of the PGS (Fig.4c).

The laryngeal vestibulum is separated by the aryepiglottic fold from the piriform fossa (Figs.4e and f). Dorsally, both spaces are bordered by the inferior constrictor pharyngis muscles, which are connected to the dorsal margins or dorsolateral part of the thyroid cartilage on both sides (Figs. 4a-e).

In the axial plane the carotid sheath is very clearly recognizable (all axial images), especially when the vessels are surrounded by adipose tissue. The carotid artery bifurcates beneath the level of the hyoid bone (Fig.4f). At this level the cervical lymphatic nodes are found. Besides small vessels and nerves, the vagus nerve is visible in a characteristic position in respect to both main vessels (all axial images).

Process of Ossification

Anatomical and radiological literature on the

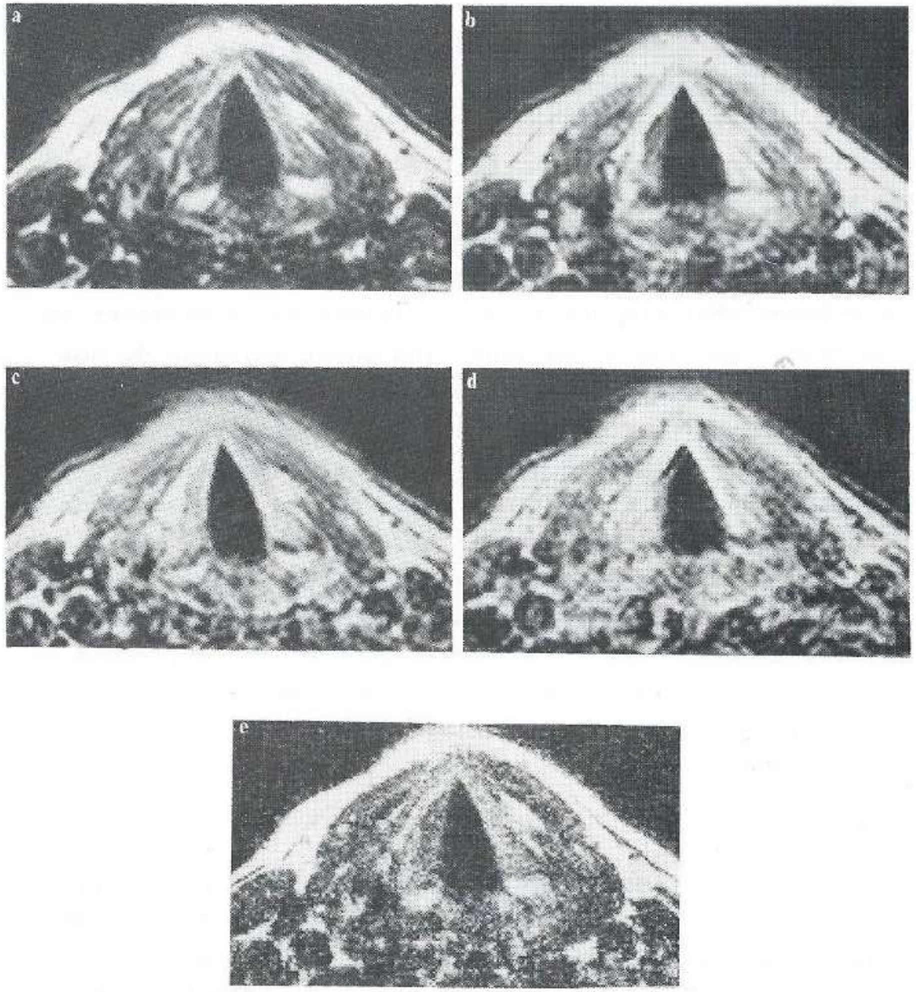

FIG. 6.
Axial images of a 31-year-Fold man; field of view: 140x140mm; slice thickness: 5mm; TE: 50ms. Surface coil.
A: Measurements: 8; TR: 250ms; matrix: 128x128.
B: Measurements: 4; TR: 500ms; matrix: 128x128.
C: Measurements: 2; TR: 1,000 ms; matrix: 128x128.
D: Measurements: 1; TR: 2,000 ms; matrix: 128x128.
E: Measurements: 4; TR: 250ms; matrix: 256x256.

ossification process suggests that the ossification occurs symmetrically according to fixed patterns (3,8). Ossification appears to occur mainly in the early twenties and is modified only slightly in the ensuing years. The dorsal ossification of the thyroid cartilage (Figs.4c and d, age 32 years) agrees with the pattern of ossification as indicated by Chievitz (8). Ossification by fixed and symmetrical patterns are questioned by Yeager et al (3). They found that the degree of ossification is greatest in the caudal portion : the inner and outer surfaces do not ossify in a corresponding pattern; the left and right laminae of the thyroid cartilage do not ossify symmetrically. Figure 5 shows the final stage of ossification in a 60-year-old man. This is in accordance with observations by Yeager et al. (3) that the ossification is asymmetrical and that the inner and outer surfaces of the thyroid lamina do not ossify in a corresponding pattern. The caudal part of the arytenoid is completely ossified. Figures 3b-e show that the caudal portions of the thyroid cartilage are completely ossified.

Imaging Techniques

Frequently CT images are degraded by streak artifacts caused by swallowing, respiratory motion, and X-ray beam hardening. According to Stark et al. (11) and Schenck et al. (7), the MR images are only minimally affected by respiration movements. However, image degradation is caused by swallowing. Prolonged scanning time (e.g., 3DFT, multislice scanning) will increase the probability of movement artifacts. With respect to sagittal imaging, the application of the surface coil (Fig.2), instead of the standard head coil (Fig.1), improves the image. The use of a surface coil in imaging the frontal and axial planes results in considerable improvement. Using the surface coil, it is possible to obtain high resolution images with 128x128 matrix with the technically minimal field of view (126x125mm, Fig.3), minimal slice thickness (3mm, not

shown). This is in accordance with a report of Axel, who described an improvement of the signal-to-noise ratio for objects close to the surface coil. This improved ratio permits higher resolution imaging of relatively superficial structures (4).

For the axial plane we find generally that images obtained with a 128x128 matrix size (Fig.6a) are more useful than 256x256 matrix size images (Fig.6e). The better signal-to-noise ratio of the former images outweighs the better resolution potential of the 256x256 images, which contain considerable noise. Images obtained with relatively short TR (250ms: Fig.6a; 500ms: Fig.6b) had a much better resolution than images with longer TR (1,000ms: Fig.6c;2,000 ms :Fig.6d). The contrast between the nonossified laryngeal skeleton and surrounding structures is slightly better in shorter TR images. Because images with TR = 250ms were applied with eight measurements, the artifacts caused by the bloodstream disappeared. Images with TE = 100ms and TE = 150ms (multiecho technique, not shown) had a rather poor signal-to-noise ratio and did not provide more information about normal anatomy. By changing the phase-encoding gradient direction to the anteroposterior direction, pulsation artifacts arising from the bloodstream in the carotid sheath appear in the anteroposterior direction and thus do not blur structures studied in the present report.

Using the IR technique, we did not succeed in differentiating between muscle tissue, compact bone, and fibrocartilage. All these structures had a low signal intensity, in accordance with findings of Stark et al. (11).

Diagnostic Implications

Local extension of the laryngeal tumors occurs in the PES, PGS, anterior commissure region, or the subglottic area. As for lymphatic spread, the area above the vocal cords drains into the internal jugular chain of nodes and the cervical nodes near the carotid bifurcation. Assessment of spread of supraglottic tumors in the horizontal direction into the PES or in the vertical direction is of importance considering indications for conservative surgical treatment or radiotherapy. A supraglottic tumor may invade the PES or the PGS; the partition membrane between the PES and PGS does offer some resistance. If the PGS is invaded, the tumor is restricted to one side. A vertical hemilaryngectomy may be adequate. Spread of tumor in the PES is limited by the boundaries of the space. When the vallecula or tongue base is invaded by the tumor, the superior extent of resection has to be increased (9). Detection of cartilage invasion is also of great clinical importance. Complications of radiation therapy such as perichondritis, necrosis, and subsequent severe edema are likely to occur when cartilage invasion is present (1).

With MR it is possible to visualize laryngeal structures with high detail in axial, sagittal, and frontal planes. In the sagittal plane the anterior, superior, and posterior wall of the PES are well delineated and furthermore the anterior commissure and the cricothyroid ligament (only midsaggital) are well appreciated. By imaging in the axial and frontal plane the lateral borders of the PES and PGS and the vocalis and thyroarytenoid muscles are shown. In both these planes the border between the PGS and the ossified thyroid cartilage is well defined (Fig.5). The border between the PGS and nonossified cartilage is not very clearly seen. In general, tumor invasion is confined to the ossified portions of the cartilage. Because the structures in the carotid sheath are surrounded by adipose tissue, MR is capable, in the axial planes, of showing lymphatic spread around the bifurcation or the internal jugular vein.

Acknowledgement: We are indepted to H.A.A. Grimbergen and P.E. Booyen for constructing the surface coil. The authors wish to thank A. Goedhart and C. Hersbach (Department of Anatomy, University of Amsterdam) for providing anatomical and pictorial support, respectively.

REFERENCES

1. Gerritsen GJ. Computed tomography and laryngeal cancer Academic thesis. Amsterdam: Free University of Amsterdam, 1984.

2. Silverman PM, Johnson GA, Korobkin M, Thompson WM. High-resolution multiplanar CT images of the larynx. Invest Radiol 1982;17:634-637.

3. Yeager VL, Lawson C, Archer CR. Ossification of laryngeal cartilages as it relates to computed tomography. Invest Radiol 1982;17:11-19.

4. Axel L. Surface coil magnetic resonance imaging. J Comput Assist Tomogr 1984;8:381-384.

5. Boskamp E. Application of surface coils in NMR tomography and decoupling of the excitation coil and the receiver (surface) coil. In: Proceedings of the third annual meeting of the Society of Magnetic Resonance in Medicine, 1984:62.

6. Roberts D, Schenck J, Joseph P, et al. Temporomandibular joint: magnetic resonance imaging. Radiology 1985;154:829-830.

7. Schenck JF, Foster TH, Henkes JL, et al. High field surface coil MR imaging of localized anatomy. AJNR 1985;6:181-186.

8. Chievitz JH. Untersuchungen ueber die Verknocherung der menschlichen Kehlknorpel. Arch f Anat Ent Gesch 1882;303-349.

9. Lam KH, Wong J. The preepiglottic and paraglottic spaces in relation to spread of carcinoma of the larynx. Am J Otolaryngol 1983;4:81-91.

10. Li KC, Henkelman M, Poon PY, Rubinstein J. MR imaging of the normal knee. J Comput Assist Tomogr 1984;8:1147-1154.

11. Stark DD, Moss AA, Gamsu G, Clark OH, Gooding GA, Webb WR. Magnetic resonance imaging of the neck. part 1: normal anatomy. Radiology 1984;150:447-454.

12. Mancuso AA, Calcaterra TC, Hanafee WN. Computed tomography of the larynx. Radiol Clin North Am 1978;16:195-208.

Chapter 5. MAGNETIC RESONANCE IMAGING OF LARYNGEAL CANCER

Authors: J.A. Castelijns (M.M.) (1,2)
M.C. Kaiser (M.D.) (1)
J. Valk (M.D.) (1)
G.J. Gerritsen (M.D.) (2)
A.H. van Hattum (M.D.) (3)
G.B. Snow (M.D.) (2)

(1) Department of Radiology
(2) Department of Otolaryngology/
Head and Neck Surgery
(3) Pathology

Institution: Free University Hospital
Amsterdam
The Netherlands

Abstract:

Forty-four consecutive patients with laryngeal carcinomas presenting at different stages of the disease were investigated by magnetic resonance (MR) imaging. Twelve patients (six with primary lesions and six with recurrent tumors) underwent laryngectomy, and the macro- and microscopic appearance of the sliced specimens were correlated with MR imaging. In the remaining patients surgery was not performed, and MR results were compared with the laryngoscopic findings. Cancerous tissue was seen on T1-weighted images as a homogeneous mass of intermediate signal intensity, slightly higher than infrahyoid muscles. The MR examinations failed mainly in patients with tumor recurrence who had undergone previous radiation treatment.
Index terms:Larynx, neoplasms- Carcinoma- Magnetic resonance imaging.

In the past, clinical examination and conventional radiological techniques (tomography and laryngography) were the diagnostic tools available for preoperative evaluation of the location and extent of carcinomas of the larynx and hypopharynx. Computed tomography added the ability to demonstrate intralaryngeal pathways of tumor spread, such as submucosal tumor growth and gross cartilage destruction. This information is very useful for staging advanced carcinomas of the larynx and hypopharynx and for deciding whether radiation therapy or surgery is indicated (1).

Nevertheless, CT of the larynx has its limitations, especially in determining early cartilage invasion and in trying to provide a three-dimensional representation of pathology. Magnetic resonance (MR) imaging displays greater soft tissue in detail in axial, frontal, and sagittal planes (2). From previously reported studies (3-7) it appears that MR shows the anatomy of the larynx, in particular the intrinsic laryngeal musculature and the intralaryngeal compartments, with excellent detail and soft tissue definition.

To evaluate how well MR can display the larynx and its surrounding structures, we compared the results of MR imaging with pathologic specimens following laryngectomy or with laryngoscopic findings when radiation treatment had to be carried out. Seven representative cases out of a series of 44 consecutive MR investigations of the larynx have been selected in which correlation with pathological specimens and laryngoscopy findings has been emphasized.

MATERIALS AND METHODS

Forty-four consecutive patients presenting with laryngeal carcinomas at different TNM stages have been investigated by MR imaging. Thirty patients had primary and 14 had recurrent disease after irradiation treatment. Primary carcinomas included six supraglottic, 19 glottic, one subglottic, and four piriform sinus tumors.

We selected the most appropriate pulse sequences and the most adequate patient and coil positioning on the basis of earlier experience with MR in 16 patients who were not included in this study. Images were acquired with a 0.6 T superconductive system (Technicare) using a solenoid surface coil placed around the anterior aspect of the neck as a receiver antenna. Routinely, a three slice technique in a sagittal plane spin echo (SE) 200/38 was obtained. The T1-weighted images in the frontal (SE 300/38) and axial planes (SE 400/38) were centered on the lesion as seen on the midline sagittal ("Scout") image. The T2-weighted images (SE 1,500/38, SE 1,500/76) were obtained in the axial plane. The slice thickness used was 4 mm with 3 mm gaps. Four measurements were obtained with T1-weighted and two measurements with T2-weighted images. Gradient zooming was used to keep the field of view as small as possible (20x20 cm). With a 256x192 matrix the images had a pixel resolution of 0,8x1,0 mm.

Twelve patients (six with primary lesions and six with recurrent tumors) underwent laryngectomy, and the specimens were obtained for sectioning. The specimens were fixed in 4% formaldehyde, then decalcified by submersion in Kristensen's solution for 2 weeks. According to the recommendations of Michaels and Gregor (8), axial slices with a 4 mm thickness were cut parallel to the plane of the axial MR slices. All slices were photographed and parts of the slices were processed for microscopic examination. Comparison between axial MR images, macroscopic sections, and microscopic findings was made to identify tumor tissue and to evaluate if infiltration of cartilage existed.

CASE REPORTS

Case 1

A 59-year-old man complained of hoarseness, swallowing difficulties, and bilateral otalgia of a few months' duration. Laryngoscopy showed an ulcerating mass on the laryngeal aspect of the epiglottis. This mass was mainly

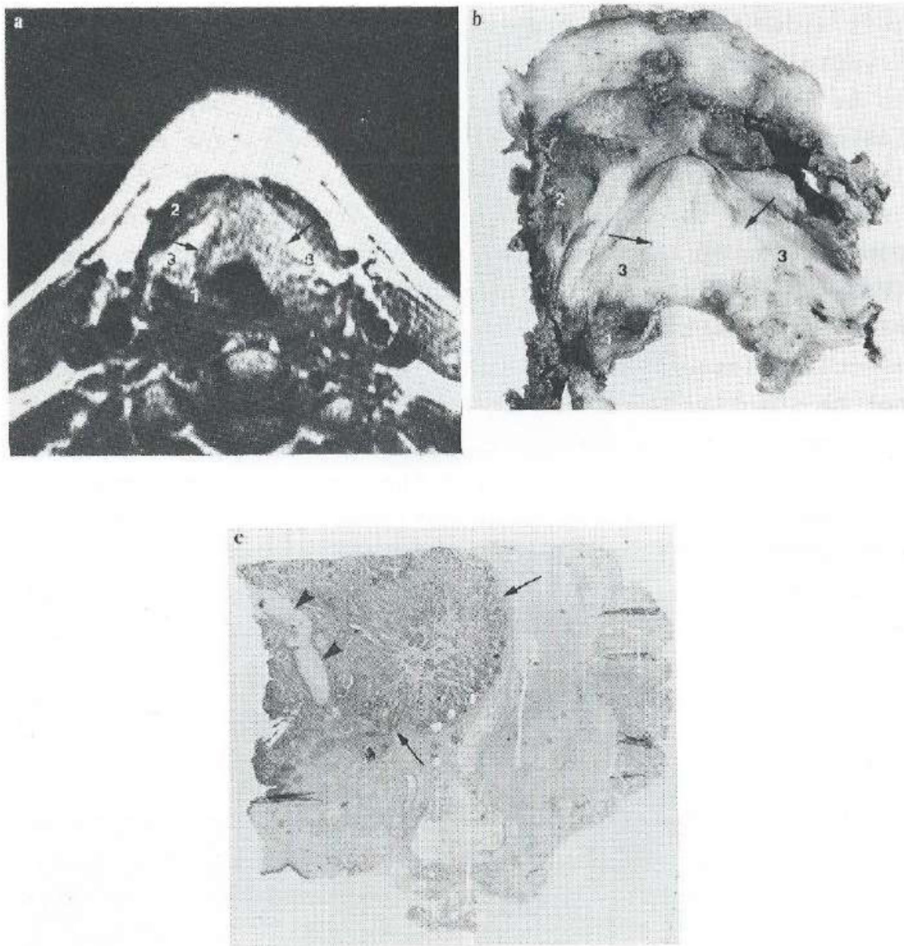

FIG. 1. Case 1. Patient with T1N0 supraglottic tumor.
A: Axial image (SE 400/38) at level of aryepiglottic fold (1) demonstrates tumor (arrows) in preepiglottic space with a slightly higher signal intensity than the infrahyoid muscles (2) but definitively lower signal intensity than fatty tissue within paraglottic space (3).
B: Axial macroscopic section corresponding to (A). Tumor is recognized as a white structure (arrows) with similar contours and a topographic relation to neighboring structures as shown by MR. The numbers are identical in (A and B).
C: Microscopic section corresponding to left posterior quadrant of (B) outlines nonossified epiglottic cartilage with obvious tumor invasion (arrowheads) located within tumor tissue (arrows).

left sided but extended to the right. The left aryepiglottic fold was involved, but the arytenoid seemed to be intact. The tumor was staged as a T1N0 supraglottic lesion. An axial T1-weighted image of the larynx at the level of the aryepiglottic fold (Fig.1a) clearly demonstrated thickening of the left aryepiglottic fold with compression of the piriform sinus. The preepiglottic space (PES) was infiltrated and enlarged by a mass with abnormal signal intensity, higher than the signal intensity of muscular tissue. The nonossified epiglottic cartilage could not be identified within the surrounding tumor.

A section of the postoperative specimen at the corresponding level showed that the contour of the tumor corresponded to the lesion as outlined by MR. This section also confirmed the MR finding of a compressed paraglottic space (PGS), normally filled by fatty tissues (Fig. 1b). On histopathological examination the nonossified cartilage within the tumor tissue showed tumor invasion (Fig. 1c).

Case 2

A 62-year-old man complained of long-standing hoarseness. Laryngoscopy showed an ulcerating tumor, originating from the posterior aspect of the right laryngeal ventricle. This mass extended superiorly into the posterior part of the false vocal cord, which was displaced cranially. The mass also extended caudally into the true vocal cord. The tumor was clinically staged as a T2-supraglottic lesion. The T1-weighted images in the frontal plane showed an intermediate intensity mass on the right side. The region of the true and false vocal cords was invaded by the process, while fat tissue of the right vocal cord was displaced upward (Fig.2a). Axial MR slices showed the false vocal cords as structures of high signal intensity. A mass of intermediate intensity was demonstrated at the posterior edge of the right false vocal cord (Fig.2b). At the level of the true vocal cord, this intermediate signal intensity mass, located in the PGS, was adjacent to the arytenoid and

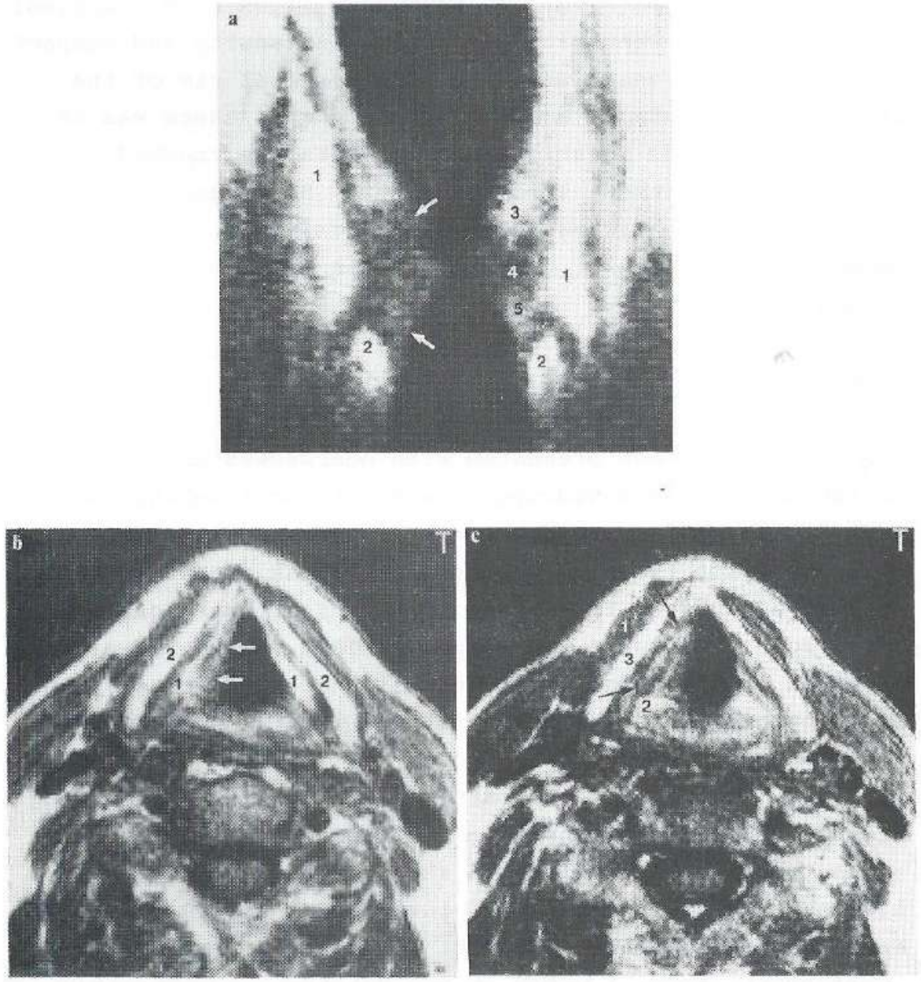

FIG. 2. Case 2. T2 supraglottic tumor on the right side.
A: A frontal image (SE 300/38) visualizes the following structures: thyroid cartilage (1), cricoid cartilage (2), false cords (3), laryngeal ventricle (4), true vocal cords (5). Note area of intermediate signal intensity on the right side due to tumor tissue (arrows).
B: Axial slice (SE 400/38) shows false cord (1), and ossified thyroid cartilage (2). Tumor compresses right vocal cord laterally (arrows).
C: Axial image (SE 400/38) at level of true vocal cords. The tumor is shown as a sharply defined mass (arrows) having a slightly higher signal intensity than the infrahyoid muscles (1). It is contiguous to arytenoid cartilage (2) and the thyroid cartilage (3).

thyroid cartilages (Fig.2c). Both cartilages were ossified; bone marrow was seen with high signal intensity and compact bone with low signal intensity. The cortical rim of the cartilage was intact, and we concluded that there was no obvious cartilage invasion. As T2 tumors are treated by irradiation treatment at our hospital, MR images could only be compared with laryngoscopic findings; correlation between the results of both diagnostic modalities was found.

Case 3

A 58-year-old man presented with hoarseness and soreness of the throat. Laryngoscopy showed a tumor invading the medial, lateral and anterior walls of the right piriform sinus, but the floor of the piriform sinus appeared uninvolved. Due to immobility of the right arytenoid and vocal cord, the tumor was staged as T3N0. Axial T1-weighted MR scans at the level of the thyroid notch showed a swelling of the anterior, medial and lateral walls of the right piriform sinus. This lesion had intermediate signal intensity and could not be differentiated from surrounding tissues (Fig.3a). Extension of the lesion in the direction of the infrahyoid muscles was shown. Although this tumor also extended dorsolaterally, invasion of the carotid artery could be excluded by MR. Macroscopic section at the level of the thyroid notch showed the tumor corresponding to the region of intermediate signal intensity on MR. The mass extended along the ventral side of the superior horn, passed over the superior edge of the thyroid cartilage, and spread toward the infrahyoid muscles (Fig.3b). Microscopic sections showed tumor involvement of the infrahyoid muscles (Fig.3c).

Case 4

A 72-year-old man complained of progressively increasing hoarsenes over a period of one year. Dyspnea with

FIG. 3. Case 3. Patient with tumor of piriform sinus
A: Axial scan (SE 400/38) at level of thyroid notch visualizes large area with intermediate signal intensity extending toward the right infrahyoid muscles (1) and the carotid sheath (2).
B: Macroscopic section at corresponding level shows the tumor (arrows), the lamina of the thyroid cartilage (1), and its superior horn (2), and the infrahyoid muscles (3).
C: Microscopic study of the right posterior quadrant of (B). Tumor (arrows) approaches the infrahyoid muscles (arrowheads).

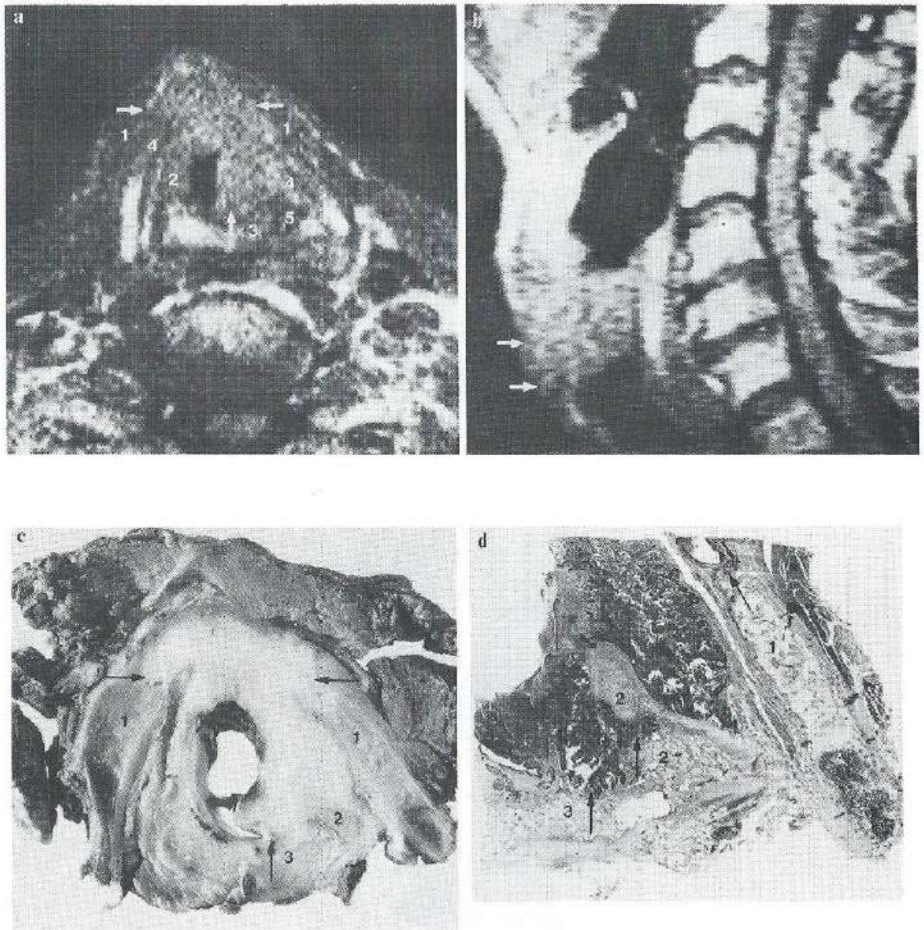

FIG. 4. Case 4. T3N0 transglottic tumor.
A: Axial image (SE 400/38) at the glottic level shows tumor (arrows) with a slightly higher signal intensity than infrahyoid (1), vocal, and thyroarytenoid muscles (2). Gross destruction of the cricoid (3), the thyroid cartilage (4), and left arytenoid cartilage (5) is present.
B: Sagittal section (SE 200/38) shows prelaryngeal (arrows) and craniocaudal extension of tumor extending from the glottic to the low subglottic level.
C: Macroscopic section corresponds to (A). Neoplastic invasion of cartilage (arrows) was confirmed: the thyroid (1), the left arytenoid (2), and the cricoid (3) showed obvious tumor invasion.
D: Microscopic examination of the left posterior quadrant of specimen (C) confirmed tumor invasion (arrows) of the thyroid (1), left arytenoid (2), and the cricoid (3) cartilages.

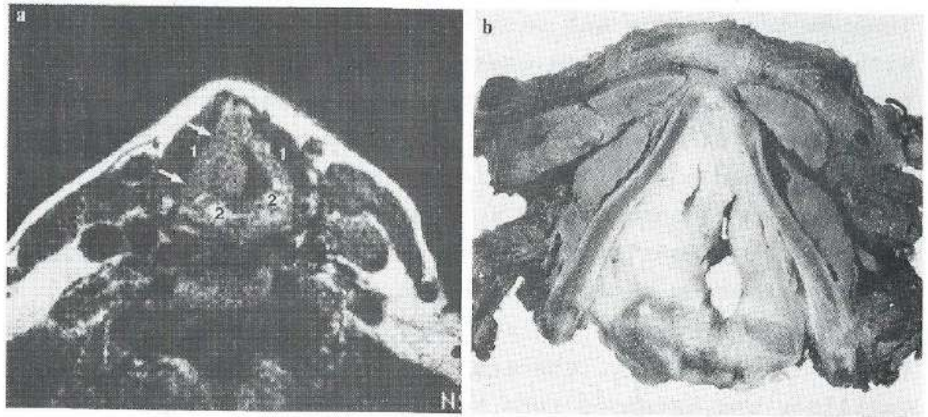

FIG. 5. Case 5. T3N0 transglottic larynx carcinoma.
A: An axial MR image (SE 400/38) at level of thyroid notch shows the thyroid cartilage with intermediate signal intensity as most of it is not yet ossified (1). The ossified arytenoids (2) have high signal intensity. Tumor (arrows) fills the right paraglottic space (PGS) and approaches the thyroid and arytenoid cartilages but no cartilage invasion was apparent.
B: Macroscopic section at same level as (A). Tumor is seen as a white tissue mass in the right PGS. Cartilage invasion was excluded.

inspiratory stridor and pain during swallowing developed within the preceding few weeks. Laryngoscopy showed a transglottic tumor on the left extending into the anterior commissure. Fixation of the vocal cords was found and the tumor was staged as T3N0. Axial MR slices at the level of the true vocal cord showed a large homogeneous area of intermediate signal intensity located within the left PGS and the anterior commissure region. This area had higher signal intensity than the neighboring infrahyoid muscles (Fig.4a). Anteriorly, the tumor invaded the thyroid cartilage and extended into the prelaryngeal infrahyoid muscles (Fig.4a and b). Posteriorly, the intermediate intensity area extended into the right arytenoid and the cricoid lamina (Fig.4a). A midsagittal scan outlined the large homogeneous mass extending from the glottic level to the low subglottic area. Macroscopic sections at the corresponding levels confirmed the MR findings (Fig.4c). Microscopic examination demonstrated invasion of the three cartilages on the left (Fig.4d) and prelaryngeal extension with invasion of the infrahyoid muscles (not illustrated).

Case 5

A 75-year-old man complained of hoarseness, dyspnea, and cough over a period of 8 months. Laryngoscopy revealed a solid glottic process on the right with submucosal extension to the supraglottic level. The false vocal cord, the laryngeal ventricle, and the aryepiglottic fold were affected. A small ulceration was seen within the anterior commissure. Clinically, the tumor was staged as T3N0. Figure 5a is an axial MR slice, displaying enlargement of the right PGS just above the glottic level. The entire PGS contained intermediate signal intensity tumor extending toward the anterior commissure. The thyroid cartilage and the right arytenoid were still intact. The corresponding macroscopic section revealed that right PGS was invade by tumor (Fig. 5b). Histopathological study confirmed that cartilage invasion was not present (not illustrated).

Case 6

A 65-year-old man complained about soreness of the throat and dyspnoea over 6 months. A progressive swelling of the right neck over 3 months was noted, due to a pathological lymph node. Laryngoscopy revealed a T4 piriform sinus tumor. A T1-weighted image (Fig. 6a) showed the lymph node with an intermediate intensity. This node had a smooth contour and was easily distinguished from surrounding fatty tissue. A T2-weighted axial scan at the corresponding level showed the node with higher signal intensity. Although the contrast definition between the enlarged node and surrounding fatty tissue was reduced, delineation from vacular structures became optimal (Fig. 6b). Total laryngectomy with en bloc neck dissection revealed malignant spread into the enlarged node, but extranodular extension was not shown (not illustrated).

Case 7

A 66-year-old man complained of swallowing difficulties, hoarseness, and left-sided otalgia. A supraglottic carcinoma, staged as T4N3, was found by laryngoscopy. A 2.5 cm lymph node was palpated in the left subdigastric region. Axial MR scans at the supraglottic level confirmed the presence of a primary carcinoma in the left aryepiglottic fold. The T1-weighted images demonstrated the pathological lymph node as an irregularly shaped soft tissue mass of intermediate signal intensity, easily differentiated from surrounding fat. Infiltration of the sternocleidomastoid muscle was present, muscular tissue having a slightly lower signal intensity than metastatic lymph node spread (Fig.7). Total laryngectomy with en bloc neck dissection demonstrated lymph node metastasis with extranodular spread into surrounding fat and muscular tissue, confirming our preoperative MR findings (not illustrated).

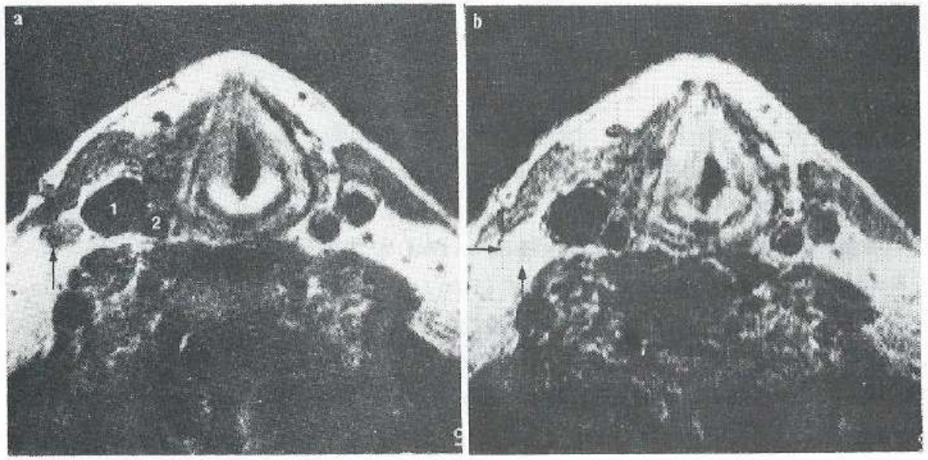

FIG. 6. Case 6. T4 piriform sinus tumor with intracapsular lymph node spread.
A: T1-weighted image (SE 400/38) demonstrates enlarged lymph node with an intermediate signal intensity (arrow) on the right, easily differentiated from the jugular vein (1), carotid artery (2), and the fatty tissues within the carotid sheath.
B: T2-weighted slice (SE 1,500/76) visualizes the malignant node (arrows) with high signal intensity optimizing its differentiation from vascular structures.

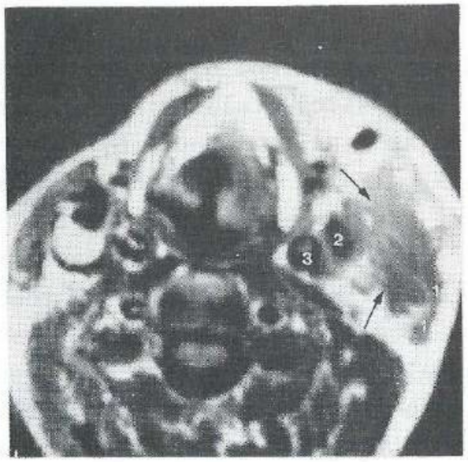

FIG. 7. Case 7. Patient with supraglottic tumor and extracapsular lymph node spread. Axial MR delineates lymphatic invasion (arrows) with intermediate signal intensity in comparison to sternocleidomastoid muscle (1), which has a relatively lower signal intensity. Metastatic spread into surrounding fat and muscle is obvious on the left. Internal jugular vein (2) and carotid artery (3) are well shown.

DISCUSSION

Magnetic resonance imaging of laryngeal carcinomas is difficult due to these patient's dyspnea, coughing and mucous secretion. Our study has, nevertheless, shown that by using shorter scanning times, MR was capable of providing good diagnostic results in almost all the cases. Further improvement of MR results may be achieved by administering drugs to inhibit coughing and mucous secretion or by sedating the patient.

In our experience MR examinations failed mainly in patients with recurrent tumors after radiation treatment, partially due to their poor clinical condition and motion artifacts (14 cases). Even when the MR images in those cases were of technically good quality, distinction among residual or recurrent tumor, radiation fibrosis, and edema was not possible. On T1-weighted images the intralaryngeal soft tissue structures could be demonstrated with intermediate signal intensity, whereas on T2-weighted images they were seen with high signal intensity. The lack of tissue differentiation by MR in cases of tumor recurrences is in agreement with the experience of Worthman et al. (7) but is contradictory to statements made by Glazer et al. (9), who claimed that, in the mediastinum, T2-weighted images (SE 1,500/90) were helpful in distinguishing recurrent tumor from radiation fibrosis.

As T1-weighted images accurately assessed the extension of primary laryngeal cancer, we stress their importance in demonstrating tumor invasion into different areas: (a) intralaryngeal region (PES, PGS, subglottic region, anterior commisure); (b) laryngeal cartilages; (c) extralaryngeal structures (piriform sinus, infrahyoid muscles, carotid sheath, lymph nodes).

The T1-weighted images in the three planes displayed the three intralaryngeal compartments (both PGS and PES) with high contrast and all bordering structures were clearly shown (5,6). In the three illustrated specimens of primary laryngeal carcinomas the topographic relation between tumor and surrounding structures corresponded well with MR findings. Site, extension and contour of the tumor mass as shown by axial MR corresponded to the actual configuration of the lesions seen on specimens (Figs.1,4, and 5). Extension of submucosal tumor in the intralaryngeal compartments was well defined by axial MR. At the supraglottic level tumor tissue was seen as a homogeneous mass of intermediate signal intensity, lower than the signal intensity of fat. On the contrary, of the level of the true vocal cords, tumor has a relatively higher signal intensity than fat and a slightly higher signal intensity than the vocal and thyroarytenoid muscles. Subglottic and craniocaudal extension is well shown in the frontal plane (Fig.2a). To perform a supraglottic laryngectomy a 3 to 5 mm tumor-free margin above the level of the anterior commissure should exist and the cartilages should not be invaded (1,10). Sagittal MR images are most appropriate to assess this tumor-free margin. In agreement with the literature we also found that this scanning plane is helpful in demonstrating or excluding infiltration of the tongue base, hyoid bone, and prelaryngeal region (Fig. 4b) (6).

Diagnosis of cartilage invasion has a major therapeutic impact. If present, perichondritis and necrosis with subsequent severe edema are likely to occur as complications following radiation therapy, and the incidence of tumor recurrence is also significantly higher (1). The cricoid, thyroid, and greater part of the arytenoid cartilages are composed of hyaline cartilage, which is subject to ossification. The epiglottic cartilage and both vocal processes are composed of yellow fibrocartilage, which does not ossify (11). If malignant invasion of hyaline cartilage occurs, it remains confined to its ossified components in most cases (12,13). Ossified cartilage, composed of compact bone surrounding marrow, has a typical three-layer appearance (Figs.2,3a, and 4a). Invasion into this cartilage can be recognized as an area of intermediate signal intensity interrupting the typical

three-layer appearance (Fig.4a). Gross cartilage invasion is routinely shown by axial MR. Nonossified epiglottic cartilage is normally shown with high contrast compared with neighboring fat (5). When cancer invades this area, the cartilage can not be identified within tumor tissue by MR (Fig.1a).

In the two cases of the piriform sinus tumors, correlation between MR and specimens was less evident. Demonstration of infiltration into extralaryngeal soft tissue structures (i.e., infrahyoid muscles, carotid sheath, and lymph nodes) is important in determining margins of surgical resection. Axial images may provide evidence of malignant invasion of the infrahyoid muscles (Figs.3a and 4a); extension into the carotid sheath can be demonstrated or excluded because contrast between fat within the carotid sheath and tumor is increased (Fig.3a). The contour of pathological lymph nodes is also well defined and contrast medium administration is not needed (Figs.6 and 7). If lymph nodes are irregularly outlined, extranodal spread should be suspected (Fig.7). If nodes are smoothly bordered on axial MR images (Fig.6), the probability of extranodal spread decreases.

Three-dimensional T1-weighted MR imaging permits calculation of the volume of the tumor mass, which is one of the most important criteria to establish a prognosis concerning the efficacy of irradiation treatment.

The T2-weighted images appear to be inappropriate to show primary tumors, as tumor tissue is visualized less homogeneously and the signal-to-noise ratio of the image is decreased (6). Tumor and reactive edema both have high signal intensity and can not be separated by MR. The T2-weighted images are useful in detecting pathological lymph nodes, which have higher signal intensity and are more easily differentiated from vascular structures (Fig.6) (14).

CONCLUSIONS

In the analysis of our series of 30 patients with primary laryngeal tumors we came to the following conclusions:

1. In seven cases with tumors clinically staged as T1aN0 glottic, MR showed either no abnormalities or no obvious pathological findings. For this reason we think that MR is not indicated in those cases.

2. In glottic tumors clinically staged as T1bN0 glottic (three cases) and T2N0 glottic (five cases) lesions, axial T1-weighted MR images showed at one level an abnormal area of homogeneous intermediate signal intensity. Important information concerning tumor extension toward the arytenoid and thyroid cartilages was obtained. Cartilage invasion could not be excluded or confirmed by MR in these relatively small lesions. Further studies including histopathological correlation will be needed for this purpose.

3. Axial MR slices of more advanced glottic tumors (three T3N0 and one T4N0) routinely demonstrated a well defined homogeneous region of intermediate signal intensity. Moreover, it was possible to show cartilage invasion and infiltration of infrahyoid muscles. In these cases frontal MR images showed obvious asymmetry between the right and left PGS so that the cranial and caudal extensions of the lesions were more precisely outlined.

4. In our experience with six cases of supraglottic tumors, sagittal MR images helped to define the distance of the abnormal signal intensity area to the root of the tongue, to the anterior commissure, and to the hyoid bone.

5. In four cases of piriform sinus tumors there was an obvious difference of signal intensity between the pathological area and the fat within the carotid sheath. Information about the relationship of the lesion to the infrahyoid and sternocleidomastoid muscles as well as about eventual extension into the posterior hypopharyngeal wall could be obtained.

6. On T1-weighted images pathological lymph nodes were seen with intermediate intensity, whereas T2-weighted images showed an increased intensity.

Magnetic resonance imaging may play a major role in the diagnostic workup of primary laryngeal tumors. Although scanning times had to be shortened due to the rather poor clinical condition of the patients, we obtained high quality T1-weighted images in patients with primary disease. It is possible to demonstrate submucosal tumor extension in the PES and PGS, cartilage invasion, and enlarged pathological lymph nodes. In our experience MR failed in patients with recurrent tumor following radiation treatment.

REFERENCES

1. Gerritsen GJ. Computed tomography and laryngeal cancer Academic thesis. Amsterdam: Free University of Amsterdam, 1984.

2. Valk J, MacLean C, Algra PR. The clinical application of NMR tomography. In: Valk J, ed. Basic principles of nuclear magnetic resonance imaging. Amsterdam: Elsevier, 1985:115-140.

3. Lufkin RB, Larsson SG, Hanafee WN. Work in progress: NMR anatomy of the larynx and the tongue base. Radiology 1983;148:173-175.

4. Stark DD, Moss AA, Gamsu G, Clark OH, Gooding GA, Webb WR. Magnetic resonance imaging of the neck. Part 1: normal anatomy. Radiology 1984;150:447-452.

5. Castelijns JA, Doornbos J, Verbeeten B Jr., Vielvoye GJ, Bloem JL. MR imaging of the normal larynx. J Comput Assist Tomogr 1985;9:919-925.

6. Lufkin RB, Hanafee WN, Wortham D, Hoover L. Larynx and hypopharynx: MR imaging with surface coils. Radiology 1986;158:747-754.

7. Wortham DG, Hoover LA, Lufkin RB, Fu YS. Magnetic resonance imaging of the larynx: a correlation with histologic sections. Otolaryngol Head Neck 1986;94:123-133.

8. Michaels L, Gregor RT. Examination of the larynx in the histopathology laboratory. J Clin Pathol 1980;33:705-710.

9. Glazer HS, Lee JK, Levitt RG, et al. Radiation fibrosis: differentiation from recurrent tumor by MR imaging. Radiology 1985;156:721-726.

10. Mancuso AA, Hanafee WN. Larynx and hypopharynx. In:

Stamathis G, eds. Computed tomography and magnetic resonance of the head and neck. Baltimore: Williams and Wilkins, 1985;241-257.

11. Chievitz JH. Untersuchungen ueber die Verknocherung der menschlichen Kehlknorpel. Arch Anat U Entwicklungsgesch 1882:303-349.

12. Kirchner JA. Two hundred laryngeal cancers: patterns of growth and spread as seen in serial sections. Laryngoscope 1977;87:474-482.

13. Pittam MR, Carter RL. Framework invasion by laryngeal carcinomas. Head Neck Surg 1982;4:200-208.

14. Dooms GC, Hricak H, Moseley ME, Bottles K, Fisher M, Higgins CB. Characterization of lymphadenopathy by magnetic resonance relaxation times: preliminary results. Radiology 1985;155:691-697.

Chapter 6. MRI OF NORMAL AND CANCEROUS LARYNGEAL CARTILAGES; HISTOPATHOLOGIC CORRELATION

Authors Jonas A. Castelijns, M.M. (1,2)
Geerten J. Gerritsen, M.D. (1)
Marc C. Kaiser, M.D. (2)
Jaap Valk, M.D. (2)
Wicher Jansen, M.D. (3)
Chris J.L.M. Meyer, M.D. (3)
Gordon B. Snow, M.D. (1)

(1) Dept. of Otolaryngology/ Head and Neck Surgery
(2) Dept. of Radiology
(3) Dept. of Pathology

Institution: Free University Hospital, Amsterdam, The Netherlands.

Abstract:

MRI appearances of laryngeal cartilages, normal or invaded by cancer, are still relatively unfamiliar to the majority of the clinicians. Twelve primary laryngeal tumors out of a series of 65 patients who were investigated by MRI were also examined postoperatively by macro- and microscopic sectioning of the surgical specimens. Images were obtained with a 0.6 Tesla superconductive system using a solenoid surface coil. The authors emphasize the value of a combined use of T1-weighted and proton density spin echo images. T1-weighted images permit differentiation between pathological and normal bone marrow. Proton density images allow separation between non-ossified cartilage and tumor tissue. MRI is an additional tool in the diagnostic work-up of cartilage invasion by cancer.

INTRODUCTION

Detection of cartilage invasion by laryngeal and hypopharyngeal carcinomas is of great clinical importance. Complications due to radiation therapy frequently occur in the presence of cartilage invasion (1). Before the introduction of CT scanning, cartilage invasion could only be diagnosed very rarely. CT has the capability to demonstrate gross cartilage invasion in an accurate manner, particularly when extralaryngeal tumor spread is present. However, CT fails in detecting early cartilage invasion (2). Due to their irregular ossification laryngeal cartilages are very difficult to investigate by CT, even when a high-resolution program is used (2,3,4,5). Uncalcified or poorly calcified cartilage may not be well shown and erosion or destruction may thus be simulated (1,2,4,5). On the other hand, tumor may grossly invade the medullary space of laryngeal cartilages and may not be detected if the surrounding bone is still intact (4,6).

Earlier experiences demonstrated that by the use of specially designed surface coils it became possible to obtain high-signal and high-resolution magnetic resonance images of the neck with excellent soft-tissue delineation (7,8,9). Comparison of MR images with sliced surgical specimens showed that primary cancerous tissue was constantly seen on spin echo (SE) T1-weighted images as a homogeneous mass of intermediate signal intensity, which was slightly higher than the signal intensity of the infrahyoid muscles (10). Gross cartilage destruction may be seen on T1-weighted images as an interruption of the cartilagineous outline (10,11). A comparative study of CT and MRI, utilizing a 0.15 Tesla (low field) resistive unit, has proven that if bone destruction caused by head and neck lesions could be demonstrated by CT scanning, it was equally well detected by MRI in all the cases (12).

The authors studied the MRI appearances of differently ossified cartilages, invaded or not, by tumor. The hyoid bone was excluded from this study, because it is always ossified at an advanced age. For the present report, images generated with different SE pulse-sequences (T1-weighted, proton density and T2-weighted images) were compared to corresponding macro- and microscopic slices of the surgical specimens obtained.

MATERIALS AND METHODS.

Sixty five consecutive patients presenting with primary laryngeal and hypopharyngeal carcinomas at different TNM stages (according to UICC, 1978) have been investigated by MR imaging at our clinic. The patient ages ranged from 48 to 86 years. Primary carcinomas included 15 supraglottic, 38 glottic, 1 subglottic and 11 piriform sinus tumors. Recurrent diseases and residual tumors after irradiation are not included in this study.

We selected the most appropriate pulse-sequences and the most adequate patient and coil positioning. Images were obtained with a 0.6 Tesla superconductive system (Technicare) using a solenoid surface coil placed around the anterior aspect of the neck as a receiver antenna. A SE pulse sequence was used to obtain all images. In all three standard directions, a T1-weighted technique which is optimal in demonstrating the anatomy, was performed using a repetition time (TR) of 200-400 ms. and an echo time (TE) of 38 ms. In the axial plane we also generated at each level images using a TR of 1500 ms and a TE of 38ms (proton density image) and 76ms (T2-weighted image). To increase the signal-to-noise ratio the acquisition was repeated four times. The slice thickness used was 0.4 cm. with a 3 mm gap. Gradient zooming was used to keep the field of view as small as possible (200x200 mm), so that with a 256x192 matrix the images had a pixel resolution of 0.8x1.0 mm. Acquisition times varied from 3 to 6 minutes.

Twelve patients out of this group of 65 underwent laryngectomy and the specimens were obtained for organ sectioning. The surgical specimens were initially fixed in a 4% formaldehyde solution for a duration of 72 hours; then

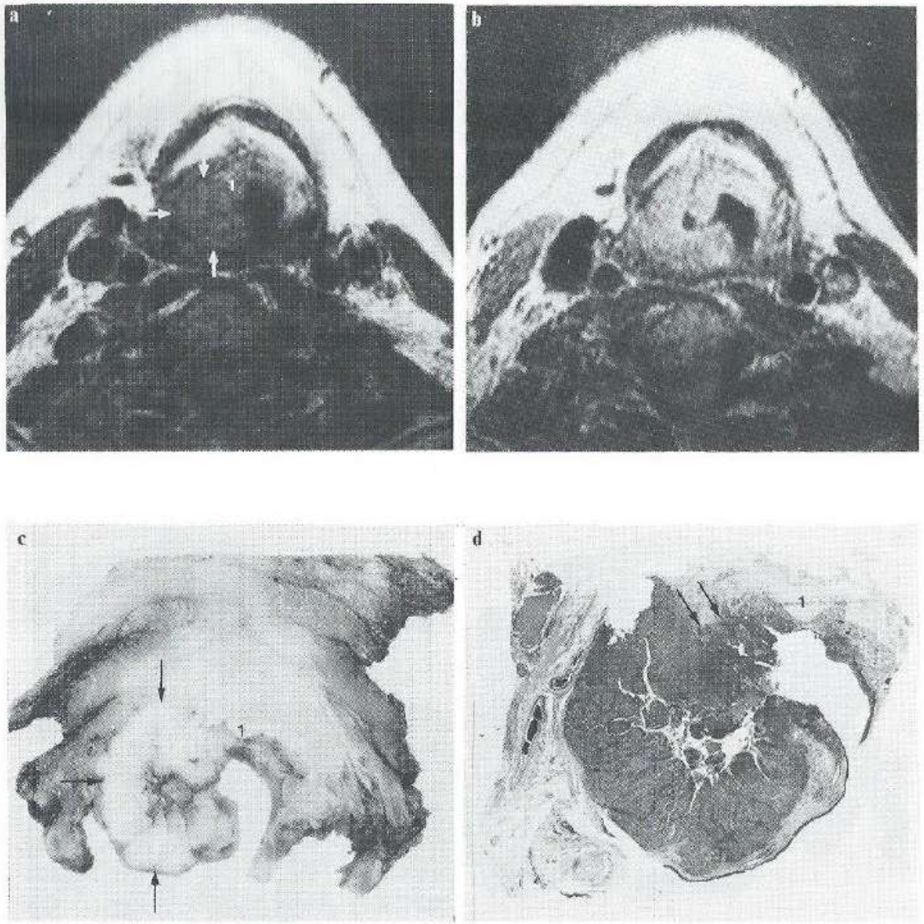

Fig.1. Patient with T3N1 hypopharyngeal tumor.
Fig.1a. T1-weighted, axial image at a supraglottic level demonstrates tumor (arrows), contacting the epiglottic cartilage (1). Both structures are seen with similar signal intensities.
Fig.1b. On a proton density image tumor and epiglottic cartilage are both seen with increased but similar signal intensities.
Fig.1c Sliced surgical specimen. Tumor (arrows) has similar contour and topographic relation to epiglottic cartilage (1) as shown by MRI.
Fig.1d. Microscopic section corresponding to the right posterior quadrant of the sliced specimen outlines non-ossified epiglottic cartilage (1) with tumor invasion (arrows).

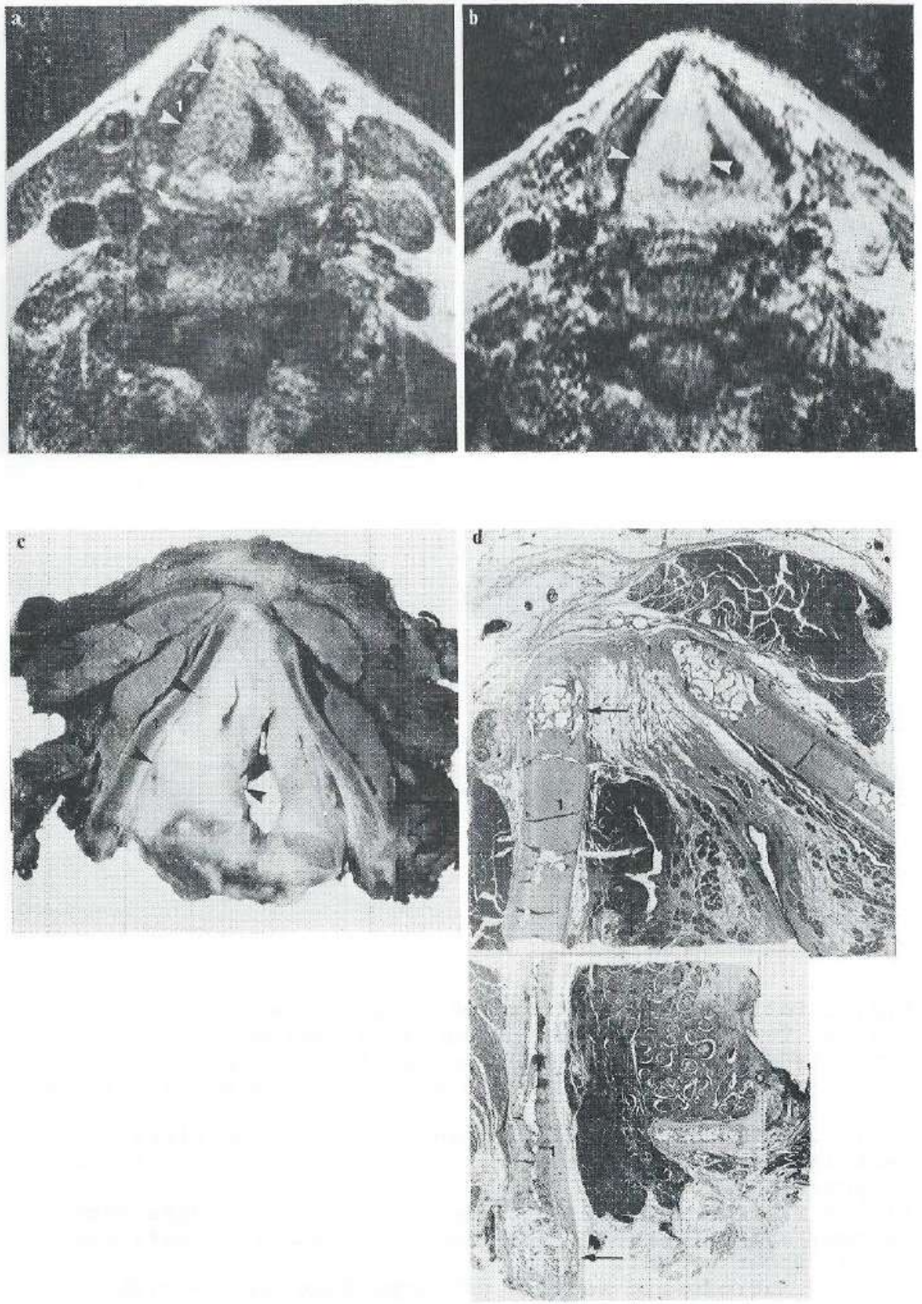

Fig.2. Patient with T3N0 supraglottic lesion.
Fig.2a. T1-weighted, axial image at the level of the false cords visualizes tumor (arrowheads) bordering the thyroid cartilage (1), which has, almost entirely, intermediate signal intensity. The ventral and dorsal ends of the right thyroid lamina are ossified (arrows).
Fig.2b. Proton density image still shows non-ossified thyroid cartilage with intermediate signal intensity. Due to increased signal intensity of cancer, contrast between tumor (arrowheads) and non-ossified cartilage has been enhanced.
Fig.2c. Macroscopic section demonstrates similar relation between tumor (arrowheads) and thyroid cartilage (1).
Fig.2d. Microscopic study of the right thyroid lamina reveals almost entirely non-ossified cartilage (1). The ventral and dorsal ends consist of bone surrounding bone marrow (arrows).

decalcification was achieved by submersion of the specimen into Kristensen's solution for approximately two weeks. According to the recommendations of Michaels and Gregor (13), axial slices with a 4 mm. thickness were cut parallel to the plane of the axial MRI-slices. All slices were photographed and parts of the slices were processed for microscopic examination. Comparison between axial MR images, macroscopic sections and complementary microscopic findings was done with a view to evaluate MR imaging of laryngeal cartilage, invaded or not by cancer.

RESULTS

Epiglottic cartilage

Fig.1a and 1b are T1-weighted and proton density images, respectively, at the supraglottic level showing the epiglottic cartilage with intermediate signal intensity. On Fig.1b the signal intensity is increased when compared to Fig.1a. On both, the thickened right ary-epiglottic fold is seen with intermediate signal intensity, which is still higher than the signal intensity of muscular tissues, but similar to that of epiglottic cartilage. This area, suspect for malignant tissue, approaches the epiglottic cartilage, but invasion of this cartilage cannot be definitely shown or excluded. Site, contour and relation of the tumor mass to the epiglottic cartilage as seen on the T1-weighted image correspond to findings shown by the surgical specimens (Fig.1c). Microscopically, the right portion of the epiglottic cartilage was suspect for tumor invasion (Fig.1d).

Consequently, cancer and epiglottic cartilage can hardly be separated due to very small contrast differences on T1-weighted and proton density images.

Thyroid cartilage

In the next part we present 2 cases, in which the normal

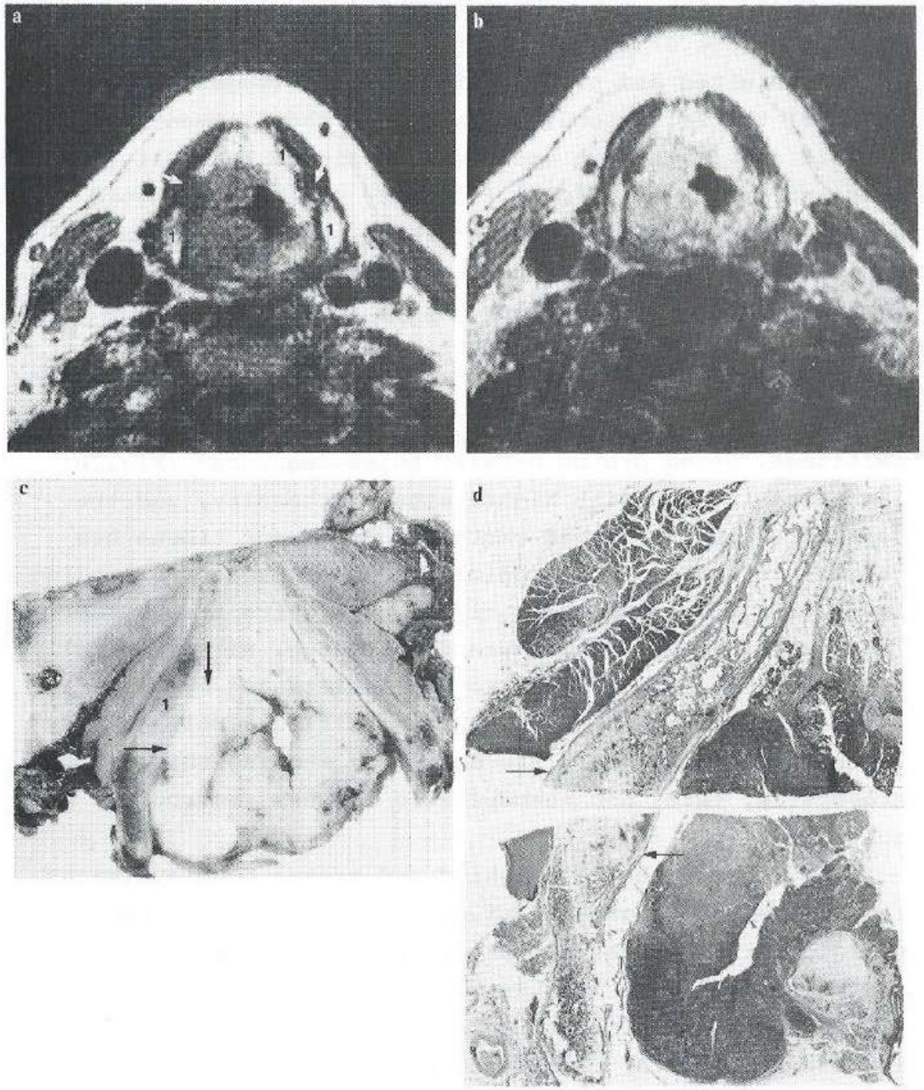

Fig.3. Same patient as in Fig.1.
Fig.3a. T1-weighted, axial image at the level of the false cords visualizes thyroid cartilage (1) which is almost entirely ossified. In the midportion of each lamina a small area of intermediate signal intensity (arrows) is seen.
Fig.3b. Proton density image still visualizes these areas with intermediate signal intensity.
Fig.3c. Corresponding sliced surgical specimen shows similar topographic relation of right lamina (1) to tumor (arrows), as seen on MRI-scans.
Fig.3d. Microscopic examination proves that intermediate signal intensity area of both MRI-images corresponds with a non-ossified portion (arrows) of the thyroid cartilage, not invaded by tumor. The remaining part of the lamina is

MRI-appearance of thyroid cartilage is shown. Fig.2a and 2b are T1-weighted and proton density axial images at the level of the false cords. Both images show segments of the thyroid cartilage with intermediate signal intensity, comparable with the signal intensity of the infrahyoid muscles. Dorsal and ventral extremes are seen with a typical three-layer appearance: a central high signal area is surrounded by rims of low signal intensity.

On Fig.2a the right paraglottic space (PGS) is infiltrated and enlarged by a homogeneous mass having an intermediate signal intensity and approaching the thyroid cartilage. Using proton density pulse-sequences (Fig.2b) this area is seen with higher signal intensity, and the contrast between thyroid cartilage and tumor tissue has become increased. Macroscopic section at the corresponding level (Fig.2c) shows tumor tissue as a white area bordering the right lamina of the thyroid cartilage. Microscopically (Fig.2d), the right lamina is not infiltrated by tumor tissue and mainly consists of non-ossified cartilage. Its ventral and dorsal ends are ossified, showing thin trabeculae, fatty and haemopoietic tissues, surrounded by a cortical rim.

In fig.3a and 3b (T1-weighted and proton density images, respectively) the greater, i.e. ossified, part of the thyroid cartilage has a typical three-layer appearance: a central high signal area is surrounded by rims of low signal intensity. In the midportion of the left and right laminae a region of intermediate signal intensity interrupts this typical appearance. In fig.3a the thickened right PGS is seen with intermediate signal intensity. Invasion of the thyroid cartilage may exist. On fig.3b, the area, which is seen on fig.3a within the laryngeal skeleton with intermediate signal intensity, is still seen with intermediate signal intensity, while neighbouring tissue in the PGS is seen with increased signal intensity. Corresponding macro- and microscopic (Fig.3c and 3d) sections reveal that the thyroid cartilage shows advanced ossification, interrupted by areas of non-ossified

cartilage within both laminae. Bone marrow consists of fat and haemapoietic tissue, lying between thin trabeculae. In this case, tumor tissue approaches the right lamina but no obvious invasion is seen.

Consequently, normal and non-ossified hyaline cartilage is seen with intermediate signal intensity on T1-weighted and proton density images, whereas ossified cartilage is demonstrated as a central high signal intensity area surrounded by rims of low signal intensity.

In the next part, 2 patients with malignant invasion of the thyroid cartilage are discussed. Fig. 4a and 4b are T1-weighted and proton density axial images just above the level of the false cords. On fig.4a the intralaryngeal area is almost entirely filled by an area of intermediate signal intensity. This area extends into the pre-laryngeal region, involving the pre-laryngeal infrahyoid muscles. The posterior portions of both laminae appear to be ossified. Fig.4b shows that most of the intermediate signal area of fig.4a has increased signal intensity which is compatible with tumor tissue. A small region of intermediate signal intensity can still be recognized within the right lamina . Macro- and microscopic examinations (Fig.4c and 4d) demonstrate invasion of the anterior part of the thyroid cartilage by cancer. The posterior segment of the right lamina proved to be ossified and unaffected, whereas the midportion of the right lamina, corresponding to the area of intermediate signal intensity on fig.4b, is non-ossified and unaffected. The greater part of the ventral end of the right lamina is invaded by cancer, in agreement with the MRI findings.

Fig.5a and 5b are T1-weighted and proton density axial images at the level of the false cords. On Fig.5a, an area of intermediate signal intensity is seen, extending laterally. This area appears to infiltrate the dorsal part of the right lamina. On fig.5b the ventral part of this area is still seen with intermediate signal intensity, whereas its dorsal part has definitely higher signal intensity. Macro- and microscopic (Fig.5c and 5d) sections

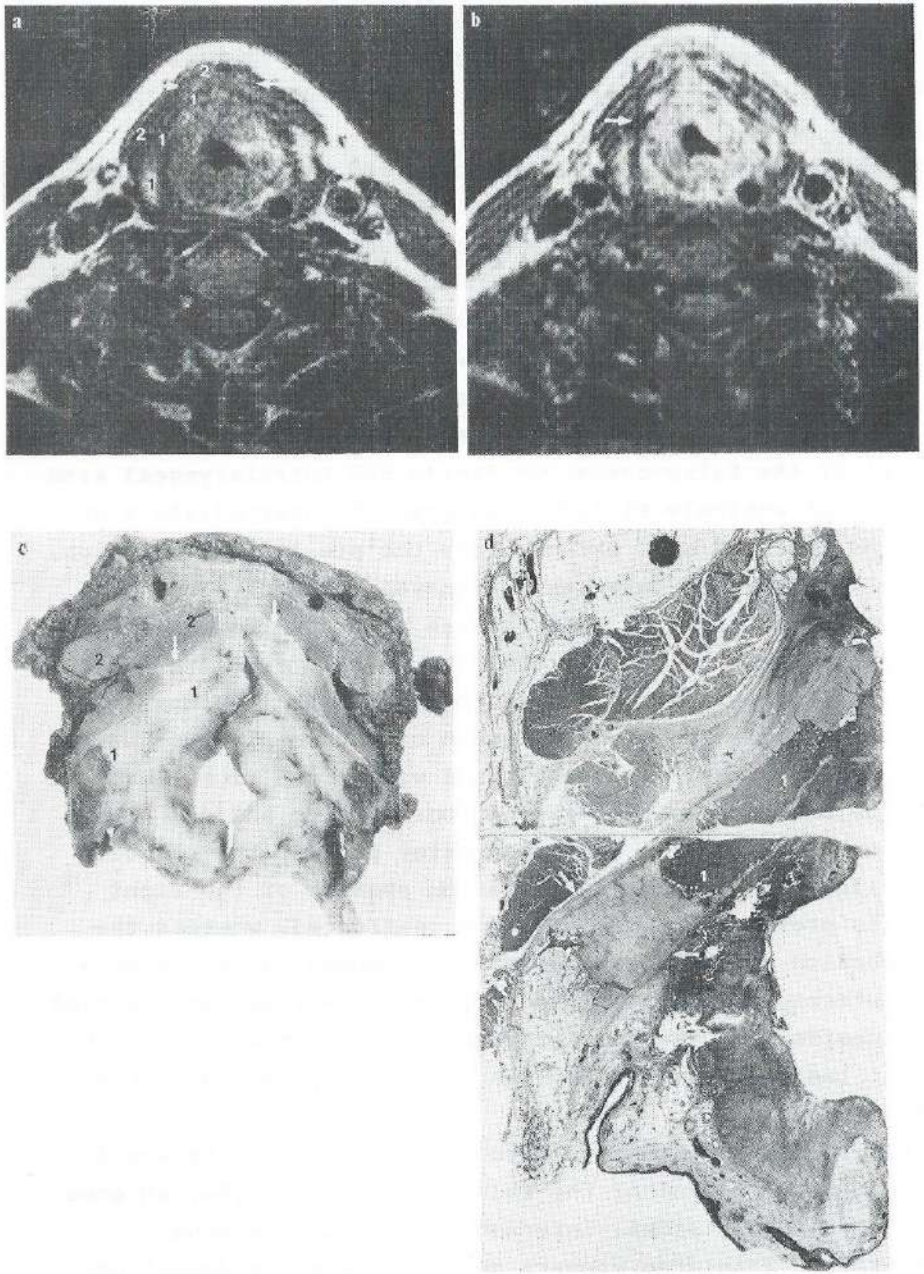

Fig.4. Patient with T4N0 transglottic lesion.
Fig.4a. T1-weighted, axial image at the level of the ary-epiglottic folds shows tumor (arrows), invading the thyroid cartilage (1) and infiltrating the infrahyoid muscles (2).
Fig.4b. Proton density image. A small area of intermediate signal intensity (arrow) separates the invaded ventral extreme and the normal ossified dorsal extreme of the right thyroid lamina.
Fig.4c. Sliced specimen demonstrates tumor (arrows) with a similar topographic relation to thyroid cartilage (1) and infrahyoid muscles (2), as demonstrated by MRI.
Fig.4d. Microscopy shows, that the area of intermediate signal intensity on Fig.4b consists of non-ossified cartilage (arrows), whereas the ventral part of the thyroid lamina (1) is invaded by cancer.

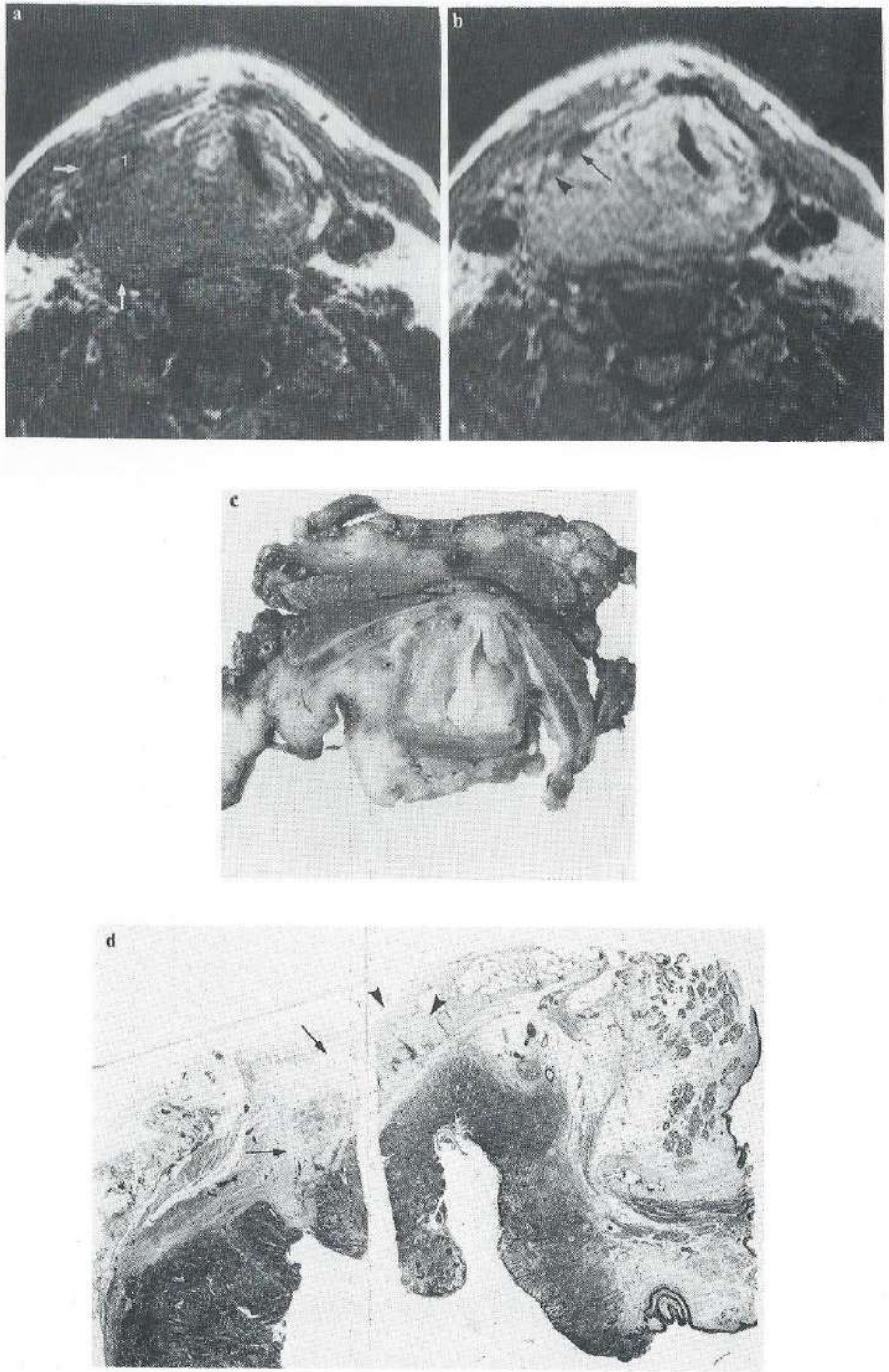

Fig.5. Patient with T4N1 hypopharyngeal tumor.
Fig.5a. T1-weighted, axial image at the level of the false cords. Large intermediate signal intensity area, suspect for tumor (arrows), extends laterally, producing intermediate signal intensity within the dorsal extreme of the right lamina (1).
Fig.5b. On the proton density image the low signal area inside the right lamina is subdivided into two regions: the ventral region (arrow) still has an intermediate signal intensity, whereas the dorsal region (arrowhead) has an increased signal intensity.
Fig.5c. Macroscopic section.
Fig.5d. Microscopy of the right posterior quadrant of Fig.5c proves that the dorsal extreme of the right thyroid lamina is invaded by cancer and reactive tissues (arrows). Ventral to this area the cartilage is not ossified (arrowheads).

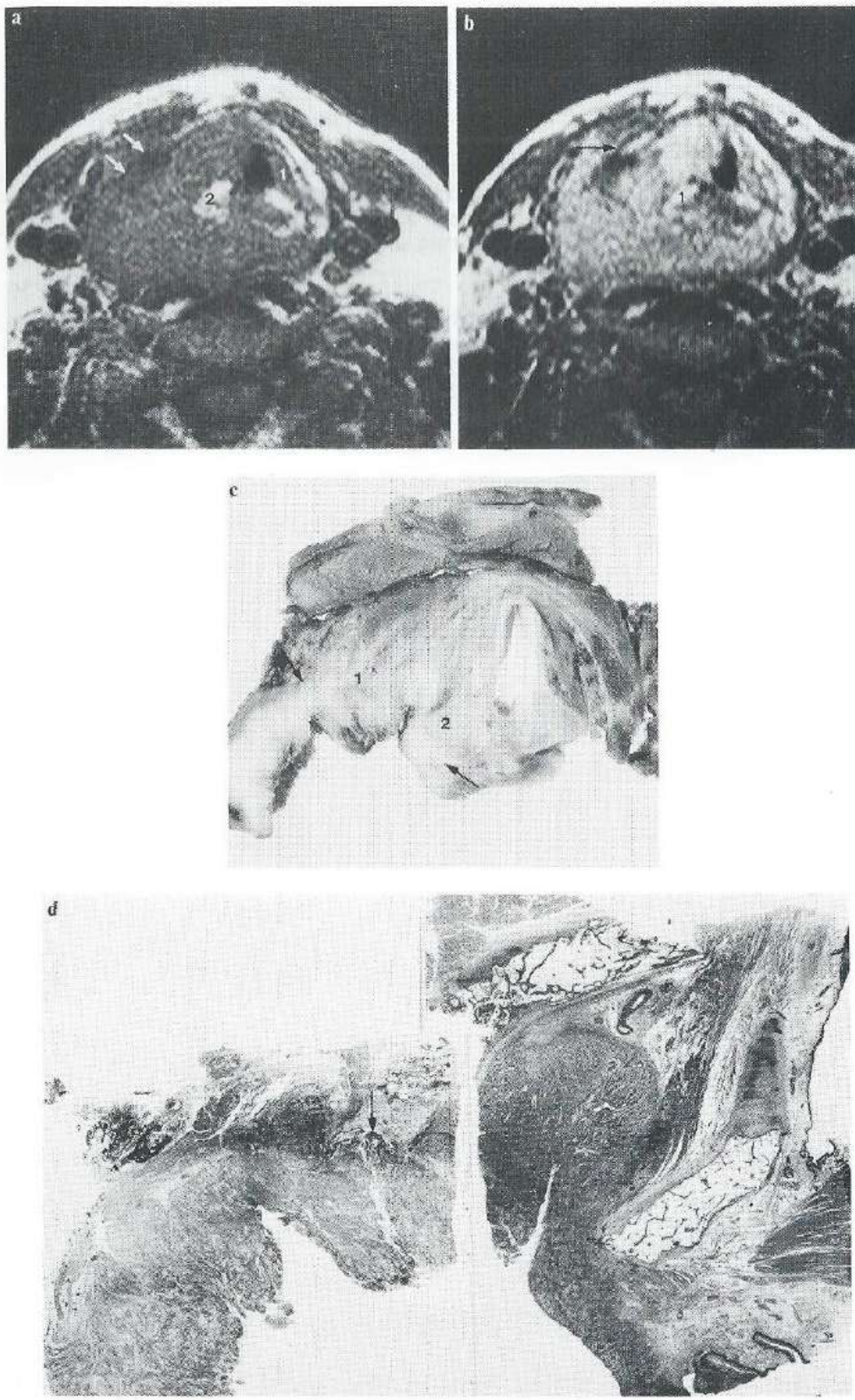

Fig.6 Same patient as in Fig.5.
Fig.6a. T1-weighted, axial image at the level of the true vocal cords (1) shows large mass of intermediate signal intensity destroying the dorsal extreme (arrows) of the right thyroid lamina, whereas the arytenoids (2) are still intact.
Fig.6b. Proton density image visualizes bone (arrow) of right thyroid lamina and the arytenoids (1) with high contrast compared to surrounding tumor.
Fig.6c. Sliced specimen shows tumor (arrows) destroying the thyroid cartilage (1) and touching the arytenoid (2).
Fig.6d. Microscopy of the right half confirms cortical destruction (arrow).

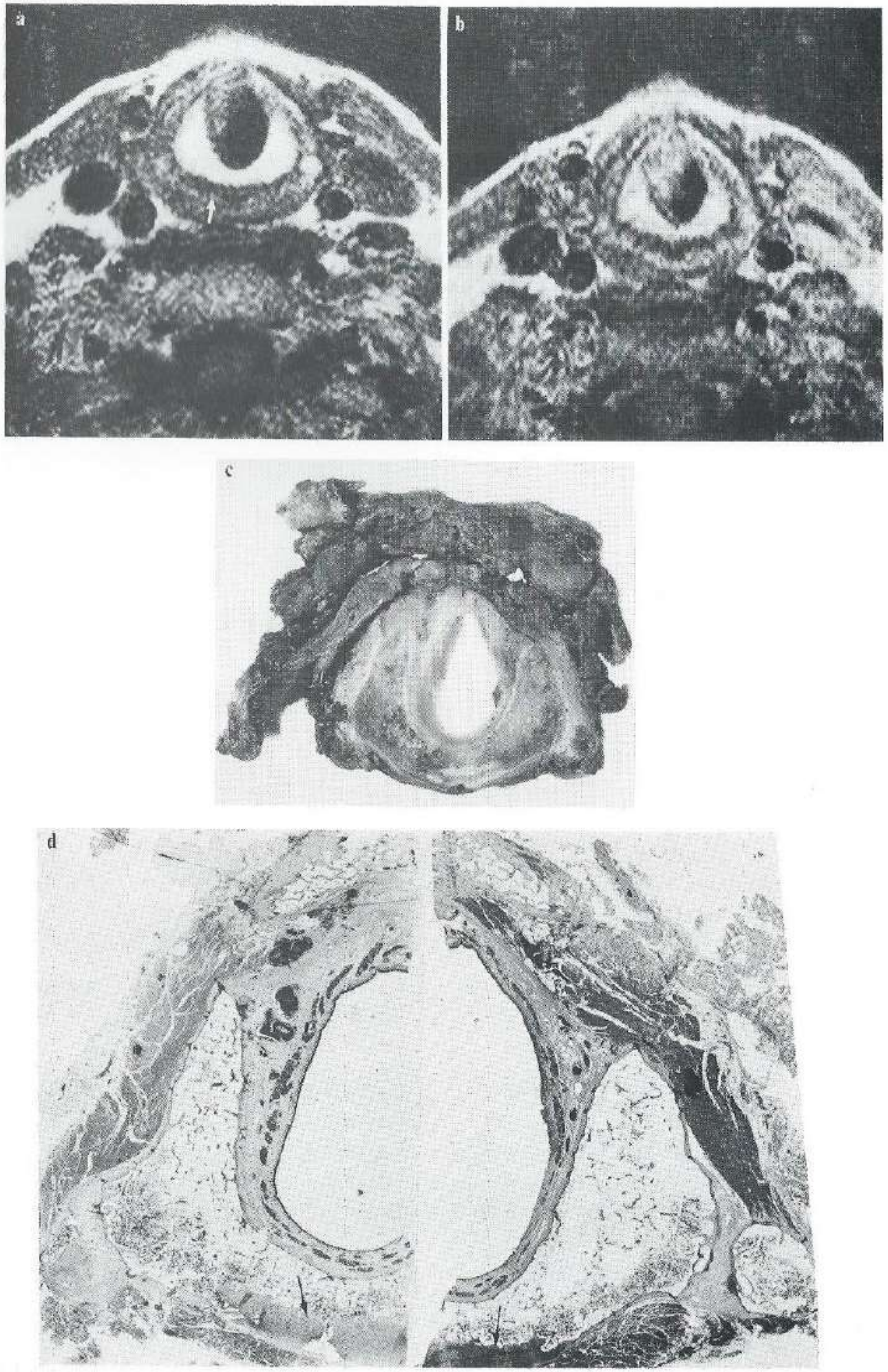

Fig.7. Same patient as in Fig.2.
Fig.7a. T1-weighted, axial image at subglottic level shows that the cricoid is almost entirely ossified. Its dorsal portion (arrow) has an intermediate signal intensity.
Fig.7b. Proton density image still visualizes the dorsal part of the cricoid with intermediate signal intensity.
Fig.7c. Macroscopic section at about the same level.
Fig.7d. Microscopy proves that the corresponding area (arrows) of intermediate signal intensity on both MRI-scans is not ossified.

at the corresponding level demonstrate that the tumor is entirely located within the region of intermediate signal intensity seen on fig.5a. The ossified and abnormal posterior portion of the right thyroid lamina (Fig.5c and 5d) corresponds to the area of cartilage having increased signal intensity (Fig.5b). Bone marrow is replaced by cancer with fibrous and inflammatory changes. Anteriorly, a small segment of normal, non-ossified cartilage borders the invaded region (Fig.5c and 5d), which corresponds to the area of intermediate signal intensity shown on fig.5b.

In the same patient an obvious asymmetry between the right and left thyroid laminae is also found at the level of the true vocal cords: the tumor has destroyed the dorsal portion of the right thyroid lamina (Fig.6a and 6b). Pathological tissue is shown with increased signal intensity on Fig.6b (proton density image), enhancing the contrast between bone and surrounding pathological tissue. Histopathological examination (Fig.6c and 6d) reveals that cancer has destroyed cartilage, the bony trabeculae being disseminated amid malignant tissue.

Consequently, malignant invasion of the thyroid cartilage is seen on T1-weighted image with intermediate signal intensity, whereas on the proton density image it is seen with increased signal intensity.

Cricoid cartilage

On fig.7a and 7b (T1- and proton density images) the cricoid is seen as a central high signal area surrounded by a low intensity rim. In this case a small edge on the posterior wall of the cricoid has a lower signal intensity. On both sides, the inferior cornu of the thyroid cartilage is clearly visible lateral to the cricoid. Macro- and microscopic examinations at about the same level (Fig.7c and 7d) demonstrate, that the cricoid cartilage is almost entirely ossified, and is composed by fat, haemopoietic tissue and bony trabeculae. Dorsally, the cricoid is not ossified; this correlates with the MRI findings.

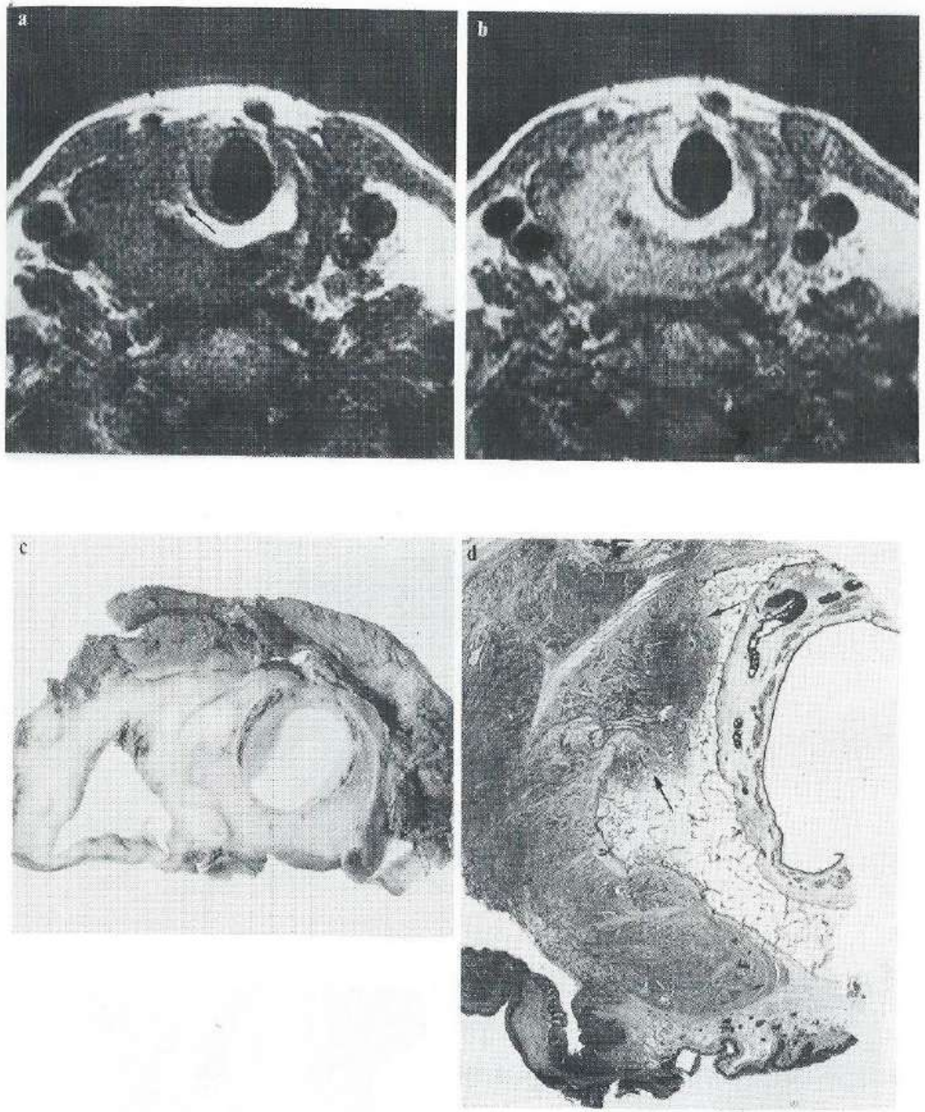

Fig.8. Same patient as in Fig.5.
Fig.8a. T1-weighted, axial image at the subglottic level shows minor infiltration (arrow) of the cricoid by a mass of intermediate signal intensity.
Fig.8b. Proton density image visualizes area, suspect for infiltration, with increased signal intensity.
Fig.8c. Sliced surgical specimen demonstrates that the right wall of the cricoid is invaded by tumor.
Fig.8d. Microscopic section of the right half demonstrates cancer infiltrating the cricoid (arrows).

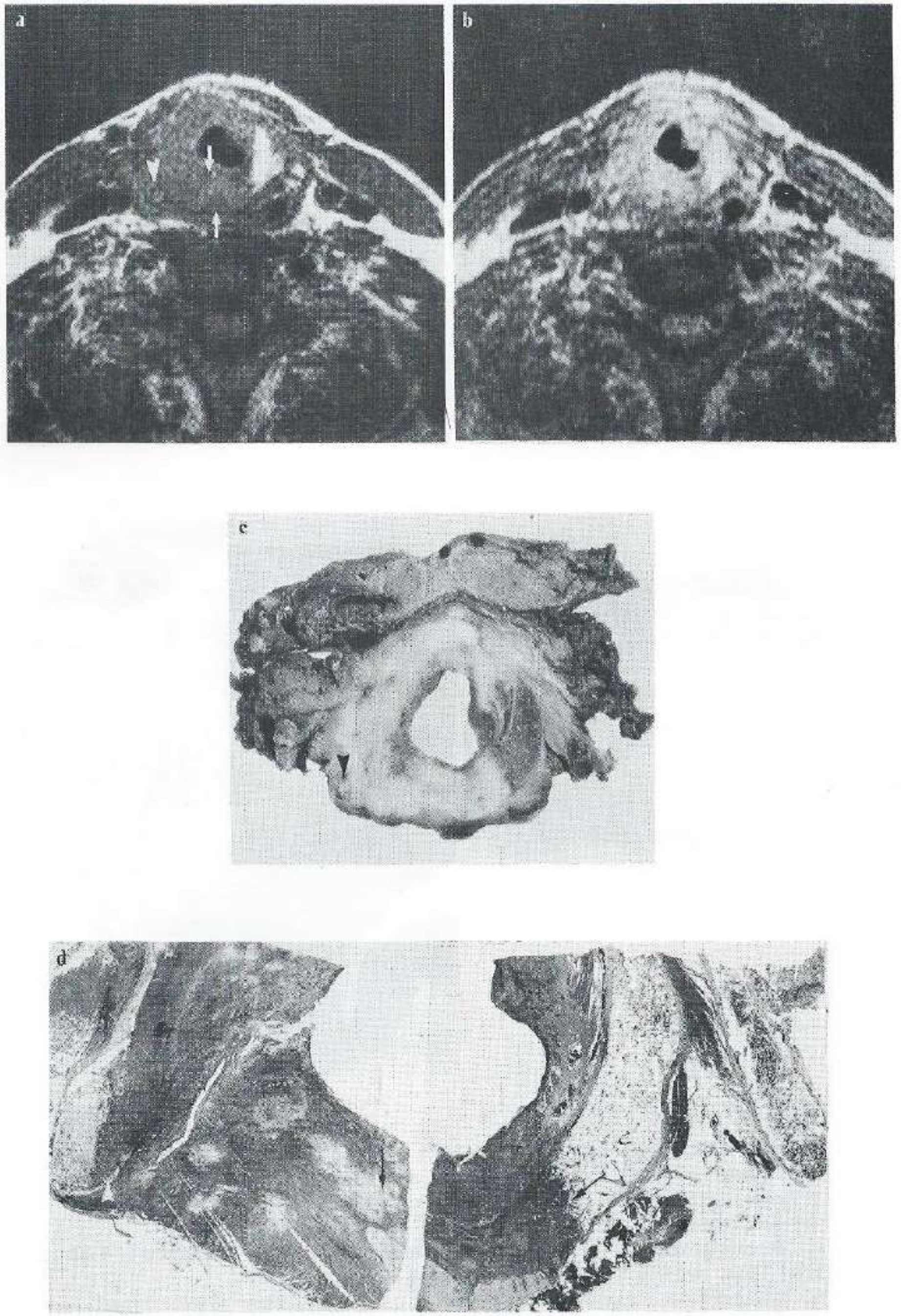

Fig.9. Same patient as in Fig.4.
Fig.9a. T1-weighted, axial image at subglottic level shows large tumorous area invading the right inferior cornu of the thyroid cartilage (arrowheads) and the greater part (arrows) of the cricoid.
Fig.9b. Proton density image visualizes tumor with increased signal intensity.
Fig.9c. A similar contour of the tumor, invading both the right inferior cornu (arrowheads) and the cricoid, is macroscopically seen.
Fig.9d. Microscopic section shows cancer infiltrating the cricoid (arrows) and the right inferior cornu (arrowhead) of the thyroid cartilage.

Fig.8a (T1-weighted) shows that the cricoid lamina is completely ossified, only a small interruption due to a mass of intermediate signal intensity is found in its right portion. This defect within the cricoid shows increased signal intensity on Fig.8b (proton density image), which raises the suspicion of cartilage invasion. Macro- and microscopic examinations (Fig.8c and 8d) confirm tumor infiltration into the ossified cricoid. Concerning tumor site and contour, a striking correlation between pathologic findings and MR images was found. Histopathologic examination (Fig.8d) demonstrates cancer, invading the ossified cricoid.

Gross invasion of cartilagineous structures is seen on Fig.9a and 9b: the right inferior cornu of the thyroid cartilage and the greater part of the cricoid lamina are imaged with intermediate (Fig.9a) and increased (Fig.9b) signal intensity. This finding is suggestive of massive invasion by cancer. MRI findings were confirmed by examination of the surgical specimens (Fig.9c and 9d).

Thus, signal intensities of normal and invaded cricoid cartilages as shown by MRI are similar to those of normal and invaded thyroid cartilages.

Arytenoid cartilage

Fig.6a and 6b show ossification of both arytenoids. On fig.6a (T1-weighted) an area with homogeneous intermediate signal intensity, suspect for cancer, borders on the right arytenoid. No evidence of invasion is seen. Slices of the surgical specimens at the corresponding level (Fig.6c and 6d) show almost complete ossification of the arytenoids. Their vocal processes are still cartilagineous. Cancer borders on the right arytenoid, but no signs of invasion are seen.

DISCUSSIONS

The signal intensity of tissues as imaged by MRI is

predominantly dependent upon their proton density and the highly heterogeneous distribution of the T1 and T2 spin-relaxation rates in the various tissues. Protons raising MRI signals are mainly located in tissue water and lipids. Protons in solid structures (e.g. bone) do not contribute to the signal. Tissue contrast may be manipulated by choosing variable pulse-sequences (TE,TR), accentuating the effects of differences in T1 or T2 spin-relaxation rates. As a rule, tumor tissue is imaged with intermediate signal intensity on T1-weighted images, whereas on more T2-weighted images its signal intensity increases (14,15).

Primary laryngeal cancer is constantly seen on T1-weighted images as a homogeneous mass of intermediate signal intensity, which in all cases is slightly higher than the signal intensity of the infrahyoid muscles. Site, extension and contour of the tumor mass as shown by axial MRI scans corresponds to the actual configuration of the lesion (10). T2-weighted images, obtained by using a long TR (1500ms) and TE (76ms), have a low signal-to-noise ratio (not shown), this statement being in agreement with Lufkin et al (11). Using a long TR (1500ms) and a short TE (38ms), T1 as well as T2 tissue-characteristics are accentuated on the images obtained. In our opinion, this technique is a good compromise between a reasonable signal-to-noise ratio and an adequate expression of T2-values, because tumor tissue is still seen with increased signal intensity.

The epiglottic cartilage and the vocal processes of the arytenoids are composed of yellow fibrocartilage, which usually does not ossify. The T1-weighted image (Fig.1a) demonstrates the epiglottic cartilage with intermediate signal intensity. On the proton density image (Fig.1b) it is seen with increased signal intensity compared to T1-weighted images. On both types of images, contrast between tumor and cartilage is minimal. Although the vicinity of a tumor to the epiglottic cartilage may be suspicious for invasion, invasion of the epiglottic cartilage may not be definitely demonstrated or excluded by

MRI. This finding agrees with earlier experiences (10).

The cricoid, thyroid and the greater part of the arytenoid consist of hyaline cartilage. These hyaline cartilages begin their ossification between the ages of 20 and 25 years. Keen and Wainwright concluded that the microscopic changes essentially consist of normal endochondral ossification (16). It remains impossible to formulate precise laws about the macroscopic pattern of this ossification, as there is a high degree of variability between individuals. Furthermore, in relation to age, ossification proceeds in a very irregular way (17). At an age when cancer is likely to occur, cartilages consist of variable amounts of hyaline cartilage, ossified tissues and bone marrow, the latter containing fat and haemapoietic tissues lying within thin trabeculae of bone.

Next MRI appearances of normal, non-ossified and ossified, hyaline cartilages are discussed. Non-ossified hyaline cartilage is imaged with intermediate signal intensity on T1-weighted as well as on proton density images (Fig.2-6). Increasing the T2-accentuation, particularly by delaying TE, non-ossified cartilage is seen with lower intensity (not shown). Tissue contrast between non-ossified cartilage and malignant tissue is minimal on T1-weighted images (Fig.2a, 3a), but is remarkably enhanced on proton density images as the signal intensity of malignant tissue strongly increases (Fig.2b, 3b). Ossified cartilage is composed by compact bone which surrounds bone marrow. On T1-weighted as well as on proton density images it has a typical three-layered appearance: a central high signal area on both sides bounded by low intensity rims (Fig.3-9). Because of its lack of mobile protons, cortical bone appears black, independently of the choice of the pulse sequences (15). Bone marrow mainly consists of fatty tissue, and in a smaller proportion, of haemopoietic tissue. With aging, there is a progressive decrease of haemapoietic tissues in bone marrow due to replacement by fat (18). This explains why T1 and T2 characteristics of bone marrow are very similar to those of fat. As a rule,

	T1 - weighted	Proton density
Elastic cartilage	Intermediate	Increased
Hyaline cartilage	Intermediate	Intermediate
Compact bone	Low	Low
Bone marrow (fatty-, haemapoietic-)	High	High
Cancer (invading and non-invading)	Intermediate	Increased

Table 1. Relative signal intensities of different tissue types on T1-weighted and proton density images

bone marrow is seen with high signal intensity on T1-weighted images, much higher than the signal intensity due to tumor.

In the majority of cases in which cartilage invasion by cancer occurs, the invasion remains confined to its ossified portions (19). On T1-weighted images cancer, invading cartilage is shown as an area of intermediate signal intensity (Fig.4a,6a,8a and 9a). If the medullary space is involved, tumor is still seen with intermediate signal intensity, which is different from the high signal intensity of normal bone marrow but similar to the MRI-appearance of non-ossified cartilage (Fig.4a,6a). As CT might not detect gross invasion of the medullary space, MRI may provide additional diagnostic information.

Differentiating invaded cartilage from non-ossified cartilage is a major diagnostic challenge in order to confirm or exclude cartilage invasion. Whereas both tissues are seen on T1-weighted images with intermediate signal intensity (Fig.4a,6a), they are imaged with high contrast on proton density images (fig.4b,6b), because tumor tissue, invading and non-invading, is found with an increased signal intensity and non-ossified cartilage still has intermediate signal intensity (Fig.2-7).

CONCLUSIONS

Gross cartilage invasion is clearly shown by MRI. In order to be able to diagnose minor invasion of hyaline cartilages the combined use of SE T1-weighted and proton density images can be very helpful (Fig.4,8). In our experience, it is possible to separate affected cartilage from normal bone marrow by the use of T1-weighted images on the one hand, and from non-ossified cartilage by proton density images on the other (table 1). Comparative assessment of MRI and CT results should ascertain the value of this statement.

REFERENCES

1. Gerritsen, G.J., Valk, J., van Velzen, D.J. and Snow, G.B. Computed Tomography: a mandatory investigational Procedure for the T-staging of advanced LaryngealCancer. Clin. Otolaryngol., 11,307-316, 1986.

2. Mafee M.F., Schild, J.A., Michael, A.S., Choi, K.H. an Capek, V.: Cartilage Involvement in Laryngeal Carcinoma: Correlation of CT and Pathologic Macrosection Studies. J. Comput. Assist. Tomogr., 8(5):969-73, 1984.

3. Hoover, L.A., Calcaterra, T.C., Walter, G.A. and Larrson, S.G. Preoperative CT Scan Evaluation for Laryngeal Carcinoma: Correlation with Pathological Findings. Laryngoscope, 94:310-315, 1984.

4. Silverman, P.M., Bossen, E.H., Fisher, S.R., Boyce Cole, T., Korobkin, L. and Halvorsen, R.A. Carcinoma of the Larynx and Hypopharynx: Computed Tomographic-histopathologic Correlations. Radiology, 151:697-702, 1984.

5. Yeager, V.L., Lawson, C and Archer C.R. Ossification of the Laryngeal Cartilages as it relates to Computed Tomography. Invest Radiol, 17:11-9, 1982.

6. Archer C.R. and Yeager V.L. Computed Tomography of Laryngeal Cancer with Histopathological Correlation. Laryngoscope, 92:1173-1180, 1982.

7. McArdle, C.B., Bailey, B.J. and Amparo, E.G. Surface Coil Magnetic Resonance Imaging of the Normal Larynx. Arch. Otolaryngol. Head Neck Surg., 112:616-622, 1986.

8. Castelijns, J.A., Doornbos, J., Verbeeten, B., Jr, Vielvoye, G.J. and Bloem, J.L. Magnetic Resonance Imaging of the Normal Larynx. J. Comput. Assist. Tomogr., 9(5):919-25, 1985.

9. Lufkin, R.B. and Hanafee, W.N.: Application of Surface Coils to MR Anatomy of the Larynx. A.J.N.R., 6:491-497, 1985.

10. Castelijns, J.A., Kaiser, M.C., Valk, J., Gerritsen, G.J. and van Hattum, A.H. and Snow, G.B. MRI of Laryngeal Cancer. J. Comput. Assist. Tomogr., 11(1), 1987. (in press)

11. Lufkin, R.B., Hanafee, W.N., Wortham, D and Hoover, L.: Larynx and Hypopharynx: MR Imaging with Surface Coils. Radiology, 158:747-754, 1986.

12. Vriapangse, C., Mancuso, A., Fitzsimmons, J. and Gainsville. Value of Magnetic Resonance Imaging in Assessing one Destruction in Head and Neck Lesions. Laryngoscope, 96:284-291, 1986.

13. Michaels, L. and Gregor, R.T. Examination of the Larynx in the Histopathology Laboratory. J. Clin. Pathol., 33:705-709, 1980.

14. Valk, J., MacLean, C. and Algra, P.R. The Clinical Application of N.M.R. tomography. In: Valk, J., eds. Basic principles of nuclear magnetic resonance imaging. Amsterdam- New York- Oxford: Elsevier, 115-140, 1985.

15. Wehrli, F.W., MacFalk, J.R. and Newton, T.H.: Parameters determining the Appearance of NMR Images.In: Advanced imaging techniques. Modern neuroradiology, Vol.2. Newton T.H. and Potts D.G. (Eds). Clavandel Press, San Anselmo, C.A., pp. 81-117, 1983.

16. Keen J.A. and Wainwright J.S. Ossification of the thyroid, cricoid and arytenoid cartilages. S. Afr. J. Lab.Clin.Med.,4:83-108, 1958.

17. Roncallo, P. Researches about Ossification and Conformation of the Thyroid Cartilage in Men. Acta Otolaryng. 36,110-134, 1948.

18. Dooms, G.C., Fisher, M.R., Hricak, H., Richardson, M., Crooks, L.E. and Genant, H.K. Bone Marrow Imaging: Magnetic Resonance Studies related to Age and Sex. Radiology, 155:429-432, 1985.

19. Kirchner, J.A. Two hundred laryngeal Cancers: Patterns of Growth and Spread as seen in serial Sections. The Laryngoscope, 87:474, 1977.

Chapter 7. DIAGNOSIS OF LARYNGEAL CARTILAGE INVASION BY CANCER: COMPARISON OF CT AND MRI

Authors: Jonas A. Castelijns, M.M. (1)
Geerten J. Gerritsen, M.D. (2)
Mark C. Kaiser, M.D. (1)
Jaap Valk, M.D. (1)
Thea E.G. van Zanten, M.D. (1)
Richard G. Golding, F.R.C.P. (1)
Chris J.L.M. Meyer, M.D. (3)
Lex H. van Hattum, M.D. (3)
Michiel Sprenger, Ph.D. (4)
P. Dick Bezemer, Ph.D. (5)
Gordon B. Snow, M.D. (2)

(1) Department of Radiology
(2) Department of Otolaryngology/ Head and Neck Surgery
(3) Department of Pathology
(4) Instruments Department
(5) Medical Statistics

Institution: Free University Hospital
Amsterdam
The netherlands

Abstract

Forty-two patients with laryngeal carcinomas were examined by Computed Tomography (CT) and Magnetic Resonance Imaging (MRI). The accuracy of CT and MRI in showing cartilage invasion was evaluated in 16 patients by comparing the results to pathological findings.

Calcified cartilage, invaded by cancer, is very frequently seen with CT as having an intact contour, whereas tumor approaching non-ossified cartilage may simulate cartilage invasion. On the other hand, T1-weighted MR images demonstrate invaded bone marrow of ossified cartilage with intermediate signal intensity, which allows to differentiate it from normal bone marrow. Proton density images show tumor with increased signal intensity, which permits to differentiate the latter from non-ossified cartilage. In our experience, specificities of CT and MRI were approximately equal, 91% and 88%, respectively. CT has a definitively lower sensitivity than MRI (46% and 89%, respectively). Gross movement artifacts, which resulted in non-diagnostic images, occurred in 16% of the MRI examinations.

We recommend MRI as the modality of choice in the diagnosis of cartilage invasion.

Index terms: Larynx, computed tomography; Larynx, magnetic resonance studies; Larynx, neoplasms; Laryngeal cartilages, Magnetic resonance studies

INTRODUCTION

The introduction of computed tomography (CT) has contributed significantly to the study of larynx and hypopharynx. The important value of CT in the diagnostic evaluation of laryngeal cancer was found in its ability to visualize submucous extension of tumor and, in particular, gross cartilage invasion (1). However, CT failed in detecting minor cartilage invasion, due to extreme variations in calcifications (2,3). In a recent publication on advanced laryngeal cancer unrecognized cartilage invasion occurred with a frequency of 25% (4).

Compared to CT, Magnetic Resonance (MR) imaging, with its improved soft-tissue contrast and its ability to perform multiplanar imaging, is an appealing modality for the study of head and neck pathology. The use of specially designed surface coils has provided the possibility to obtain high-signal and high-resolution MR images of the neck with excellent soft tissue delineation (5,6,7,8). A previous study showed, that although the patients suffered from dyspnea MRI succeeded to provide diagnostic images by using shorter scan times by an appropriate choice of pulse parameters, acquisition matrices and a minimal number of slices (14). In our hands MR examinations failed in patients with recurrent tumors after irradiation treatment, because distinction between residual or recurrent tumor, radiation fibrosis and edema was not possible (14). In a previous report, it was stated that by the combined use of T1-weighted and proton density images in the axial plane MRI is a promising additional tool in the diagnostic work-up of cartilage invasion in non previously treated patients. T1-weighted axial images permit differentiation between pathological and normal bone marrow. Proton density axial images allow separation between non-ossified cartilage and tumor tissue (9,10).

In the present study we compared CT- and MR-appearances of laryngeal cartilage invasion by cancer in non previously treated patients by using macro- and microscopic specimens as a standard of reference. In addition, we evaluated the diagnostic accuracy of MRI and CT for the diagnosis of cartilage invasion by comparing findings of multiple observers with histopathologic observations.

MATERIALS AND METHODS

Forty two patients with clinically proven and non previously treated laryngeal or hypopharyngeal cancer were examined by MRI and CT. Sixteen patients underwent surgery. Twenty six patients were treated with irradiation treatment. There were 38 (15) men and 4 (1) women with ages ranging between 46 (52) and 87 (76) years. Patients which underwent surgery are summarized between brackets. Primary carcinomas included 17 (4) supraglottic, 16 (8) (trans)glottic, 1 (0) subglottic and 8 (4) hypopharyngeal tumors. All patients had a squamous cell carcinoma.

The CT scans were obtained within two weeks before and after the MRI study: 22 scans were obtained before MRI, and 20 CT scans after MR scanning. MRI and CT were performed independently. To avoid bias caused by patient selection, our MR series was a consecutive one, although patients carrying a pacemaker, or being in poor clinical condition, had to be excluded from this study. At our institution, all patients with supraglottic tumor and patients with an advanced glottic or subglottic tumor, clinically staged as T3 and T4, routinely undergo CT-examination.

Imaging Techniques

CT scanning was performed using a third generation scanner, (Philips Tomoscan 350). The slice thicknesses used were 3 , 4.5 or 6 mm with no interslice gap. Field of view was 240x240 mm. The scanning time was 9 seconds. Patients were asked to breath normally.

MR images were obtained on a 0.6 Tesla superconductive system (Technicare- Teslacon I) using a half saddle-shaped surface coil placed around the anterior aspect of the neck.

Patient	Clin. st.	Computer Tomography					Magnetic Resonance Imaging					Pathology				
		e.c.	t.c.	l.a.	r.a.	c.c.	e.c.	t.c.	l.a.	r.a.	c.c.	e.c.	t.c.	l.a.	r.a.	c.c.
1	Supra T1b	=	=	=	=	=	+	+	-	=	=	++	++	=	=	=
2	Gl, T3	=	++	-	=	++	-	++	+	=	++	=	++	++	=	++
3	Supra, T3	=	-	=	=	=	=	+	=	-	=	=	++	=	=	=
4	Gl, T3	=	-	=	=	=	+	+	=	-	=	++	++	=	=	=
5	Gl, T3	-	++	+	-	-	++	++	-	++	++	++	++	=	++	++
6	Gl, T3	-	+	=	-	=	++	-	=	-	=	++	++	=	++	=
7	Gl, T3	++	++	+	=	++	++	++	++	-	+	++	++	++	=	=
8	Gl, T3	+	++	=	-	-	++	++	+	++	++	++	++	=	++	++
9	Gl, T3	=	+	=	=	=	++	++	+	-	+	++	++	++	=	++
10	Supra, T4	+	=	=	=	=	+	=	=	=	=	++	=	=	=	=
11	Supra, T1b	+	=	=	=	=	+	=	=	=	=	++	=	=	=	=
12	Gl, T3	=	=	=	=	=	+	+	+	=	-	++	++	++	=	=
13	Hypo, T3	+	+	=	=	=	+	++	=	++	-	++	=	=	=	=
14	Hypo, T3	+	+	=	++	-	-	+	-	+	=	++	++	=	=	=
15	Hypo, T4	-	++	=	++	=	-	++	=	-	++	=	++	=	++	++
16	Hypo, T2	=	=	-	=	=	=	=	=	=	=	=	=	=	=	=

Table 1. Clinical, CT-, MRI- and histopathological findings for the cartilages of each patient surgically treated

ec=epiglottic cartilage
tc=thyroid cartilage
la=left arytenoid cartilage
ra=right arytenoid cartilage
cc=cricoid cartilage

Supra=supraglottic tumor
Gl=glottic tumor
Hypo=hypopharyngeal tumor

++ evident cartilage invasion
\+ invasion probably
\- invasion improbably
= no invasion

differently from pathological findings

A multisection two-dimensional Fourier transform spin-echo (SE) pulse sequence was used in all cases. In sagittal, axial and frontal planes T1-weighted images were obtained using a repetition time (TR) of 200-400 ms and an echo time (TE) of 38 ms. In the axial plane we also generated proton density (SE 1500/38) and T2-weighted (SE 1500/76) images at each corresponding level. The acquisition of T1-weighted images was repeated four times for signal averaging, whereas the acquisition of proton density images and T2-weighted images was repeated two times. The slice-thickness used was 4 mm with a 3 mm interslice gap. The field of view was kept as small as possible (200x200 mm.), so that with a 256x192 acquisition matrix the T1-weighted images had a pixel resolution of 0.8x1.0 mm. Proton density and T2-weighted images had a 256x128 acquisition matrix. Acquisition times varied from 3 to 6 minutes. Patients were instructed to breath quietly and to refrain from swallowing.

Image Interpretation

All CT and MRI studies were retrospectively reviewed by two couples of two independent observers, who were asked to assess the presence of cartilage invasion. Observers of CT-scans (T.v.Z.,R.G.) were familiar with the evaluation of CT-examinations of the larynx. MRI-observers (M.K.,J.V.) were trained in evaluating MRI-examinations. The observers were "blind" about the result of the other study, about previus interpretations of the studies, and about clinical information and therapeutical decisions. At the end of the first set of readings, the reviewers of each modality compared their findings. In cases of discordance, both readers of each modality reviewed the examinations together to reach a consensus. The radiological and pathological findings are tabulated in table 1. There were 16 cases of disagreement (one observer diagnosed "probably" or "evident" cartilage invasion and the other one diagnosed "probably no" or "no" invasion) between CT-observers and 18 cases of disagreement between MR observers. To evaluate movement artifacts, all observers were asked whether adequate interpretation of images was possible.

Pathological Findings

Thirteen patients underwent total laryngectomy and three patients supraglottic laryngectomy (15 patients within one month after using both scans). The margins of resection of three supraglottic specimens being free of tumor, we concluded that the arytenoids and the cricoid were not invaded in these patients. The surgical specimens were obtained for organ sectioning. They were initially fixed for a period of 72 hours in a 4% formaldehyde solution; then decalcified by submersion of the specimen into Kristensen's solution for approximately two weeks. According to the recommendations of Michaels and Gregor (11), axial 4 mm. thick slices were cut parallel to the plane of the axial CT- and MR-images. Parts of all the slices were processed for microscopic examination.

RESULTS

-Epiglottic cartilage

An axial CT-scan (Fig.1a) at the supraglottic level of a male patient (no.16) with a hypopharyngeal lesion, clinically staged as T2N1, shows the left piriform sinus filled with a tumor mass. Tumor which is seen with increased density, does not extend to the region of the epiglottic cartilage. Therefore, invasion of this cartilage may be excluded. Patient also underwent MRI examination. On Fig.1b, which is a T1-weighted image, the same area is seen with intermediate signal intensity, suggestive of cancer. Because the epiglottic cartilage is surrounded by tissue having normally high signal intensity of fat, invasion of the epiglottic cartilage may be excluded. Microscopy confirmed MRI findings (Fig.1d).

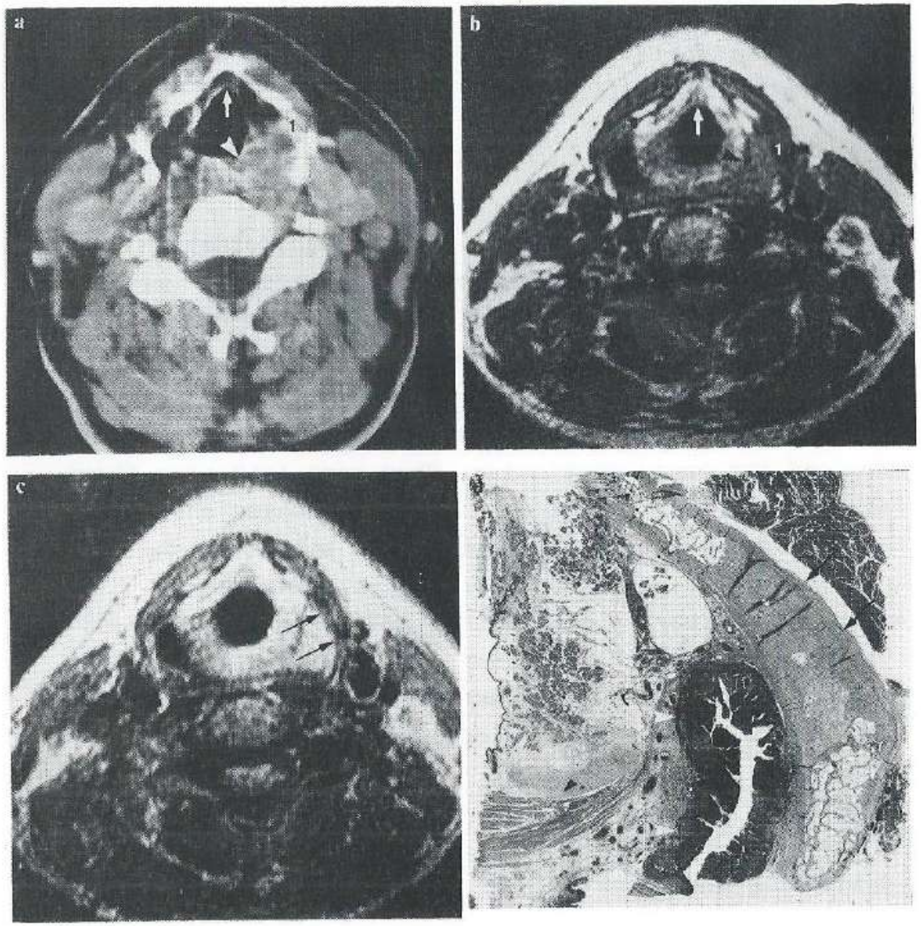

Fig.1. Patient with a T2 hypopharyngeal lesion.
Fig.1a. Axial CT-scan at a supraglottic level. Left piriform sinus is filled with tumor (arrowhead), which does not reach the area of the epiglottic cartilage (arrow). Left thyroid lamina (1) may have been invaded by tumor or consist of non-ossified cartilage.
Fig.1b. Axial, T1-weighted MR-scan (SE 400ms/38ms) at a corresponding level shows tumor (arrowhead) with homogeneously intermediate signal intensity. It does not approach the epiglottic cartilage area (arrow), but borders the left thyroid lamina (1).
Fig.1c. Proton density scan (SE 1500ms/38ms) at a corresponding level. Tumor, which is seen with increased signal intensity, has not invaded non-ossified cartilage (arrows), which is still seen with intermediate signal intensity.
Fig.1d. Left posterior quadrant of an axial sliced specimen. Microscopy shows tumor (arrowheads) bordering non-ossified cartilage (arrows).

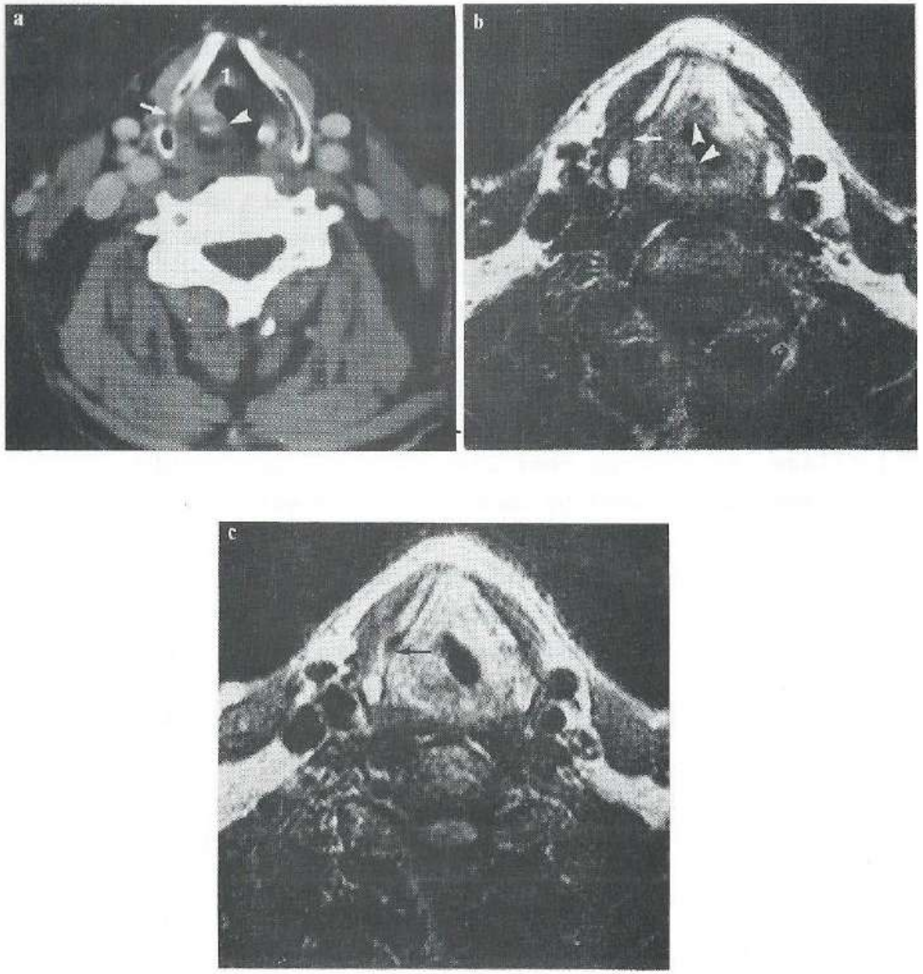

Fig.2. Patient with a T4 transglottic lesion.
Fig.2a. Axial CT-scan, just above level of the false cords. Tumor (arrowhead) extends towards epiglottic cartilage (1), but no clear invasion is found. Thyroid cartilage is locally (arrow) seen with isodensity as tumor: invasion or non-ossified cartilage.
Fig.2b. Axial, T1-weighted MR image (SE 400ms/38ms) on a corresponding level shows tumor (arrowheads) invading the epiglottic cartilage. The medial wall of the thyroid cartilage is irregularly outlined (arrow).
Fig.2c. Proton density image (SE 1500ms/38ms) demonstrates tumor with high contrast compared to non-ossified cartilage (arrow) which is still seen with intermediate signal intensity.

An axial CT-scan (Fig.2a), just above the level of the false cords in a male patient (no.4) with a T3N0 transglottic lesion, shows thickening within the dorsal portion of the right paraglottic space (PGS). Tumor which is seen with increased density, also extends towards the pre-epiglottic space (PES). Our CT-observers concluded that the CT-scans do not show obvious invasion of the epiglottic cartilage. T1-weighted MR scan (Fig.2b) at the corresponding level shows tissue suspect for cancer, extending into the PES. Because of the close relation of tumor to the epiglottic cartilage, both MR-observers concluded that there might be invasion of epiglottic cartilage. Microscopy confirmed that the epiglottic cartilage was invaded by cancer (not shown).

In 6 patients there were false negative CT-interpretations and in another patient one false-negative MRI finding (table 1). Of the six false negative CT-examinations, five patients had (trans) glottic tumors (patient 4,5,6,9,12). Extension of the tumor into PES was underestimated, because the region around the epiglottic cartilage was neither seen with increased density nor was it enlarged by tumor. In contrast, MRI showed an abnormal intermediate signal intensity around the epiglottic cartilage.

-Thyroid cartilage

On Fig.1a the thyroid cartilage is irregularly, but symmetrically calcified. Tumor abuts on the left thyroid lamina, which has partly an isodensity, suggestive for tumor invasion or for non-ossified cartilage. The CT-observers concluded that invasion was absent. The T1-weighted MR (Fig.1b) shows tumor, suspect for cancer, bordering the left thyroid lamina. The proton density image (Fig.1c) shows tumorous tissue with increased signal intensity. The left thyroid lamina, adjacent to the tumor tissue, is still seen with intermediate signal intensity, indicating non-ossified cartilage. Malignant invasion is

unlikely, due to its regularly outlined medial wall. Pathological examination (Fig.1d) confirmed MRI findings.

On Fig.2a, tumor approaches the right thyroid lamina, and irregularity of the right lamina is found. Cartilage invasion may not be definitively proved, because tumor tissue may border on non-ossified cartilage. Both CT-observers concluded that there might be cartilage invasion. The corresponding T1-weighted MR scan (Fig.2b) shows a suspect area in the right PGS. The tumor appears to border on non-ossified cartilage, because both the T1-weighted (Fig.2b) and the proton density image (Fig.2c) show thyroid cartilage, adjacent to tumor tissue, with intermediate signal intensity. The medial wall of the thyroid lamina is irregularly outlined. MRI-observers concluded that there might be invasion of non-ossified cartilage. Microscopy (not shown) demonstrated minor invasion of non-ossified cartilage.

An axial CT-scan (Fig.3a), at the level of the false cords in a male patient (no.15) presenting with a T4 hypopharyngeal lesion, shows the right piriform sinus filled by a tumorous mass. The thyroid cartilage is almost entirely calcified. Because the medial wall of the right lamina shows a minimal irregularity adjacent to tumor tissue, one may conclude that minor invasion exists. Because at a lower level invasion of thyroid cartilage was more obvious, both CT-observers agreed that invasion of the right lamina exists. On the corresponding T1-weighted MR scan (Fig.3b), the pathological area includes the dorsal portion of the right thyroid lamina. Fig.3c (proton density image) shows that the pathological area entirely has an increased signal intensity. Although the cortical rim is intact, the dorsal extreme of the right thyroid lamina appears to be invaded. Ventrally, this area borders on non-ossified cartilage, still being imaged with intermediate signal intensity. Microscopy (Fig.3d) revealed that the dorsal extremity of the right thyroid lamina is invaded by pathological tissue: inflammatory and fibrous tissue with nests of cancer are present.

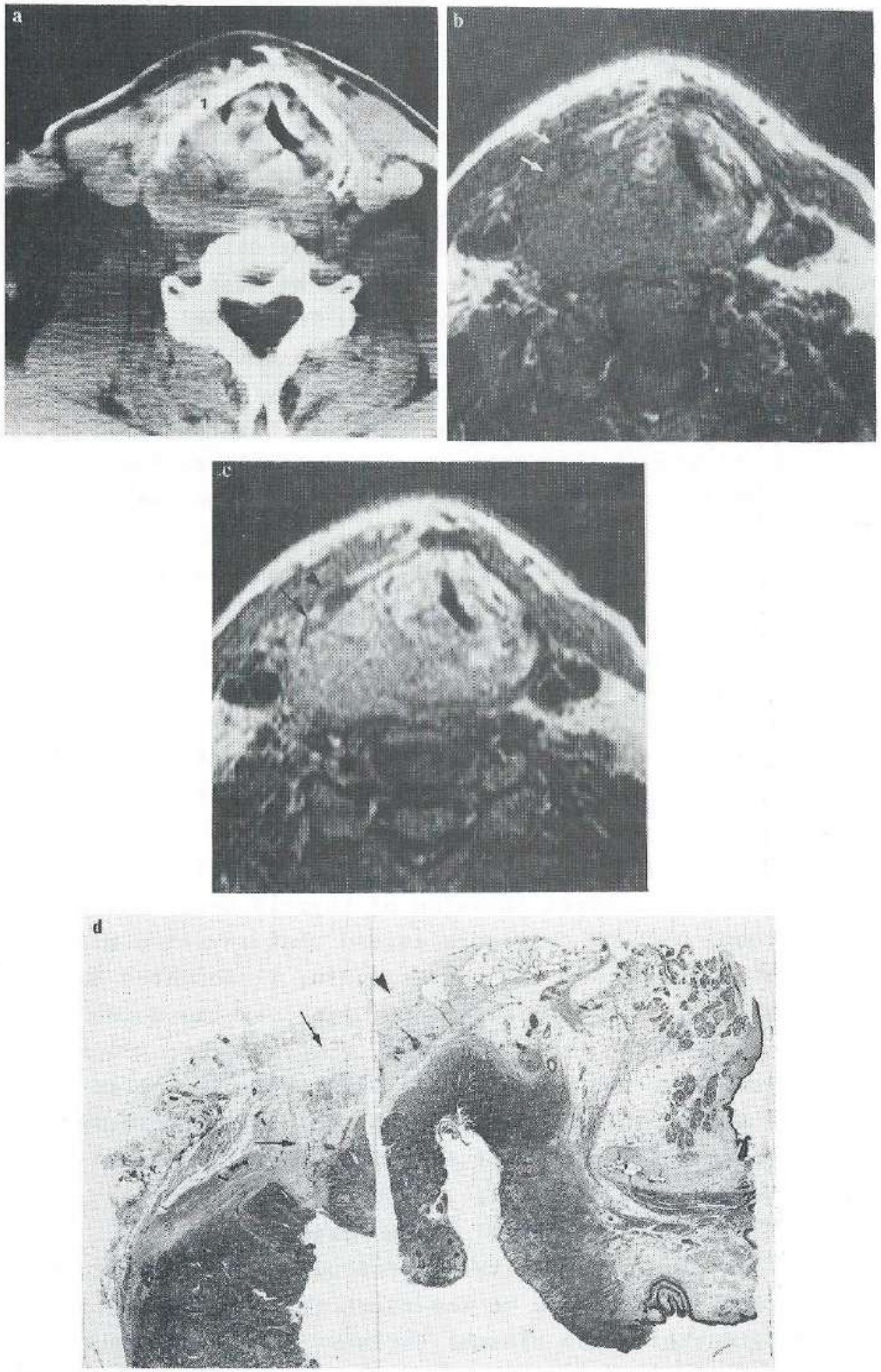

Fig.3. Patient with T4 hypopharyngeal lesion.
Fig.3a. Axial CT-scan at the level of the false cords. Tumor borders right thyroid lamina (1). The medial wall of the lamina is irregularly outlined, suggesting minor cartilage invasion.
Fig.3b. Axial, T1-weighted scan (SE 400ms/38ms) on a corresponding level shows right piriform sinus filled by a pathological mass. The dorsal extremity of the right thyroid lamina is seen with intermediate signal intensity (arrows).
Fig.3c. Axial, proton density image (SE 1500ms/38ms) demonstrates that the dorsal extremity of the right thyroid lamina is invaded by tumor, the cortical rim being intact (arrow). Ventrally this area borders non-ossified cartilage (arrowhead) which is still seen with intermediate signal intensity.
Fig.3d. Microscopy of an axial sliced specimen confirms MR- and contradicts CT-findings. A large tumor mass infiltrates (arrows) the dorsal extremity of the right thyroid lamina. Ventral to this area, non-ossified cartilage (arrowheads) is found which suggests cartilage invasion on the CT-scan.

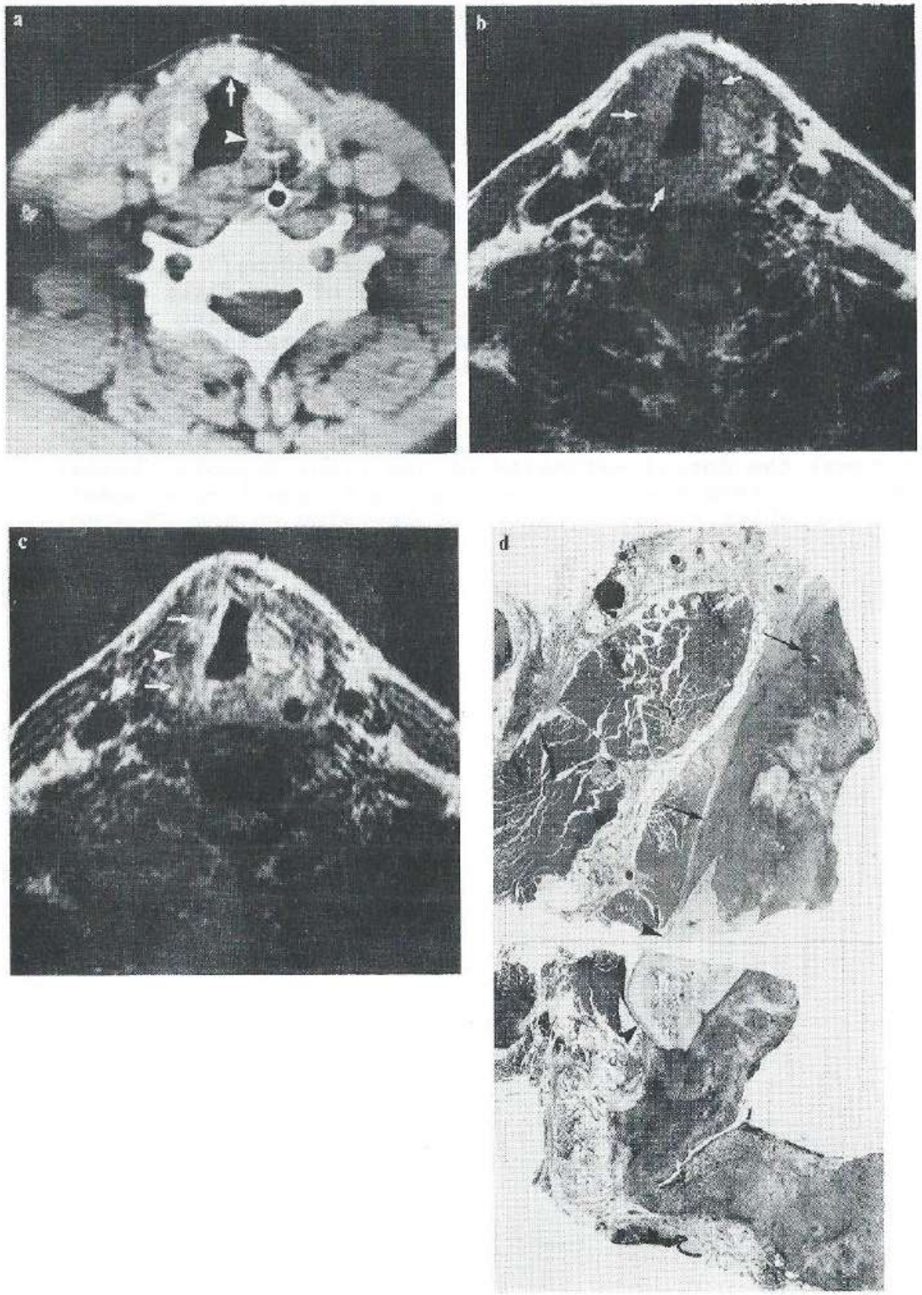

Fig.4. Patient with T4 glottic lesion.
Fig.4a. Axial CT-scan at the level of false cord. Tumor (arrowhead) is found in the dorsal portion of the left PGS. The right compartment and the anterior commissure (arrow) show no thickening. Whereas tumor is found on the left, calcification pattern is more affected in the right thyroid lamina.
Fig.4b. T1-weighted MR image (SE 400ms/38ms) shows cancer (arrows) with homogeneously intermediate signal intensity, extending circumferentially around the walls of the laryngeal cavity.
Fig.4c. The proton density image (SE 1500ms/38ms) shows almost the entire area between the thin cortical layers (arrows) of both thyroid lamina with increased signal intensity, demonstrating cartilage invasion by pathological tissues. A small area of non-ossified cartilage (arrowhead) is still seen with intermediate signal intensity.
Fig.4d. Microscopic examination of the axial sliced right lamina confirms the greater part of the right lamina invaded by tumor (arrows). Non-ossified cartilage (arrowheads) is found in agreement with MRI findings.

An axial CT-scan (Fig.4a), at the level of the false cords in a male patient (no.5) with a glottic lesion, clinically staged as T3N0, demonstrates thickening of the dorsal portion of the left PGS, whereas the right compartment and the anterior commissure show no thickening. Thyroid cartilage is irregularly and asymmetrically calcified. Whereas tumor is found on the left side, the calcification pattern is more affected in the right thyroid lamina. Both CT-observers concluded that invasion of the thyroid cartilage exists. On the T1-weighted MR image of the corresponding level (Fig.4b), an intermediate signal area extends circumferentially around the laryngeal cavity, which is suggestive for cancer in both the right and left PGS's. Thyroid cartilage is found almost entirely with intermediate signal intensity, indicating non-ossified cartilage or cartilage invasion. The dorsal portion of the left thyroid lamina appears to be ossified and not invaded by tumor. On the proton density image (Fig.4c), almost the whole area between the thin cortical layers of the right and left thyroid lamina has an increased signal intensity, representing invasion by pathological tissue. A small area in the right lamina still has intermediate signal intensity: non-ossified cartilage. Microscopic examination of the right lamina (Fig.4d) confirmed the MRI-findings of invasion of the ventral and dorsal portions of the right lamina, being separated by normal and non-ossified cartilage.

There were four false negative diagnoses by CT and one false negative diagnosis by MRI (table 1). All four false negative diagnosis by CT-observers (no.1,3,4,12) were due to the intact contour of the calcified cartilages. In contrast, MRI showed invasion of bone marrow or showed an irregular outline of the medial wall of non-ossified thyroid cartilage. In one patient (no.6), MRI failed to detect cartilage invasion due to movement artifacts on the proton density images. Both CT- and MRI-observers made one false positive interpretation in the same patient (no.13).

-Arytenoid cartilage

An axial CT-scan (Fig.5a) at the glottic level of the same patient as Fig.4 shows thickening in the left PGS. No tumor was seen around the right arytenoid. It was stated by CT-observers that the left arytenoid is invaded by tumor and that the right arytenoid is intact. T1-weighted MR scan (Fig.5b) demonstrates normal bone marrow of the left arytenoid, whereas the right arytenoid has an intermediate signal intensity. On the corresponding proton density scan (Fig.5c), the area of the right arytenoid has an increased signal intensity, resulting from the invasion by pathological tissue. Microscopic examination of the left half confirmed the MRI findings that the left arytenoid was not invaded by cancer (Fig.5d).

The failures of CT consisted of six false negative and two false positive diagnoses of invasion of the arytenoids. There were two false negative and three false positive interpretations of MRI-examinations (table 1). In five out of six CT-false negative cases of invasion (no.2,6,8,9,12), the arytenoid was neighbouring a tumor mass, but the calcification pattern and the contour of the cartilage was still intact. In contrast, MRI showed in this group in all but one patient a mass of intermediate signal intensity invading the marrow of the arytenoids. One false negative interpretation (no.6) was made by MRI-observers, because in this case MRI did not show abnormality. In the patient (no.5) of Fig.6, a false positive and a false negative diagnosis by CT-observers was caused by wrong interpretation of soft tissue swelling.

Invasion of the right arytenoid of one patient (no.14) was wrongly diagnosed by both CT- and MRI-observers. CT showed a hypodense arytenoid and MRI demonstrated an irregularly-shaped arytenoid among tumor tissue. In one patient (no.8) MRI-observers made a false positive interpretation, because the arytenoid was found among a large tumor mass. In a third false positive case (no.13), micrscopy showed fibrous tissue but no cancer in the

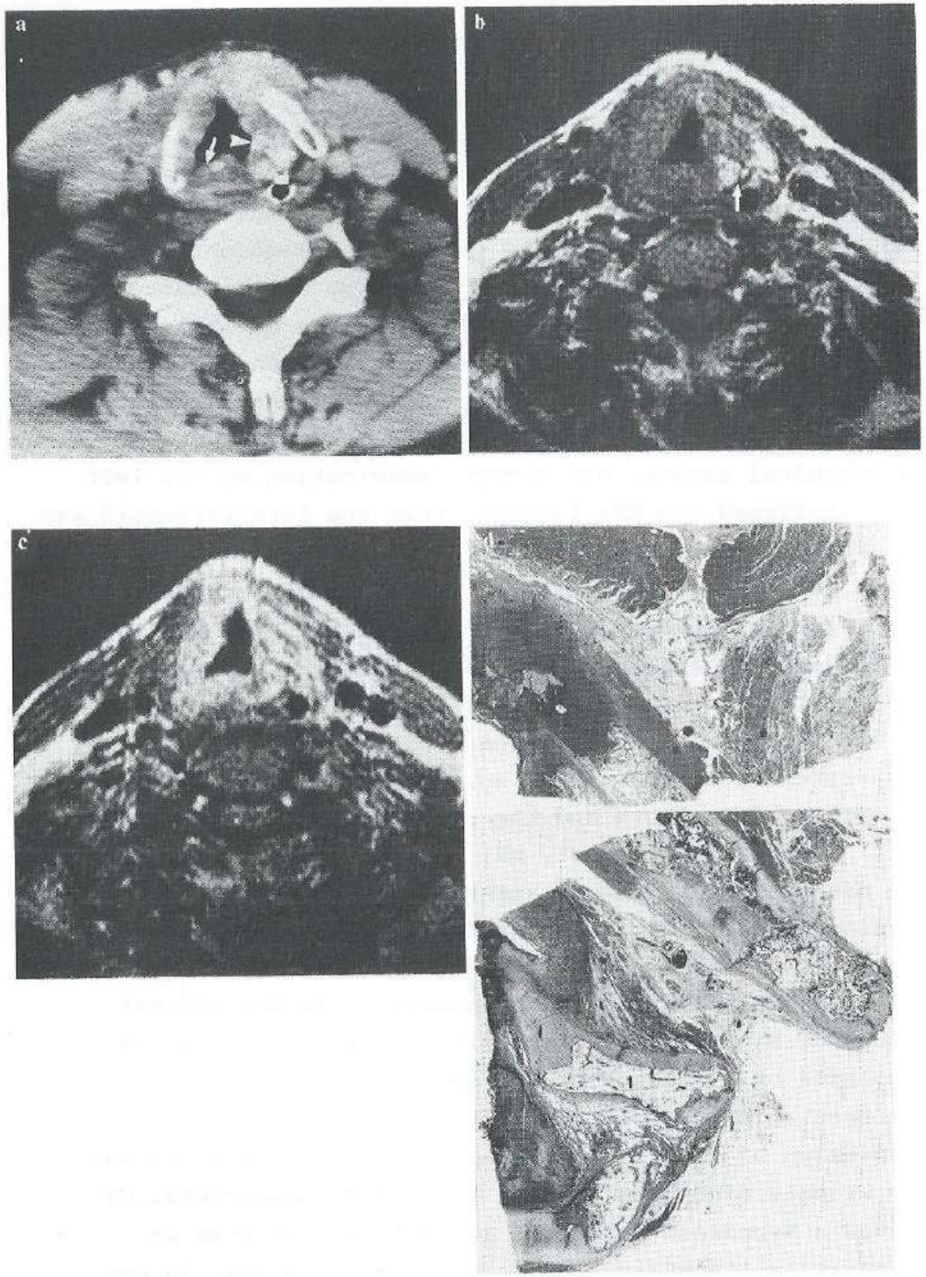

Fig.5. Same patient as Fig.4.
Fig.5a. Axial CT-scan at the level of the glottis. The surroundings of the left arytenoid (arrowhead) are thickened, but no tumor is found in the area of the right arytenoid (arrow).
Fig.5b. Axial, T1-weighted scan (SE 400ms/38ms) on a corresponding level shows that marrow of the left arytenoid (arrow) is not invaded by cancer, whereas the area around the right arytenoid has an intermediate signal intensity.
Fig.5c. Proton density scan (SE 1500ms/38ms) demonstrates the area of the right arytenoid with increased signal intensity suggesting cartilage invasion.
Fig.5d. Microscopic examination of an axial sliced specimen confirms that the left arytenoid (1) is not invaded by cancer.

arytenoid.

-Cricoid cartilage

An axial CT-scan at the subglottic level (Fig.6a) of the same patient as shown in Fig.3 (no.15) demonstrates the right piriform sinus filled with a large tumorous mass. The cricoid has a calcified rim, but no obvious invasion is found. MR images (Fig.6b and 6c) demonstrates minor invasion into the right border of the cricoid. Microscopic study confirmed MRI findings (Fig.6d).

Whereas CT-examinations of 4 patients were false negative diagnosed, MRI observers made no false negative interpretation. In 3 out of 4 patients (no.8,9,15) CT did not show invasion of the cricoid, because the calcification pattern and the contour of the cricoid were intact, or showed locally even more calcification. In contrast, MRI showed invasion of the bone marrow of the ossified cricoid. In one patient (no.5) CT-observers made a false positive interpretation, because the tumor was left sided, whereas the calcification pattern was affected on the right side. Both CT- and MRI-observers did one false positive interpretation in the same patient (no.7). An asymmetrical cricoid, bordering on a large tumor, caused a false positive interpretation on both CT- and MR-images.

Group of patients, of which no pathologic correlation was available.

Fig.7a is an axial CT-scan at the glottic level (Fig.7a) of a patient with a T2N0 glottic lesion. Both arytenoids appear not to be invaded, because the contours of both arytenoids is intact. In contrast, MR scans (Figs.7b and 7c) demonstrated obvious invasion of the right arytenoid.

On an axial CT-scan at the high subglottic level of the same patient (Fig.8a), a tumor is found, adjacent to the anterior commissure, but thyroid cartilage appears to be normal and calcified. The T1-weighted MR scan (Fig.8b)

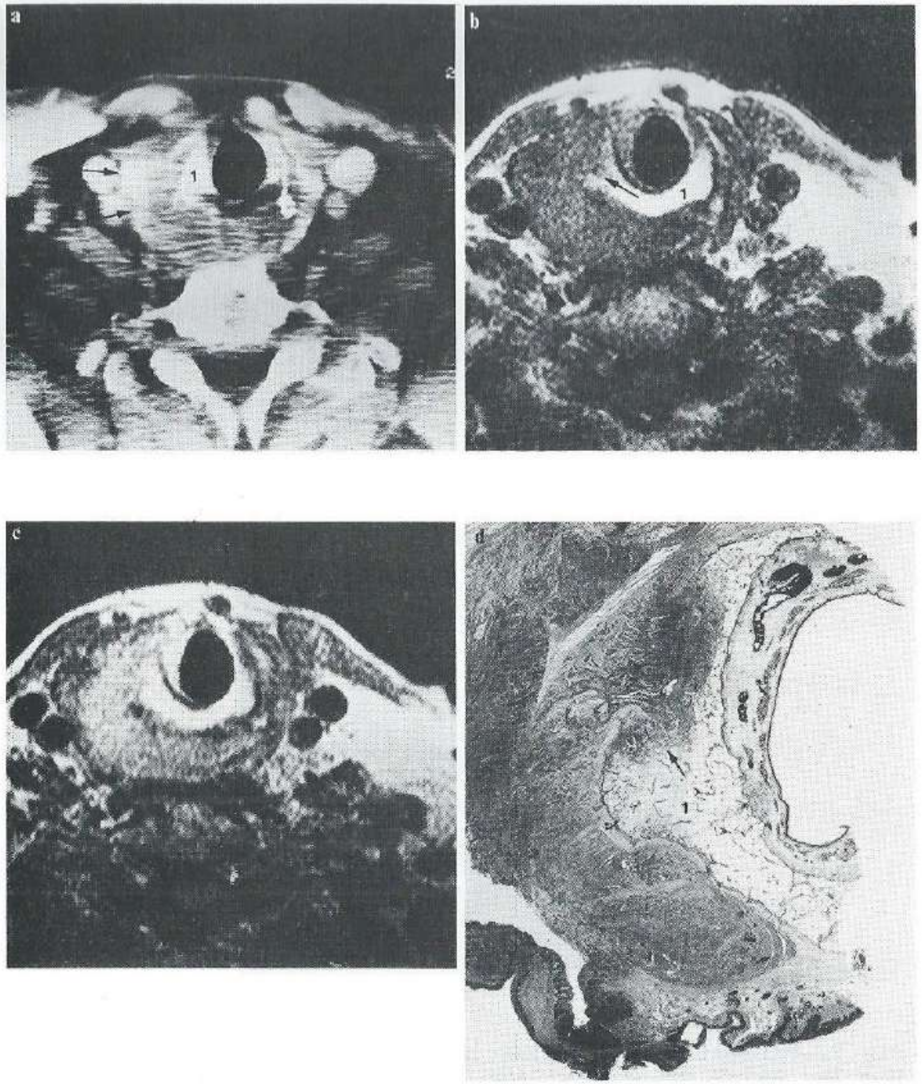

Fig.6. Same patient as in fig.3.
Fig.6a. Axial CT-scan at the subglottic level. Large tumor (arrows) borders the cricoid (1), but no invasion is found.
Fig.6b. Axial, T1-weighted scan (SE 400ms/38ms) at a corresponding level. Minor invasion (arrow) of the bone marrow of the cricoid (1) is found.
Fig.6c. Axial, proton density scan (SE 1500ms/38ms) shows entire tumor mass with increased signal intensity.
Fig.6d. Microscopic study of the axial sliced right part of the cricoid confirms MR finding of invasion (arrow) of the cricoid (1).

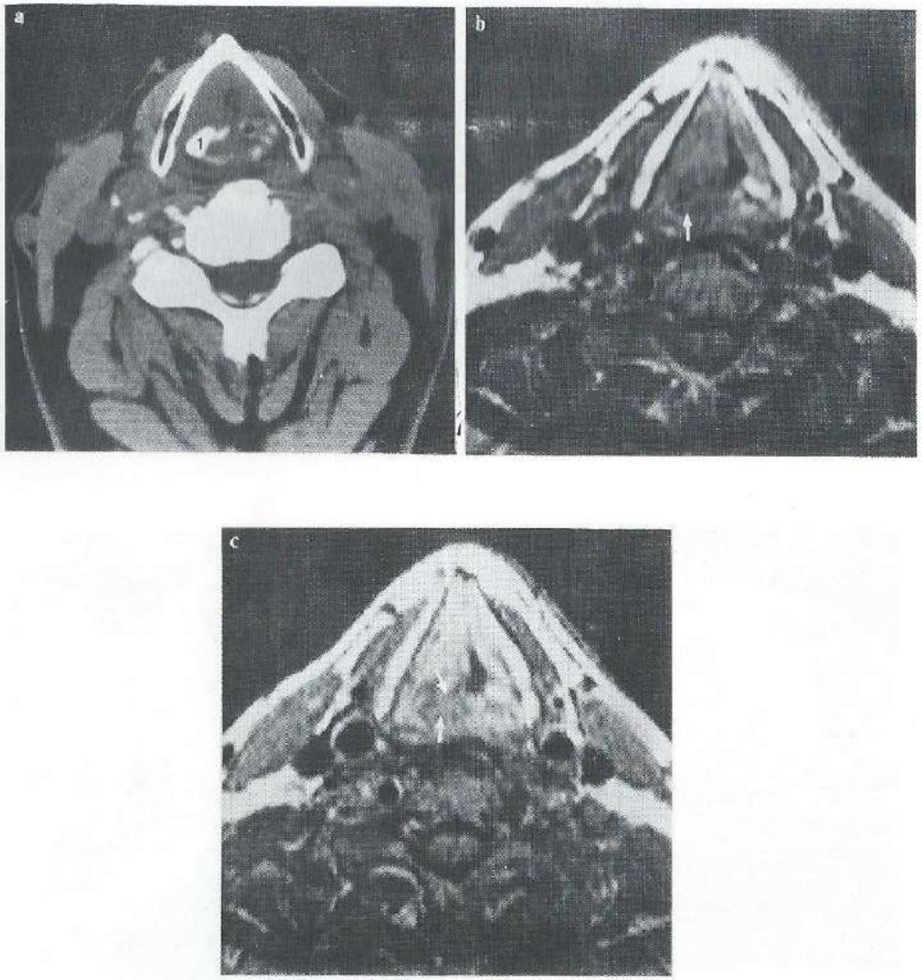

Fig.7. Patient with T2 glottic lesion.
Fig.7a. Axial CT-scan at the level of the glottis. No obvious invasion of the right arytenoid (1) exists.
Fig.7b. Axial, T1-weighted scan (SE 400ms/38ms) shows right arytenoid with intermediate signal intensity (arrow).
Fig.7c. Axial, proton density scan (SE 1500ms/38ms) shows bone marrow (arrows) in the right arytenoid with increased signal intensity which strenghtens the suspicion of cartilage invasion.

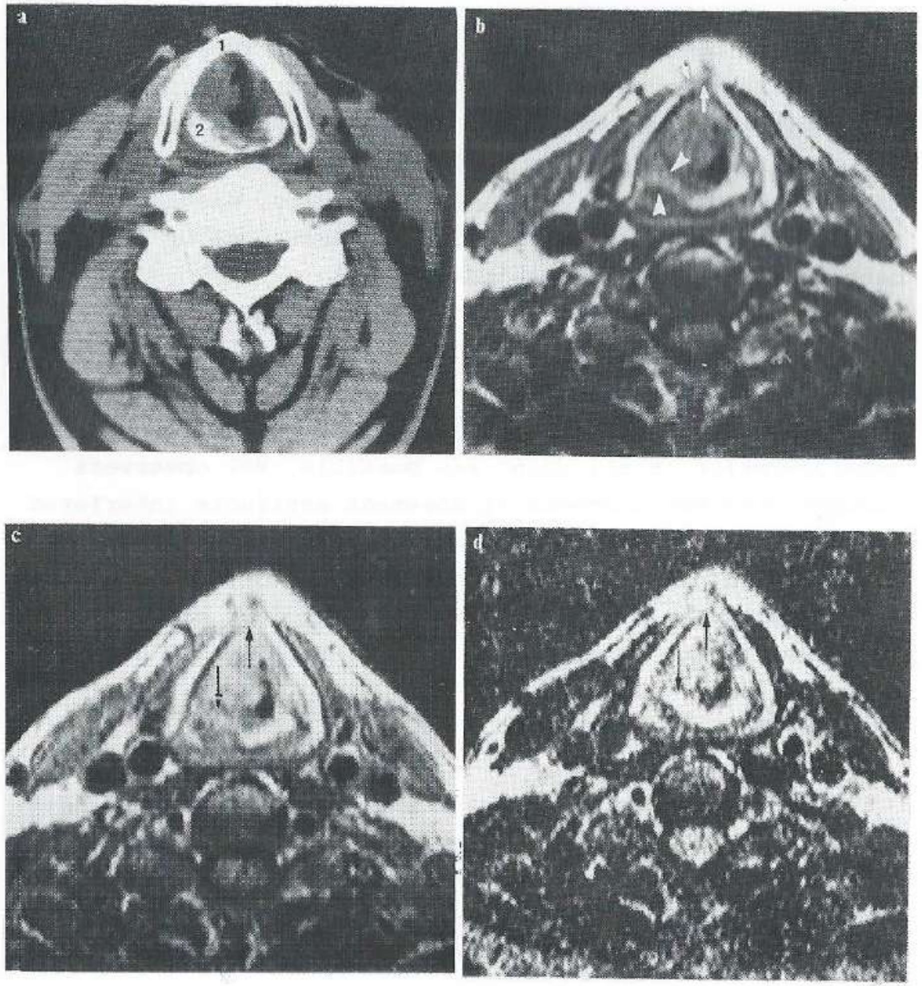

Fig.8. Same patient as in Fig.7.
Fig.8a. An axial CT-scan at a high subglottic level. Tumor is found narrowing the intralaryngeal lumen. Both thyroid (1) and cricoid (2) cartilages do not show obvious cartilage invasion.
Fig.8b. T1-weighted MR image (SE 400ms/38ms) suggests invasion of the right half of the cricoid cartilage (arrowheads) and the anterior commissure (arrows).
Fig.8c. Proton density image (SE 1500ms/38ms). The bone marrow of both thyroid and cricoid cartilages (arrows) is seen with increased signal intensity.
Fig.8d. T2-weighted images (SE 1500ms/76ms) demonstrate tumor, invading the cartilages (arrows), with even more signal intensity, indicating invasion by tumor.

suggests invasion of the anterior commissure and the right portion of the cricoid. Proton density and T2-weighted images (Fig.8d even more than Fig.8c) demonstrate that both regions are invaded by tumor.

In this group of patients, CT-readers observed evident cartilage invasion in 2 out of 26 patients, whereas MRI-observers concluded that in 6 patients one or more cartilages were evidently invaded.

Movement artifacts

Whereas CT-observers concluded that adequate interpretation of all scans was possible, MRI observers thought that the presence of movement artifacts interfered with adequate diagnosis in 7 out of 42 examinations. Four out of seven patients had chronic respiratory disease, or severe dyspnoea in their histories. Only four patients in the remaining group of 35 had chronic respiratory disease.

DISCUSSION

The laryngeal skeleton consists of 2 types of cartilages. The epiglottic cartilage consists of elastic cartilage and in general does not ossify. The cricoid, the thyroid cartilage, and the greater part of the arytenoids consist of hyaline cartilage and ossify. Often, the process of ossification and calcification is very irregular.

Detection of cartilage invasion is of great clinical importance. Complications due to irradiation treatment frequently occur in the presence of cartilage invasion. Demonstration of such an invasion may contribute to better selection between irradiation treatment and surgery (1). Partial laryngectomy is contraindicated if the cartilages have undergone invasion by tumor (2).

-Elastic cartilage: epiglottic cartilage

In the present study, invasion of the epiglottic cartilage was frequently false positive diagnosed, due to underestimation of the extension of tumor tissue into the PES. In contrast with earlier expectations (13,14), the MRI observers succeeded very well in detecting invasion of the epiglottic cartilage. T1-weighted images show tumor in high contrast with surrounding fat, normally present at the supraglottic level (Fig.1b,2b). Although the epiglottic cartilage is not always recognizable, the vicinity of tumor to the area of the epiglottic cartilage appears to be very suspicious for cartilage invasion. In contrast, if surrounding tissues of the epiglottic cartilage are seen with normally high signal intensity, invasion of the cartilage can be excluded (Fig.1b). Proton density images have little value for detection of invasion of the epiglottic cartilage, because contrast between pathological tissue and fat is minimal (Fig.1c,2c).

-Hyaline cartilage: thyroid, cricoid and arytenoid cartilages

The changes in hyaline cartilages are the subject of long discussion. Roncallo has reviewed the literature on this subject. Some authors consider ossification and calcification the same processes, whereas others maintain that calcification precedes ossification. Roncallo himself favours the view, originally put forward by Chievitz, that the two processes are absolutely independent of each other (15,16).

CT-appearance of normal hyaline cartilages is mainly determined by the state of calcification. The hyaline cartilages may be variably composed of calcified and non-calcified cartilage, or of bone with a marrow cavity (17). Uncalcified cartilage and bone marrow are much less well visualized on CT than calcified cartilage. The cortical rim of ossified cartilage with relatively abundant marrow may appear thinner than ossified cartilage, containing extensive bony trabeculae within the marrow cavity. Its margins may be indistinct (18).

MRI of hyaline cartilages correlates very well with the histological appearance: the process of endochondral ossification. As previously described, both T1-weighted and proton density images show non-ossified cartilage with intermediate signal intensity (9). Both types of images show ossified cartilage with a typically three-layered appearance: bone marrow showing high signal intensity and the bony rims having low signal intensity (5,9,14).

Cancer preferably invades ossified cartilage. Very frequently CT failed severely in detecting invasion of calcified thyroid, cricoid and arytenoid cartilages (Figs.3a,6a,7a,8a,etc.). The contour or pattern of calcification did not show deformities, whereas in some cases invaded cartilage was even seen with increased density. In all ossified cartilages, tumor may grossly invade the medullary space of the laryngeal cartilages, and may not be detected by CT if the surrounding bone is still intact. Tumor growth infiltrating the marrow cavity without destroying bony trabeculae or surrounding bone may escape detection because the presence of these bony structures enables reconstruction of an apparently normal cartilage on CT. In contrast, MRI is capable of showing early invasion of ossified cartilage. On T1-weighted images invasion of bone marrow is found with intermediate signal intensity (Fig.3b,6b,7b,8b).

In some patients CT may suggest invasion of cartilage (Fig.2a,3a). Because uncalcified or poorly calcified cartilage may not be well shown by CT, and therefore erosion or destruction may be simulated. In contrast, proton density MR images are capable of differentiating between invaded bone marrow and non-ossified cartilage (Figs.2c,3c), by showing tumor with increased signal intensity.

Sometimes, CT fails in detecting invasion of the arytenoid and cricoid, because no tumor was found around these cartilages (Fig.4a,5a). On CT, usual indicators of tumor are thickening of soft tissue structures, distortion

or displacement of the adjacent lumen, and the presence of an area with mostly increased density (18). Cancer localisation is not always possible by CT, and sometimes leads astray from assessing the real extent of tumor spread. MRI has greater possibilities than CT for the assessment of the site and the extension of tumor (14) (Figs.4b,5b).

In a minority of cases cancer invades non-ossified cartilage. Whereas cancer spreads rapidly in bone marrow of ossified cartilage after invading through the cortical rim, infiltration of non-ossified cartilage occurs gradually. Contrast between non-ossified cartilage and tumor is higher on proton density images than it is on T1-weighted images. The probability of invasion of non-ossified cartilage increases, if an irregularity of non-ossified cartilage adjacent to tumor is found on proton density images (Fig.2c).

Because diagnosis of cartilage invasion may result in laryngectomy, evaluation of false positive interpretations of MR images is most important. The MRI-observers made five false positive diagnoses of cartilage invasion. In one patient (no.13), the MRI-readers observed invasion in an arytenoid, which was filled with fibrous tissue. The four other false positive diagnoses were due to different reasons: difficult interpretation of invasion of non-ossified cartilage, low signal-to-noise ratio of some proton density images, irregularities of cartilages and movement artifacts.

The previous discussion indicates that "probable" and "evident" cartilage invasion, as shown by MRI, are good parameters for the detection of cartilage invasion and that "no" and "probably no" cartilage invasion, as shown by MRI, are good parameters for the absence of cartilage invasion. MRI findings in the patients, treated by surgery, would raise the clinical stage of all but three patients. To calculate the accuracy of the detection of cartilage invasion, the numbers of "probable" and "evident" cartilage invasion were summarized, and so were the numbers of "probably no" and "no" cartilage invasion. In our experience, specificities (percentage of cases, in which the absence of cartilage invasion was correctly diagnosed) of CT and MRI for detecting invasion of the laryngeal cartilages are approximately equal, resp. 39/43=91% and 38/43=88%. CT has a much lower sensitivity (percentage of cases, in which the presence of cartilage invasion was correctly diagnised) than MRI, resp. 17/37=46% and 33/37=89%.

We recommend MRI as the modality of choice for the diagnosis of cartilage invasion. If diagnostic use of MRI examinations of, for instance, patients with chronic respiratory disease is impossible by movement artifacts (in our hands 16% of the cases), CT will be necessary.

Summary.

MRI is superior to CT in detecting invasion of the laryngeal cartilages. Frequently calcified cartilage, invaded by cancer, is found on CT with an intact contour and intact calcification pattern. Tumor tissue bordering on non-calcified cartilage may simulate cartilage invasion. In contrast, MRI offers clear criteria to demonstrate or exclude cartilage invasion. This results in a specificity equal to CT, and a much higher sensitivity. The existence of movement artifacts interfered with adequate diagnosis in 16% of the MRI examinations.

REFERENCES

1. Gerritsen GJ, Valk J, van Velzen DJ, Snow GB. Computed tomography: a mandatory investiogational procedure for the T-staging of advanced laryngeal cancer. Clin Otolaryngol 1986;11:307-316.

2. Yeager VL, Lawson C, Archer CR. Ossification of laryngeal cartilages as it relates to computed tomography. Invest Radiol 1982;17:11-19.

3. Hoover LA, Calcaterra TC, Walter GA, Larrson SG. Preoperative CT scan evaluation for laryngeal carcinoma: correlation with pathological findings. Laryngoscope 1984;94:310-315.

4. Decker JW, Price JC, Goldstein JC. Advanced Laryngeal Cancer. Relevance of Pathologic Stage to Survival and Therapy. Arch Otolaryngol Head Neck Surg 1986;112:1163-1167.

5. McArdle CB, Bailey BJ, Amparo EG. Surface coil magnetic resonance imaging of the normal larynx. Arch Otolaryngol Head Neck Surg 1986;112:616-622.

6. Castelijns JA, Doornbos J, Verbeeten B Jr., Vielvoye GJ, Bloem JL. Magnetic resonance imaging of the normal larynx. J Comput Assist Tomogr 1985;9(5):919-25.

7. Lufkin RB, Hanafee WN. Application of surface coils to MR anatomy of the larynx. AJNR 1985;6:491-497.

8. Lufkin RB, Hanafee WN, Wortham D, Hoover L. Larynx and hypopharynx: MR imaging with surface coils. Radiology 1986;158:747-754.

9. Castelijns JA, Gerritsen GJ, Kaiser MC, Valk J, Jansen W, Meyer CJLM, Snow GB. MRI of laryngeal cartilages, normal or invaded by primary cancer; MRI-histopathologic correlation. Laryngoscope (in press).

10. Castelijns JA. Laryngeal cancer. In: Valk J,ed. Magnetic Resonance Imaging of the brain, head, neck and spine- a teaching atlas of clinical applications. Dordrecht: Martinus Nijhoff Publishers, 1987 (in press).

11. Michaels L, Gregor RT. Examination of the larynx in the histopathology laboratory. J Clin Pathol 1980; 33:705-709.

12. Moss WT, Brand WN, Battifora H. The endolarynx, hypopharynx, and thyroid. In: Moss WT, ed. Radiation Oncology. Saint Louis: The C. V. Mosby Compagny, 1973:195-232.

13. Castelijns JA, Valk J, Kaiser MC, Gerritsen GJ, Jansen W, Snow GB. MRI of laryngeal tumors. In: RSNA Scientific Program of the 72nd Scientific Assembly and Annual Meeting. 1986: 366.

14. Castelijns JA, Kaiser MC, Valk J, Gerritsen GJ, van Hattum AH, Snow GB. MRI of laryngeal cancer. J Comput Assist Tomogr 1987;11(1),134-140.

15. Roncallo, P. Researches about ossification and conformation of the thyroid cartilage in men. Acta Otolaryng 1948;36;110-134.

16. Chievitz JH. Untersuchungen ueber die verknocherung der

menschlichen kehllnorpel. Arch anat u entwickelingsgesch 1882;4:200-208.

17. Sagel SS, Aufderheide JF, Aronberg DJ, Stanley RJ, Archer CR. High resolution computed tomography in the staging of carcinoma of the larynx. The Laryngoscope 1981;91,292-300.

18. Archer CR, Yeager VL. Computed tomography of laryngeal cancer with histopathological correlation. Laryngoscope 1982;92,1173-1180.

Chapter 8. GENERAL DISCUSSION

Employing standard head and body coils, the structures of the neck are particularly difficult to image by MR. Head coils will not cover the middle and inferior regions of the neck because the shoulders interfere with positioning. Body coils are inefficient because of the small size of the region of interest. The application of specially designed surface coils has been proven to be the ideal solution of these problems. The use of these type of coils results in a considerable improvement of the signal-to-noise ratio of laryngeal imaging. It is also possible to obtain high signal resolution images with a field of view as small as possible and with a minimal slice thickness which is necessary to demonstrate delicate laryngeal structures.

CT images are frequently degraded by streak artifacts caused by swallowing, respiratory motion and/or X-ray beam hardening. A disadvantage of MRI is that at the present stage of technology, scan times for MRI are considerably longer, in the order of minutes, versus seconds for CT. Consequently, MR imaging is much more susceptible to degradation by gross motion. Occasionally, in this study 16% of the examinations, image quality may interfere with the minimal requirements for diagnostic work-up. In accordance with Stark, we find that MR images are only minimally affected by normal respiration movements (1). Patients with great difficulty in swallowing, excessive coughing or patients with chronic respiratory disease and/or forced breathing are unsuitable candidates. Furthermore, due to the long scanning times it is not yet possible to image laryngeal structures without motion artifacts, while performing phonation or other physiological manoeuvers. However, the recent introduction of the fast scanning technique offers new prospects (2).

Applying the MR inversion recovery technique, we could not differentiate between muscular, bony and cartilagineous structures. MR Spin Echo (SE) images display greater soft tissue detail. In contrast to the findings of Stark et al, images, obtained with short repetition time (TR) and short echotime (TE), are preferable to demonstrate the laryngeal anatomy (1). SE T1-weighted images show relevant intralaryngeal structures (intrinsic musculature and the intralaryngeal compartments), the laryngeal cartilages and extralaryngeal structures (infrahyoid muscles, vascular structures in the carotid sheath) with excellent detail and soft tissue definition. Particularly, non-ossified and ossified cartilages are seen with clear contrast. Non-ossified cartilage is demonstrated with an intermediate signal intensity. Ossified cartilage has a typically three-layer appearance: high signal bone marrow being surrounded by low signal cortical rims. Cortical bone is imaged with low signal intensity due to the lack of mobile protons. Bone marrow, irrespective of the proportion of fatty and haemopoietic content, is always seen with high signal intensity. In fact, haemopoietic marrow consists of 25%-50% fat.

Surgery, partial or total laryngectomy, and/or radiation therapy are the modalities of choice for the treatment of laryngeal cancer. The choice between these modalities is, amongst others, influenced by the site and the extent of the lesion. Particularly, the question whether cartilage invasion is present or absent is of importance. Radiation therapy, particularly high doses, may be contra-indicated and total laryngectomy may be indicated, if cartilage invasion exists. If the cartilages are invaded by tumor, radiation often results in perichondritis, necrosis or sequestration of the cartilages, particularly if high doses of radiation are given. Furthermore, accurate assessment of the extent of the primary lesion is highly important with regards to the feasibility and the application of the various techniques of partial and total laryngectomy and the techniques of irradiation treatment.

Direct and indirect laryngoscopic examinations offer a great deal of information about the site, the volume, and the extent of the intralaryngeal lesion, but do not provide

information about the submucosal extension of the lesion and some hidden regions, such as the subglottic area or areas concealed by a large tumor mass.

The conventional radiological modalities, such as contrast laryngography and conventional tomography, may provide additional information about the extent of the disease. However, these modalities have been largely supplanted by CT. The introduction of CT has been a break-through in demonstrating the submucosal extent of the disease in the axial plane, particularly extralaryngeal spread and major cartilage invasion. CT provides helpful information about areas that may be hidden from visual inspection by bulky tumors, such as the subglottis. More important, it reveals submucosal extension not visible by other means.

However, information about the extent of the tumor can only indirectly be inferred from CT images, by assessing the distortion of the laryngeal structures or narrowing of the laryngeal lumen. This study demonstrates that MR T1-weighted images appear to be more appropriate than CT to assess the extent of laryngeal cancer. On T1-weighted images, tumor tissue is found with homogeneously intermediate signal intensity, slightly higher than the signal intensity of muscular tissue, but definitively lower than that of fat. Images, accentuating T2-characteristics (proton density or T2-weighted images), show tumor tissue with less homogeneous signal intensity. Tumor is found with increased signal intensity, minimizing the contrast between pathological tissue and fat and increasing the contrast between the tumor on the one hand and muscular and cartilagineous tissues on the other. T2-weighted images have a relatively low signal-to-noise ratio. The use of proton density images is a good compromise between a reasonable signal-to-noise ratio and an adequate expression of T2 tissue-characeristics.

The axial imaging technique is, above other scan directions, appropriate to study the site and the extent of tumor in intralaryngeal compartments (pre-epiglottic space and right and left paraglottic spaces), laryngeal cartilages as well as in extralaryngeal structures, such as the infrahyoid muscles, piriform sinus, subcutaneous fat and lymph nodes along the carotid sheath.

MRI has the advantage over CT, that it is capable of imaging in the frontal and sagittal planes in a sufficiently accurate manner. On frontal images, the cranio-caudal extension of the tumor, particularly a subglottic extension, and the relationship between the caudal margin of the tumor and the upper border of the cricoid, is more clearly demonstrated. The laryngeal ventricles may be seen open on frontal images, but this is not a constant finding in patients who do not have abnormalities at the level of the laryngeal ventricles.

On sagittal images infiltration of the root of the tongue by tumor tissue is well visualized. The distance between the caudal margin of a supraglottic tumor and the anterior commissure can be assessed.

Three-dimensional representation of pathology, as may be demonstrated by MRI, enables calculation of the tumor volume to provide the basis for radiation therapy.

In this study we demonstrate that the main advantage of MRI over any other diagnostic modality appears to be its capability to demonstrate laryngeal cartilage invasion by cancer. This will be discussed firstly for the epiglottic cartilage. The epiglottic cartilage consists of elastic fibrocartilage and generally does not ossify. All other laryngeal cartilages consist of hyaline cartilage and ossify at an advanced age. This study demonstrates that the vicinity of tumor to the epiglottic cartilage, as shown by MR T1-weighted, axial and sagittal images, appears to be very suspicious for cartilage invasion. Using these criteria, the sensitivity of MRI to detect invasion of the epiglottic cartilage is much higher than that of CT. Whereas on CT, the extent of the lesion is often underestimated due to low contrast differences between pathological tissue and pre-epiglottic fat, SE T1-weighted images show more contrast between both tissues.

The changes in hyaline cartilage are the subject of long discussion in literature. In some studies it is maintained that both processes (ossification and calcification) are interrelated, whereas other authors favour the view that both processes are totally independent of each other. This confusion continues in recent reports, concerning MRI of the neck area (3,4,5). In this study, changes in the cartilages as visualized by CT, are defined with the term "calcification", and changes in hyaline cartilages observed in MR images, with the term "ossification". Comparison of CT and MRI images with corresponding microscopic sections suggest that patterns of calcification and ossification agree to a certain degree.

It has been stated that CT is superior to MRI in depicting laryngeal cartilages and detection of cartilage invasion (6). However, the present study demonstrates that MR imaging, by combined use of axial T1-weighted and proton density images, is more appropriate than CT to detect invasion of laryngeal cartilages. Due to irregular calcification and high degree of variability of calcification between individuals, minor cartilage invasion cannot be detected by CT. Uncalcified or poorly calcified cartilage is inadequately shown by CT, and therefore erosion or destruction may thus be simulated. On the other hand, very frequently the tumor may grossly invade the medullary space of the laryngeal cartilages without destroying bony trabeculae and surrounding bone and may therefore escape detection because the presence of these bony structures allows for reconstruction of an apparently normal cartilage on CT. Comparison of results of CT- and MRI-observers indicates that MRI detects cartilage invasion with a higher accuracy and, in particular, a much higher sensitivity than CT does. Detection of invasion into hyaline cartilages (cricoid, arytenoid and thyroid cartilages) is highly improved by the use of both T1-weighted and proton density images. T1-weighted images allow separation between pathological and normal bone marrow. Proton density images permit differentiation between non-ossified cartilage and tumor tissue.

In this study, MRI appears to be less effective in patients suspect of a recurrent or a residual tumor after previous irradiation treatment. Distinction between cancer, edema and irradiation fibrosis is not possible. This agrees with the findings of Lufkin et al (7), but is in contrast to preliminary reports of Glazer et al, in which it is maintained that MR imaging is very encouraging in evaluating the post-treatment neck.

In patients with squamous cell carcinoma of the upper air- and food passages MRI appears to be promising with regard to detection of spread to regional lymph nodes in the neck. It is generally recognized that the status of the cervical lymph nodes is the most important factor in these patients. Clinical assessment of the status of neck nodes is still based on palpation. However, the overall error in assessing the presence or absence of cervical node metastasis by palpation, is reported to be within a range of 20-30%. Moreover, some areas of the neck are not accessible to palpation, such as the para- or retropharyngeal spaces. There is thus a great need for other, hopefully more reliable, methods of detection of metastatic lymph nodes in the neck. MRI has, by the use of both T1-weighted and proton density images, great potential for the detection of the smaller, metastatic lymph nodes. Lymph nodes and vessels are demonstrated on T1-weighted images with intermediate and low signal intensity, respectively, both being imaged with high contrast to surrounding fat. Vessels are clearly identified on proton density images, lymph nodes being demonstrated with increased signal intensity.

In summary, the comparison with histological findings and statistical evaluation suggest a superiorty of MR imaging over CT in delineating the site and the extent of laryngeal cancer. MRI therefore, should be included in the diagnostic work-up of all patients with laryngeal cancer who have not been treated previously, except those patients with small tumors such as glottic T1-lesions. If MRI fails due to movement artifacts, claustrophobia, metallic inplants in the region of interest or if MRI is impossible in patients bearing a pacemaker or surgical clips, CT may still be necessary.

REFERENCES

1. Stark DD, Moss AA, Gamsu G, Clark OH, Gooding GA, Webb WR. Magnetic resonance imaging of the neck. Part 1: normal anatomy. Radiology 1984;150:447-54.

2. Van der Meulen P, Groen JP, Cuppen JJM. Very fast MR Imaging by field echoes and small angle excitation. Magn Reson Imaging 1985;3:297-299.

3. Wortham DG, Hoover LA, Lufkin RB, Fu YS. Magnetic resonance imaging of the larynx: a correlation with histologic sections. Otolaryngol head neck surg 1986;94:123-133.

4. Glazer HS, Niemeyer JH, Balfe DM et all. Neck neoplasms: MR Imaging. Part 1. Initial evaluation. Radiology 1986;160:343-348.

5. Lufkin RB, Hanafee WN. Application of surface coils to MR anatomy of the larynx. AJNR 1985;6:491-497.

6. McArdle CB, Bailey BJ, Amparo EG. Surface coil magnetic resonance imaging of the normal larynx. Arch Otolaryngol Head and Neck Surg 1986;112:616-622.

7. Lufkin RB, Hanafee WN, Wortham D, Hoover L. Larynx and hypopharynx: MR imaging with surface coils. Radiology 1986;158:747-754.

Summary

Chapter 1 deals with general aspects of laryngeal cancer. An accurate assessment of the extent of the primary tumor is essential for both the choice and the technique of the treatment procedure. Laryngoscopic examination provides valuable information about the intralaryngeal extent of the lesion but is deficient in assessing the submucosal extent of the lesion.
In chapter 2, the clinical relevance of various radiological examinations of the larynx is discussed. Conventional radiological modalities, such as contrast laryngography and conventional tomography have largely been supplanted by computer tomography (CT). CT is a major contribution to the diagnostic work-up of laryngeal carcinoma, particularly with regards to the demonstration of submucosal changes, major cartilage invasion and extralaryngeal extension. However, CT still has its limitations concerning its ability to image accurately in frontal and axial planes and concerning its potential to discriminate soft tissues and the detection of minor cartilage invasion.
Chapter 3 deals with the basic principles of MRI and reviews its technical potentials and limitations. MRI is a non-ionizing diagnostic method, providing images with high soft-tissue contrast in any plane of the human body.
In chapter 4, the experiences obtained in this study in optimizing MR images of the larynx are discussed. The application of specially designed surface coils results in a considerable improvement of the signal-to-noise ratio with both a field of view and a slice thickness as small as possible, necessary to demonstrate the delicate laryngeal structures. Spin echo T1-weighted images are preferable in the study of the laryngeal anatomy. Intralaryngeal structures (intrinsic musculature, intralaryngeal compartments), laryngeal cartilages and extralaryngeal structures (infrahyoid muscles, vascular strucures in the carotid sheath) are seen in detail. In particular,

non-ossified and ossified cartilage are imaged with high contrast to each other.
Chapter 5 deals with the MR imaging of laryngeal cancer, particularly in non-previously treated patients, by comparing pre-operative MRI findings with post-operative histopathological findings in corresponding sections of surgical specimens. Cancerous tissue is constantly seen on spin echo T1-weighted images as a homogeneous mass of intermediate signal intensity, which is slightly higher than the signal intensity of the infrahyoid muscles but much lower than that of fat. MRI appears to have less value for the diagnostic work-up of recurrent tumor: differentiation between recurrent tumor, irradiation fibrosis and edema is not possible.
Chapter 6 gives a detailed description of MR images of non-ossified and ossified cartilages, both normal and invaded by cancer. MRI has great potential in the detection of cartilage invasion by the combined use of T1-weighted and proton density images. T1-weighted images permit differentiation between pathological and normal bone marrow. Proton density images allow separation between non-ossified cartilage and tumor tissue.
In chapter 7, the capability of MRI and CT to detect cartilage invasion is evaluated, by comparing CT- and MR-images with histopathological findings in corresponding sections of surgical specimens and by comparative assessment of the accuracy of observations, done by CT- and MRI-observers. CT results in much more false negative diagnoses than MRI does, because calcified cartilage, invaded by cancer, is very frequently seen with CT as having an intact contour. On the other hand, tumor approaching non-ossified cartilage may simulate cartilage invasion. In our experience, specifities of CT and MRI to detect cartilage invasion are approximately equal (91% vs. 88%). However, CT has a much lower sensitivity than MRI (46% vs. 89%).

This study shows that MRI is superior to CT in delineating the site and the extent of laryngeal cancer.

This holds particularly true for the detection of laryngeal cartilage invasion by cancer. MRI therefore, is to be included in the diagnostic work-up of all laryngeal cancer patients, who have not been previously treated, with the exception of patients with small tumors, such as glottic T1 lesions.

Samenvatting

In hoofdstuk 1 wordt een aantal algemene aspecten van larynxkanker behandeld. Zowel voor de keuze als de uitvoering van de behandeling -bestraling of operatie- is nauwkeurige bepaling van de uitbreiding van de primaire tumor essentieel. Laryngoscopisch onderzoek verschaft goede informatie omtrent de intralaryngeale uitbreiding maar schiet tekort wat betreft de submucosale uitbreiding, terwijl sommige gebieden zoals de subglottis voor dit onderzoek niet voldoende toegankelijk zijn.

In het tweede hoofdstuk wordt de clinische relevantie van verschillende radiologische onderzoeksmethoden van de larynx besproken. Conventionele radiologische technieken, zoals contrast laryngografie en conventionele tomografie, zijn grotendeels verdrongen door computer tomoprafie (CT). CT draagt in belangrijke mate bij aan de diagnostiek van larynx kanker, in het bijzonder wat betreft de weergave van submuceuze veranderingen, grove kraakbeeninvasie en extralaryngeale uitbreiding. CT heeft echter een aantal beperkingen, met name wat betreft contrastrijke weergave van zachte weefsels, het verschaffen van sagittale en frontale afbeeldingen en het aantonen van geringere vormen van kraakbeeninvasie.

In hoofdstuk 3 worden enige algemene aspecten van MRI besproken en wordt een overzicht van haar beperkingen gegeven.

In hoofdstuk 4 worden de ervaringen besproken, opgedaan tijdens deze studie, in het verkrijgen van een optimale weergave van de larynx. De toepassing van speciaal ontworpen oppervlaktespoelen in MR beeldvorming van de larynx maakt een aanzienlijke verbetering van de signaal-ruis verhouding mogelijk, terwijl gebruik gemaakt kan worden van een zo klein mogelijk gezichtsveld en een zo dun mogelijk coupedikte, die noodzakelijk zijn om de verfijnde laryngeale structuren weer te geven. Spin echo T1-gewogen afbeeldingen verdienen de voorkeur voor de bestudering van de anatomie van de larynx. Intralaryngeale structuren, zoals de intrinsieke musculatuur en intralaryngeale compartimenten, larynxkraakbeenderen en extralaryngeale structuren, zoals de mm. infrahyoidei en vasculaire structuren in de vaat-zenuwstreng, laten zich tot in detail afbeelden. In het bizonder niet-verbeend kraakbeen en verbeend "kraakbeen" vertonen een hoog contrast met elkaar.

In hoofdstuk 5 wordt de MRI van larynx kanker behandeld van in het bizonder onbehandelde patienten aan de hand van een vergelijking van pre-operatieve MRI beelden met post-operatieve pathologisch-anatomische bevindingen in operatiepreparaten. Kankerweefsel wordt op T1-gewogen afbeeldingen steeds gezien als een homogene massa met een intermediaire intensiteit, die iets hoger is dan de intensiteit, waarmee de infrahyoide spieren weergegeven worden en veel lager dan de intensiteit, waarmee vetweefsel weergegeven wordt. MRI lijkt slechts beperkte waarde te hebben voor de diagnostiek van recidief carcinoom na bestraling: onderscheid tussen recidief tumor, bestralingsfibrose en oedeem lijkt niet mogelijk.

In hoofdstuk 6 wordt een gedetailleerde beschrijving gegeven van MR afbeeldingen van niet-verbeend en verbeend kraakbeen, zowel normale kraakbeenderen als kraakbeenderen geinvadeerd door kankerweefsel. MRI heeft grote mogelijkheden in het aantonen van kraakbeeninvasie door een gecombineerd gebruik van T1-gewogen en zogenaamde "proton density" beelden. T1-gewogen afbeeldingen maken differentiatie mogelijk tussen pathologisch en normaal beenmerg. Met behulp van "proton density" beelden is het mogelijk om te differentieren tussen niet-verbeend kraakbeen en tumorweefsel.

In het zevende hoofdstuk wordt het vermogen van MRI en CT om kraakbeeninvasie aan te tonen geevalueerd met behulp van enerzijds een vergelijking van CT- en MRI-beelden met histopathologische bevindingen in corresponderende coupes van operatiepreparaten en anderzijds het bepalen van de sensiviteit en de specifiteit van de bevindingen, zoals gedaan door CT- en MRI-waarnemers. CT leidt tot veel meer

vals negatieve bevindingen dan MRI. Verkalkt kraakbeen, dat geinvadeerd is, wordt met behulp van CT toch vaak gezien met een intacte contour. Tumor, die aanligt tegen niet-verbeend kraakbeen, kan anderzijds de verdenking van kraakbeeninvasie geven. Hoewel CT en MRI in dit onderzoek een vrijwel gelijke specificiteit (resp. 91% en 88%) blijken te hebben in het aantonen van kraakbeeninvasie, heeft CT een veel lagere sensitiviteit dan MRI (resp. 46% en 89%).

Deze studie toont aan dat MRI beter dan CT in staat is de localisatie en uitbreiding van larynxcarcinomen te bepalen; in het bizonder geldt dit voor het aantonen van kraakbeeninvasie. MRI is dan ook geindiceerd bij alle patienten met een niet eerder behandeld larynxcarcinoom, met uitzondering van patienten met kleine tumoren, zoals bijvoorbeeld glottische T1 lesies.

WOORD VAN DANK:

Aan het tot stand komen van dit proefschrift hebben velen een wezenlijke bijdrage geleverd. Allen ben ik daarvoor dank verschuldigd. Een aantal van hen wil ik met name noemen:

-Mijn promotor Prof.Dr. J.Valk. U ben ik dankbaar voor uw enthousiaste begeleiding, deskundigheid en steun.

-Mijn promotor Prof.Dr. G.B.Snow. Ik heb uw kundigheid als waardevol ervaren. U ben ik erkentelijk voor uw inspirerende inzet.

-Mijn referent Prof.Dr. A.E. van Voorthuisen dank ik voor de kritische beschouwing van dit manuscript. Ik ben zijn afdeling zeer dankbaar, dat ik de gelegenheid kreeg om dit onderzoek te beginnen.

-Prof.Dr. C.J.L.M.Meyer ben ik erkentelijk voor de stimulerende kritiek en ook voor de geboden voorzieningen om mijn wetenschappelijke arbeid uit te voeren.

-Prof.Dr. A.H.M.Lohman. U ben ik dankbaar voor de tijd die u heeft besteed aan het kritisch doornemen van het manuscript.

-Mw. M.Smeenk, mw. K. van der Vegt, mw A.Mast, mw. W.Rood en de heer R.A.Prinsze ben ik veel dank verschuldigd voor de deskundige bediening van de N.M.R.-scanner. Mw. E. van der Straten en mw. J. van den Abbeelen wil ik danken voor de secretariele steun. Zonder hen allen was dit proefschrift niet tot stand gekomen.

-Drs. B.Verbeeten Jr., Dr. W.Jansen en Drs. M.M.Roganovic ben ik in het bijzonder erkentelijk voor hun stimulerende en bemoedigende opmerkingen.

-Voorts ben ik dank verschuldigd aan de overige medewerkers van dit onderzoek, met name wil ik noemen Drs. M.C.Kaiser, Dr. G.J.Gerritsen, Dr. A.H. van Hattum, Dr. J.Doornbos en Drs. J.L.Bloem. Behalve een essentiele bijdrage aan de artikelen, ontving ik van hen vaak nuttige adviezen.

-Ook wil ik danken de volgende personen, die ieder een bijdrage aan de totstandkoming van dit proefschrift leverden: de heren A.P.J.Castelijns, P.H.Castelijns, A.J.M.Peters en D.Campbell en mw. F.Noorderijk. De medewerkers van de audiovisuele dienst met name de heren G.J.Lijnzaad, J.T.A. van Ederen, G.J.Oskam en J.T. van Veldhuisen dank ik voor het enthousiasme en de deskundige hulp waarmee het werk uitgevoerd werd.

-De (overige) stafleden en assistenten en andere medewerkers van de afdelingen Radiodiagnostiek, KNO en Pathologische Anatomie wil ik danken. Jullie ondersteuning en belangstelling waren zeer bemoedigend. Enkelen wil ik met name noemen: Dr. A.J.M.Balm, mw. O. von Freytag Drabbe, Dr. F.B.J.M.Thunnissen, de heer W.J.E.Verra en Dr. R.G.M. de Slegte.